atoms

MDPI

Article

Extended Atomic Structure Calculations for W^{11+} and W^{13+}

Narendra Singh [1], Sunny Aggarwal [1,*] and Man Mohan [2]

[1] Department of Physics, Shyamlal College, University of Delhi, Delhi 110032, India; nsingh76@yahoo.co.in
[2] Department of Physics & Astrophysics, University of Delhi, Delhi 110007, India; drmanmohan.05@gmail.com
* Correspondence: sunny.du87@gmail.com

Received: 1 August 2020; Accepted: 3 December 2020; Published: 7 December 2020

check for updates

Abstract: We report an extensive and elaborate theoretical study of atomic properties for Pm-like and Eu-like Tungsten using Flexible Atomic Code (FAC). Excitation energies for 304 and 500 fine structure levels are presented respectively, for W^{11+} and W^{13+}. Properties of the 4*f*-core-excited states are evaluated. Different sets of configurations are used and the discrepancies in identifications of the ground level are discussed. We evaluate transition wavelength, transition probability, oscillator strength, and collisional excitation cross section for various transitions. Comparisons are made between our calculated values and previously available results, and good agreement has been achieved. We have predicted some new energy levels and transition data where no other experimental or theoretical results are available. The present set of results should be useful in line identification and interpretation of spectra as well as in modelling of fusion plasmas.

Keywords: oscillator strength; FAC; NIST; EBIT; spectroscopy

PACS: 32.70; Cs oscillator strengths

1. Introduction

There has been strong interest in the spectroscopy of tungsten as it is planned to be used in plasma facing components of future fusion devices, such as International Thermonuclear Experimental Reactor (ITER) due to its favourable physical and chemical properties, e.g., high energy threshold of sputtering, low sputtering yield, low tritium retention, and high melting temperature [1,2]. Since tungsten is a high-*Z* element ($Z = 74$), where Z is the atomic number, it will contribute a large fraction of energy carried out from the plasma, which leads to plasma cooling. Atomic data such as energy levels, radiative transition rates, and photoionization cross sections for low-charged and medium-charged ions are of great importance in the ITER plasma diagnostics [3]. In the past few decades, atomic data for several highly charged tungsten ions have been determined using different experimental and theoretical methods [4–8], but still there is demand for more accurate atomic data, especially for low and medium ionization states of tungsten.

In the present work, spectra of moderately charged states of tungsten (W^{11+} and W^{13+}) are theoretically investigated. Several observations and theoretical calculations have been performed for Pm-like W but, for Eu-like W, only a few experimental data are available in the literature. In fact, only one theoretical energy value can be found for Eu-like W in the Atomic Spectra Database of the National Institute of Standards and Technology (NIST) [9]. These ionized states of tungsten are complex due to an open 4f shell, and obtaining accurate atomic data for these ions is a largely unsolved problem. For example, by inclusion of different configuration sets in the calculations, one will obtain a different ground state. The accuracy of a calculation can be estimated by considering (i) the convergence rate, (ii) the agreement between experimental measurements and theoretical calculations, and (iii) the difference between the velocity and length gauges of oscillator strength. Furthermore, results of calculations depend on the configuration-interaction (CI) effects, and, to ensure good accuracy, the most essential interactions must be included. In the past few years, we have calculated accurate atomic data by taking into account the essential interactions [10–15]. Brage and Froese Fischer [16] and Froese Fischer [17] presented a detailed review of analysis and evaluation of the CI effect in different atomic structure codes. In our present work, we have compared our calculated results with the available theoretical and experimental results and found good agreement.

2. Available Atomic Data

2.1. Pm-Like W (W^{13+})

Promethium-like ions have been studied both experimentally and theoretically over many years. There is still no full understanding of this sequence due to the open 4f shell, and obtaining accurate atomic data for this sequence is a largely unsolved problem. There is contradiction over the ground state for various charged states of Pm-like ions. Reliable atomic data for Pm-like ions are much needed, as some of these ions are promising candidates for the development of future optical clocks [18] and measurement of variation of the fine structure constant [19,20]. Curtis and Ellis [21] by their Hartree-Fock-Pauli (HFP) calculations showed that, in Pm-like W, the ground state is $4f^{14}5s\ ^2S_{1/2}$ and dominant resonance lines are 5s-5p doublets. Theodosiou and Raftopoulos [22] performed a fully relativistic but single configuration calculation, using the Dirac-Fock approximation, and determined that the ground state of W^{13+} is odd parity $4f^{13}5s^2\ ^2F_{7/2.}$ Hutton et al. [23] identified the transitions $4f^{14}5s\ ^2S_{1/2}$- $4f^{14}5p\ ^2P_{1/2,3/2}$ using an electron beam ion trap (EBIT). Vilkas et al. [24] evaluated transition wavelengths and lifetimes in Pm-like ions (including W^{13+}) by taking $4f^{13}5s^2$, $4f^{13}5p^2$, $4f^{13}5s5p$, $4f^{12}5s^25p$, $4f^{12}5s5p^2$, and $4f^{12}5p^3$ configurations using relativistic multi-reference Møller-Plesset second order perturbation theory (MR-MP). They claim to have accuracy of a predicted wavelength of about 0.25 Å for Pm-like W. Their [24] work targeted the $4f^{14}5s\ ^2S_{1/2}$- $4f^{14}5p\ ^2P_{1/2,3/2}$ transitions between excited states.

Kramida and Shirai [25] predicted that the ground state of Pm-like W is $4f^{13}5s^2\ ^2F_{7/2}$ while the first excited state is $4f^{13}5s^2\ ^2F_{5/2}$, which is separated by 18,000 cm^{-1} from the ground state. Wu and Hutton [26] discussed the behaviour of relative intensities of strong lines at different electron beam energies. Kramida [27] in his review noted the effect on the calculated energies from inclusion of two additional configurations ($4f^{11}5s^25p^2$ and $4f^{10}5s^25p^3$). Safronova et al. [28] calculated excitation energies of some levels in Pm-like ions (including Pm-like W) using relativistic many body perturbation theory (RMBPT), Hebrew university Lawrence Livermore atomic code (HULLAC), and Hartree-Fock relativistic method (Cowan's code). They confirmed that the ground state is $4f^{13}5s^2\ ^2F_{7/2}$. Qiu et al. [29] studied the visible and soft X-ray spectral regions and concluded that 4f collapse is not complete in W^{13+}. According to them [29], four lines that were identified in the Berlin EBIT spectra [30] do not appear to originate from tungsten. Kobayashi et al. [31] observed extreme ultraviolet and visible spectra of W^{13+} using EBIT. Zhao et al. [32] observed visible transitions in W^{13+} using Shanghai high temperature superconducting EBIT. They predicted that, out of eight observed lines, five belong to transitions from $4f^{12}5s^25p$. Recently, Ding et al. [33] calculated wavelengths and transition rates of the 5s-5p transitions of tungsten ions (including W^{13+}) using the relativistic configuration interaction method as implemented in the Flexible Atomic Code (FAC) [34].

2.2. Eu-Like W (W^{11+})

Ions of the Eu isoelectronic sequence (63 electron systems) are complex systems due to open 5s, 5p, and 4f subshells, but atomic structure calculations for these ions are needed to interpret the observed features. In the past, no extensive calculations for Eu-like W have been carried out. In fact, no spectral lines are available at the NIST website [9] for this particular ion. However, some authors reported selected transition wavelengths. Several studies contradict over the ground state for this ion. Kramida and Shirai [25] predicted that the ground state of Eu-like W is $4f^{13}5s^25p^2\,{}^4F_{7/2}$, while the first excited state is $4f^{14}5s^25p\,{}^2P_{1/2}$ located approximately 11,000 cm^{-1} above it. They showed that the ground state of this ion is uncertain. Li et al. [30] reported spectra for some transitions in the range of 150–400 Å using the Shanghai high-temperature superconducting electron beam ion trap (SH-HtscEBIT). They have also performed calculations using the fully relativistic FAC using nine configurations, which generated 2538 fine-structure levels. They confirmed that the ground state is $4f^{13}5s^25p^2\,{}^4F_{7/2}$. Mita et al. [34] observed EUV spectra for multiple charged tungsten ions (including W^{11+}). They have compared experimental measurements with collisional-radiative (CR) model calculations.

3. Theoretical Method

In spite of calculations performed by different authors for Pm-like and Eu-like W, there are no medium-scale calculations for these ions, and the shortage of complete and accurate data for these ions motivates this work. Most past calculations included very limited CI with an arbitrary choice of configurations. Therefore, in the present work, extensive calculations for W^{11+} and W^{13+} have been performed within the framework of FAC, which was developed by Gu [35]. FAC is a fully relativistic program used to compute the atomic structure, photoionization cross sections, and other atomic data. It is based on the Dirac-Hartree-Fock-Slater (DHFS) method, which uses perturbation theory. Optimization of orbitals is performed in a self-consistent-field iterative procedure in which the average energy of a fictitious mean configuration is minimized. This mean configuration represents the average electron cloud of the configurations retained in the CI expansion. In FAC, the Hamiltonian and configuration atomic state functions are similar to those of the MCDF (multi-configuration Dirac-Fock) method, including relativistic effects and higher-order QED effects, e.g., the Breit interaction in the zero-energy limit for the exchanged photon, and hydrogenic approximations for self-energy and vacuum polarization effects.

The effective Hamiltonian for an N-electron system is given by:

$$\hat{H} = \sum_{i=1}^{N} \hat{H}_i + \sum_{i=1}^{N-1} \sum_{j=i+1}^{N} V_{ij}, \tag{1}$$

where $\hat{H}_i$ is the Dirac one-particle operator for the ith-electron and V_{ij} represents effective electron-electron interactions.

An atomic state function (ASF) with total angular momentum J, its z-projection M, and parity p is assumed in the following form.

$$\psi_s\left(JM^P\right) = \sum\nolimits_m c_m(s)\phi\left(\gamma_m JM^P\right) \tag{2}$$

where $\phi\left(\gamma_m JM^P\right)$ are configuration state functions (CSF), $c_m(s)$ are configuration mixing coefficients for the states, and γ_m represents all information required to uniquely define a certain CSF. A detailed description of this theoretical approach can be found in the literature [35].

4. Result and Discussion

4.1. Eu-Like W

There is scarcity of complete, consistent, and reliable atomic data for Eu-like W in the literature. Therefore, in the present calculations, we have evaluated energy levels and radiative transition rates using FAC for Eu-like W with a set of electronic configurations ([Kr]$4d^{10}$) $4f^{12}5s^25p5d^2$, $4f^{12}5s^25p^25d$, $4f^{12}5s^25p^3$, $4f^{12}5s5p^25d^2$, $4f^{13}5s^25p5d$, $4f^{13}5s^25p^2$, $4f^{13}5p^25d^2$, $4f^{13}5s5p5d^2$, $4f^{13}5s5p^25d$, $4f^{13}5s5p^3$, $4f^{14}5s^25d$, $4f^{14}5d5f^2$, $4f^{14}5d^25f$, $4f^{14}5d^3$, $4f^{14}5s^25f$, $4f^{14}5f^3$, $4f^{14}5s^25p$, $4f^{14}5p5d5f$, $4f^{14}5p5d^2$, $4f^{14}5p5f^2$, $4f^{14}5p^25d$, $4f^{14}5p^25f$, $4f^{14}5p^3$, $4f^{14}5s5d^2$, $4f^{14}5s5f^2$, $4f^{14}5s5p5d$, $4f^{14}5s5p5f$, and $4f^{14}5s5p^2$, which generate

20,573 fine structure levels. Previous studies have not included so many configurations. Our ground state with this set of configurations is $4f^{13}5s^25p^2\ ^2F_{7/2}$, which is also shown by Li et al. [30].

We found complexity in the energy levels of Eu-like W. We have performed several calculations with different configurations included and found significant differences in the results, especially for the ground state. We are discussing one such difference. We have performed calculations by including the $4f^{14}5l^3$ (l = s,p,d,f,g), $4f^{13}5s^25p^2$, $4f^{13}5s5p^3$, $4f^{13}5s^25p5d$, $4f^{13}5s5p^25d$, $4f^{12}5s^25p^3$, and $4f^{12}5s^25p^25d$ configurations, which generate 4653 fine structure levels. Using these configurations, the ground state is found to be $4f^{14}5s^25p\ ^2P_{1/2}$. This problem is due to an insufficient account for inter-electron correlations, as accurate calculation of energies of open-f-shell configurations requires accounting for single and double excitations not only from the valence shells (including 4f), but also from the core shells such as 4d, which makes the study of Eu-like W more difficult. Therefore, we decided to check the reliability of our calculated results by comparison with the other available theoretical and experimental results, as suggested by Froese Fischer [17].

We present energy levels (in Ryd.) of the lowest 304 levels in Table 1 calculated using FAC. In the column "configuration," we give the configuration in *LS* coupling, while, in the "2*J*" column, the relativistic designation ending with the 2*J* value of a particular level is provided. Each shell is denoted so that 4f+7(7) represents seven electrons in the $4f_{7/2}$ subshell (J = 7/2), and 4f-5(5) represents five electrons in the $4f_{5/2}$ subshell (J = 5/2). The number in parentheses is two times the total angular momentum of the coupled shell. Immediately after the parentheses, there is a number indicating the 2*J* value obtained after all preceding shells are coupled. Completely filled relativistic subshells, such as $(4f_{5/2})^6$ and $(5s_{1/2})^2$, are omitted in the '2*J*' designations. For example, 4f+6(8)p+1(3)11 represents $[(4f_{5/2}{}^6)_0(4f_{7/2}{}^6)_4(5s^2)_0(5p_{1/2}{}^2)_0(5p_{3/2}{}^1)_{3/2}]$ (J = 11/2).

Table 1. Energies (in eV) of 304 lowest levels of Eu-like W.

Level	Configuration	2*J*	Energy (eV)
0	$4f^{13}5s^25p^2$	4f+7(7)7	0.000000
1	$4f^{14}5s^25p^1$	5p-1(1)1	1.487410
2	$4f^{13}5s^25p^2$	4f-5(5)5	2.635751
3	$4f^{13}5s^25p^2$	4f+7(7)7.5p-1(1)6.5p+1(3)9	10.406621
4	$4f^{13}5s^25p^2$	4f+7(7)7.5p-1(1)8.5p+1(3)5	11.338412
5	$4f^{13}5s^25p^2$	4f+7(7)7.5p-1(1)6.5p+1(3)3	11.495144
6	$4f^{13}5s^25p^2$	4f+7(7)7.5p-1(1)8.5p+1(3)7	11.982615
7	$4f^{13}5s^25p^2$	4f-5(5)5.5p-1(1)6.5p+1(3)3	12.116363
8	$4f^{13}5s^25p^2$	4f+7(7)7.5p-1(1)8.5p+1(3)11	12.306080
9	$4f^{13}5s^25p^2$	4f+7(7)7.5p-1(1)6.5p+1(3)5	12.599174
10	$4f^{13}5s^25p^2$	4f+7(7)7.5p-1(1)8.5p+1(3)9	12.897008
11	$4f^{13}5s^25p^2$	4f+7(7)7.5p-1(1)6.5p+1(3)7	12.986980
12	$4f^{12}5s^25p^3$	4f+6(12)12.5p+1(3)15	13.168432
13	$4f^{13}5s^25p^2$	4f-5(5)5.5p-1(1)4.5p+1(3)7	13.903781
14	$4f^{13}5s^25p^2$	4f-5(5)5.5p-1(1)6.5p+1(3)5	14.122897
15	$4f^{12}5s^25p^3$	4f+6(8)8.5p+1(3)11	14.291251
16	$4f^{13}5s^25p^2$	4f-5(5)5.5p-1(1)6.5p+1(3)9	14.621510
17	$4f^{12}5s^25p^3$	4f+6(12)12.5p+1(3)13	14.631127
18	$4f^{13}5s^25p^2$	4f-5(5)5.5p-1(1)4.5p+1(3)1	14.679897
19	$4f^{12}5s^25p^3$	4f+6(8)8.5p+1(3)9	14.759824
20	$4f^{12}5s^25p^3$	4f-5(5)5.4f+7(7)10.5p+1(3)7	15.082206
21	$4f^{13}5s^25p^2$	4f+7(7)7.5p-1(1)8.5p+1(3)9	15.398633
22	$4f^{12}5s^25p^3$	4f+6(8)8.5p+1(3)11	15.501744
23	$4f^{13}5s^25p^2$	4f-5(5)5.5p-1(1)4.5p+1(3)5	15.508532
24	$4f^{14}5s^25p^1$	5p+1(3)3	15.538168
25	$4f^{12}5s^25p^3$	4f+6(8)8.5p+1(3)7	15.864304
26	$4f^{13}5s^25p^2$	4f-5(5)5.5p-1(1)4.5p+1(3)3	15.922657
27	$4f^{12}5s^25p^3$	4f-5(5)5.4f+7(7)10.5p+1(3)13	16.076542

Table 1. *Cont.*

Level	Configuration	2*J*	Energy (eV)
28	$4f^{12}5s^25p^3$	4f+6(8)8.5p+1(3)5	16.145582
29	$4f^{12}5s^25p^3$	4f-5(5)5.4f+7(7)8.5p+1(3)7	16.400673
30	$4f^{12}5s^25p^3$	4f+6(4)4.5p+1(3)5	16.824471
31	$4f^{12}5s^25p^3$	4f-5(5)5.4f+7(7)10.5p+1(3)9	16.857139
32	$4f^{12}5s^25p^3$	4f-5(5)5.4f+7(-7)10.5p+1(3)11	17.125132
33	$4f^{12}5s^25p^3$	4f+6(4)4.5p+1(3)3	17.421249
34	$4f^{12}5s^25p^3$	4f-5(5)5.4f+7(7)6.5p+1(3)7	17.509417
35	$4f^{12}5s^25p^3$	4f-5(5)5.4f+7(7)8.5p+1(3)11	17.527564
36	$4f^{12}5s^25p^3$	4f-5(5)5.4f+7(7)8.5p+1(3)9	17.779745
37	$4f^{12}5s^25p^3$	4f-4(8)8.5p+1(3)5	17.834973
38	$4f^{12}5s^25p^3$	4f+6(4)4.5p+1(3)1	17.891446
39	$4f^{12}5s^25p^3$	4f-5(5)5.4f+7(7)6.5p+1(3)5	18.053266
40	$4f^{12}5s^25p^3$	4f-5(5)5.4f+7(7)6.5p+1(3)7	18.202150
41	$4f^{12}5s^25p^3$	4f-5(5)5.4f+7(7)6.5p+1(3)9	18.356867
42	$4f^{12}5s^25p^3$	4f-5(5)5.4f+7(7)8.5p+1(3)7	18.596612
43	$4f^{12}5s^25p^3$	4f-5(5)5.4f+7(7)6.5p+1(3)3	19.061518
44	$4f^{12}5s^25p^3$	4f-5(5)5.4f+7(7)8.5p+1(3)5	19.422447
45	$4f^{12}5s^25p^3$	4f-4(8)8.5p+1(3)7	19.635564
46	$4f^{12}5s^25p^3$	4f-4(8)8.5p+1(3)11	19.732177
47	$4f^{12}5s^25p^3$	4f-4(8)8.5p+1(3)9	19.983774
48	$4f^{12}5s^25p^3$	4f-5(5)5.4f+7(7)4.5p+1(3)5	20.239222
49	$4f^{12}5s^25p^3$	4f-5(5)5.4f+7(7)12.5p+1(3)15	20.693116
50	$4f^{12}5s^25p^3$	4f-5(5)5.4f+7(7)4.5p+1(3)7	20.821427
51	$4f^{12}5s^25p^3$	4f+6(4)4.5p+1(3)1	20.856783
52	$4f^{12}5s^25p^3$	4f+6(4)4.5p+1(3)3	20.905069
53	$4f^{12}5s^25p^3$	4f-5(5)5.4f+7(7)12.5p+1(3)9	21.326702
54	$4f^{12}5s^25p^3$	4f+6(0)0.5p+1(3)3	21.575392
55	$4f^{12}5s^25p^3$	4f-5(5)5.4f+7(7)2.5p+1(3)5	22.169730
56	$4f^{12}5s^25p^3$	4f-5(5)5.4f+7(7)12.5p+1(3)11	22.498936
57	$4f^{12}5s^25p^3$	4f-5(5)5.4f+7(7)2.5p+1(3)1	22.737919
58	$4f^{12}5s^25p^3$	4f-5(5)5.4f+7(7)12.5p+1(3)13	22.989126
59	$4f^{12}5s^25p^3$	4f-4(4)4.5p+1(3)5	23.102462
60	$4f^{12}5s^25p^3$	4f-5(5)5.4f+7(7)2.5p+1(3)3	23.176613
61	$4f^{12}5s^25p^3$	4f-4(4)4.5p+1(3)7	23.443646
62	$4f^{12}5s^25p^3$	4f-5(5)5.4f+7(7)4.5p+1(3)3	23.652780
63	$4f^{12}5s^25p^3$	4f-4(4)4.5p+1(3)1	24.886345
64	$4f^{12}5s^25p^3$	4f+6(12)12.5p-1(1)11.5p+2(4)15	25.198660
65	$4f^{13}5s^25p^2$	4f+7(7)7.5p+2(4)11	25.225674
66	$4f^{13}5s^25p^2$	4f+7(7)7.5p+2(4)9	25.463906
67	$4f^{13}5s^25p^2$	4f+7(7)7.5p+2(4)7	25.560618
68	$4f^{13}5s^25p^2$	4f+7(7)7.5p+2(4)3	25.845469
69	$4f^{12}5s^25p^3$	4f+6(12)12.5p-1(1)11.5p+2(4)13	26.159966
70	$4f^{13}5s^25p^2$	4f+7(7)7.5p+2(4)5	26.641175
71	$4f^{12}5s^25p^3$	4f+6(8)8.5p-1(1)7.5p+2(4)11	26.677789
72	$4f^{12}5s^25p^3$	4f+6(12)12.5p-1(1)13.5p+2(4)9	26.929062
73	$4f^{12}5s^25p^3$	4f+6(12)12.5p-1(1)13.5p+2(4)11	27.017239
74	$4f^{13}5s^25p^2$	4f-5(5)5.5p+2(4)5	27.183576
75	$4f^{12}5s^25p^3$	4f+6(8)8.5p-1(1)9.5p+2(4)7	27.403642
76	$4f^{13}5s^25p^2$	4f-5(5)5.5p+2(4)3	27.583722
77	$4f^{12}5s^25p^3$	4f+6(8)8.5p-1(1)7.5p+2(4)9	27.737449
78	$4f^{13}5s^25p^2$	4f-5(5)5.5p+2(4)9	27.825543
79	$4f^{13}5s^25p^2$	4f-5(5)5.5p+2(4)1	27.843724
80	$4f^{12}5s^25p^3$	4f+6(8)8.5p-1(1)9.5p+2(4)5	28.013025
81	$4f^{13}5s^25p^2$	4f-5(5)5.5p+2(4)7	28.016205
82	$4f^{12}5s^25p^3$	4f+6(12)12.5p-1(1)13.5p+2(4)17	28.046730
83	$4f^{12}5s^25p^3$	4f-5(5)5.4f+7(7)10.5p-1(1)11.5p+2(4)9	28.073077

Table 1. *Cont.*

Level	Configuration	2*J*	Energy (eV)
84	$4f^{12}5s^25p^3$	4f-5(5)5.4f+7(7)10.5p-1(1)11.5p+2(4)11	28.092883
85	$4f^{12}5s^25p^3$	4f-5(5)5.4f+7(7)10.5p-1(1)9.5p+2(4)13	28.093387
86	$4f^{12}5s^25p^3$	4f+6(12)12.5p-1(1)13.5p+2(4)15	28.284992
87	$4f^{12}5s^25p^3$	4f-5(5)5.4f+7(7)10.5p-1(1)11.5p+2(4)7	28.296631
88	$4f^{12}5s^25p^3$	4f+6(12)12.5p-1(1)13.5p+2(4)13	28.439835
89	$4f^{12}5s^25p^3$	4f-5(5)5.4f+7(7)8.5p-1(1)9.5p+2(4)7	28.636467
90	$4f^{12}5s^25p^3$	4f-5(5)5.4f+7(7)8.5p-1(1)9.5p+2(4)5	28.890217
91	$4f^{12}5s^25p^3$	4f-5(5)5.4f+7(7)6.5p-1(1)5.5p+2(4)9	29.031733
92	$4f^{12}5s^25p^3$	4f+6(8)8.5p-1(1)9.5p+2(4)13	29.106108
93	$4f^{12}5s^25p^3$	4f-5(5)5.4f+7(7)8.5p-1(1)7.5p+2(4)11	29.109282
94	$4f^{12}5s^25p^3$	4f+6(12)12.5p-1(1)11.5p+2(4)7	29.138058
95	$4f^{12}5s^25p^3$	4f-5(5)5.4f+7(7)6.5p-1(1)7.5p+2(4)5	29.247008
96	$4f^{12}5s^25p^3$	4f-5(5)5.4f+7(7)10.5p-1(1)11.5p+2(4)9	29.463518
97	$4f^{12}5s^25p^3$	4f-5(5)5.4f+7(7)6.5p-1(1)7.5p+2(4)3	29.510742
98	$4f^{12}5s^25p^3$	4f+6(4)4.5p-1(1)3.5p+2(4)7	29.581339
99	$4f^{12}5s^25p^3$	4f+6(8)8.5p-1(1)7.5p+2(4)3	29.660947
100	$4f^{12}5s^25p^3$	4f-5(5)5.4f+7(7)8.5p-1(1)7.5p+2(4)11	29.690268
101	$4f^{12}5s^25p^3$	4f+6(4)4.5p-1(1)5.5p+2(4)1	29.785016
102	$4f^{12}5s^25p^3$	4f-5(5)5.4f+7(7)6.5p-1(1)7.5p+2(4)7	29.802755
103	$4f^{12}5s^25p^3$	4f+6(8)8.5p-1(1)9.5p+2(4)11	29.835407
104	$4f^{12}5s^25p^3$	4f+6(12)12.5p-1(1)11.5p+2(4)9	29.935173
105	$4f^{12}5s^25p^3$	4f+6(8)8.5p-1(1)7.5p+2(4)9	29.992789
106	$4f^{12}5s^25p^3$	4f-4(8)8.5p-1(1)9.5p+2(4)5	30.135794
107	$4f^{12}5s^25p^3$	4f+6(8)8.5p-1(1)7.5p+2(4)7	30.208798
108	$4f^{12}5s^25p^3$	4f-4(0)0.5p+1(3)3	30.252252
109	$4f^{12}5s^25p^3$	4f-5(5)5.4f+7(7)10.5p-1(1)11.5p+2(4)15	30.315463
110	$4f^{12}5s^25p^3$	4f-5(5)5.4f+7(7)6.5p-1(1)7.5p+2(4)5	30.367034
111	$4f^{12}5s^25p^3$	4f-5(5)5.4f+7(7)10.5p-1(1)11.5p+2(4)13	30.420168
112	$4f^{12}5s^25p^3$	4f-4(8)8.5p-1(1)9.5p+2(4)5	30.515569
113	$4f^{12}5s^25p^3$	4f-5(5)5.4f+7(7)10.5p-1(1)9.5p+2(4)11	30.618863
114	$4f^{12}5s^25p^3$	4f-4(8)8.5p-1(1)9.5p+2(4)9	30.650657
115	$4f^{12}5s^25p^3$	4f+6(8)8.5p-1(1)7.5p+2(4)3	30.755836
116	$4f^{12}5s^25p^3$	4f-4(8)8.5p-1(1)9.5p+2(4)7	30.950833
117	$4f^{13}5s^25p^2$	4f+7(7)7.5p+2(0)7	31.028018
118	$4f^{12}5s^25p^3$	4f-5(5)5.4f+7(7)10.5p-1(1)9.5p+2(4)5	31.135297
119	$4f^{12}5s^25p^3$	4f-5(5)5.4f+7(7)8.5p-1(1)9.5p+2(4)13	31.239437
120	$4f^{12}5s^25p^3$	4f-5(5)5.4f+7(7)10.5p-1(1)9.5p+2(4)9	31.300041
121	$4f^{12}5s^25p^3$	4f+6(12)12.5p-1(1)11.5p+2(0)11	31.395345
122	$4f^{12}5s^25p^3$	4f-5(5)5.4f+7(7)6.5p-1(1)5.5p+2(4)1	31.455875
123	$4f^{12}5s^25p^3$	4f-4(8)8.5p-1(1)9.5p+2(4)11	31.524113
124	$4f^{12}5s^25p^3$	4f-5(5)5.4f+7(7)10.5p-1(1)9.5p+2(4)9	31.631040
125	$4f^{12}5s^25p^3$	4f+6(4)4.5p-1(1)5.5p+2(4)5	31.660101
126	$4f^{12}5s^25p^3$	4f-5(5)5.4f+7(7)10.5p-1(1)9.5p+2(4)7	31.690291
127	$4f^{12}5s^25p^3$	4f-5(5)5.4f+7(7)6.5p-1(1)7.5p+2(4)11	31.716101
128	$4f^{12}5s^25p^3$	4f-4(8)8.5p-1(1)9.5p+2(4)7	31.778531
129	$4f^{12}5s^25p^3$	4f-5(5)5.4f+7(7)8.5p-1(1)7.5p+2(4)3	31.849222
130	$4f^{14}5s^15p^2$	5s+1(1)1	31.888981
131	$4f^{12}5s^25p^3$	4f-5(5)5.4f+7(7)8.5p-1(1)9.5p+2(4)11	32.085578
132	$4f^{12}5s^25p^3$	4f+6(4)4.5p-1(1)3.5p+2(4)1	32.085592
133	$4f^{12}5s^25p^3$	4f-5(5)5.4f+7(7)8.5p-1(1)7.5p+2(4)5	32.119796
134	$4f^{12}5s^25p^3$	4f+6(4)4.5p-1(1)3.5p+2(4)3	32.155819
135	$4f^{12}5s^25p^3$	4f-5(5)5.4f+7(7)10.5p-1(1)9.5p+2(4)7	32.172054
136	$4f^{12}5s^25p^3$	4f+6(4)4.5p-1(1)5.5p+2(4)9	32.219276
137	$4f^{12}5s^25p^3$	4f+6(12)12.5p-1(1)13.5p+2(0)13	32.250253
138	$4f^{12}5s^25p^3$	4f-5(5)5.4f+7(7)6.5p-1(1)5.5p+2(4)3	32.284567
139	$4f^{12}5s^25p^3$	4f-5(5)5.4f+7(7)6.5p-1(1)7.5p+2(4)9	32.310825

Table 1. *Cont.*

Level	Configuration	2*J*	Energy (eV)
140	$4f^{12}5s^25p^3$	4f+6(4)4.5p-1(1)3.5p+2(4)5	32.430748
141	$4f^{12}5s^25p^3$	4f-4(8)8.5p-1(1)7.5p+2(4)7	32.599412
142	$4f^{12}5s^25p^3$	4f-5(5)5.4f+7(7)2.5p-1(1)1.5p+2(4)5	32.710532
143	$4f^{12}5s^25p^3$	4f+6(8)8.5p-1(1)9.5p+2(0)9	32.722893
144	$4f^{12}5s^25p^3$	4f-5(5)5.4f+7(7)6.5p-1(1)5.5p+2(4)3	32.726514
145	$4f^{12}5s^25p^3$	4f-4(8)8.5p-1(1)9.5p+2(4)13	32.788252
146	$4f^{12}5s^25p^3$	4f-5(5)5.4f+7(7)6.5p-1(1)7.5p+2(4)7	32.803691
147	$4f^{13}5s^25p^2$	4f-5(5)5.5p+2(0)5	33.190258
148	$4f^{12}5s^25p^3$	4f-5(5)5.4f+7(7)12.5p-1(1)13.5p+2(4)9	33.311662
149	$4f^{12}5s^25p^3$	4f-4(8)8.5p-1(1)9.5p+2(4)11	33.320945
150	$4f^{12}5s^25p^3$	4f-5(5)5.4f+7(7)12.5p-1(1)11.5p+2(4)15	33.356951
151	$4f^{12}5s^25p^3$	4f+6(8)8.5p-1(1)7.5p+2(0)7	33.409179
152	$4f^{12}5s^25p^3$	4f-4(8)8.5p-1(1)7.5p+2(4)3	33.506910
153	$4f^{12}5s^25p^3$	4f-4(8)8.5p-1(1)7.5p+2(4)5	33.541559
154	$4f^{12}5s^25p^3$	4f-4(4)4.5p-1(1)5.5p+2(4)1	33.637808
155	$4f^{12}5s^25p^3$	4f-5(5)5.4f+7(7)8.5p-1(1)7.5p+2(0)7	33.638887
156	$4f^{12}5s^25p^3$	4f-5(5)5.4f+7(7)12.5p-1(1)13.5p+2(4)11	33.703349
157	$4f^{12}5s^25p^3$	4f-5(5)5.4f+7(7)10.5p-1(1)9.5p+2(0)9	33.705428
158	$4f^{12}5s^25p^3$	4f-5(5)5.4f+7(7)8.5p-1(1)9.5p+2(0)9	33.869720
159	$4f^{12}5s^25p^3$	4f-4(8)8.5p-1(1)7.5p+2(4)3	33.944386
160	$4f^{12}5s^25p^3$	4f-4(8)8.5p-1(1)9.5p+2(4)13	34.004247
161	$4f^{12}5s^25p^3$	4f-4(8)8.5p-1(1)7.5p+2(4)3	34.099755
162	$4f^{12}5s^25p^3$	4f+6(4)4.5p-1(1)5.5p+2(0)5	34.102104
163	$4f^{12}5s^25p^3$	4f-5(5)5.4f+7(7)10.5p-1(1)11.5p+2(0)11	34.135950
164	$4f^{12}5s^25p^3$	4f-4(8)8.5p-1(1)7.5p+2(4)7	34.455709
165	$4f^{12}5s^25p^3$	4f-4(8)8.5p-1(1)7.5p+2(4)5	34.503115
166	$4f^{12}5s^25p^3$	4f-5(5)5.4f+7(7)4.5p-1(1)5.5p+2(4)1	34.566251
167	$4f^{12}5s^25p^3$	4f-5(5)5.4f+7(7)6.5p-1(1)7.5p+2(0)7	34.581228
168	$4f^{12}5s^25p^3$	4f-4(8)8.5p-1(1)7.5p+2(4)9	34.785497
169	$4f^{12}5s^25p^3$	4f-4(4)4.5p-1(1)5.5p+2(4)9	34.912240
170	$4f^{12}5s^25p^3$	4f-4(4)4.5p-1(1)3.5p+2(4)5	34.933144
171	$4f^{12}5s^25p^3$	4f-5(5)5.4f+7(7)4.5p-1(1)5.5p+2(4)3	35.233127
172	$4f^{12}5s^25p^3$	4f-5(5)5.4f+7(7)12.5p-1(1)11.5p+2(4)13	35.331629
173	$4f^{12}5s^25p^3$	4f-4(4)4.5p-1(1)5.5p+2(4)7	35.335261
174	$4f^{12}5s^25p^3$	4f-5(5)5.4f+7(7)2.5p-1(1)3.5p+2(4)1	35.353611
175	$4f^{12}5s^25p^3$	4f-4(8)8.5p-1(1)7.5p+2(4)5	35.358568
176	$4f^{12}5s^25p^3$	4f-5(5)5.4f+7(7)4.5p-1(1)3.5p+2(4)3	35.443479
177	$4f^{12}5s^25p^3$	4f-5(5)5.4f+7(7)12.5p-1(1)13.5p+2(4)17	35.506997
178	$4f^{12}5s^25p^3$	4f-5(5)5.4f+7(7)12.5p-1(1)11.5p+2(4)11	35.519342
179	$4f^{12}5s^25p^3$	4f-5(5)5.4f+7(7)12.5p-1(1)13.5p+2(4)15	35.687177
180	$4f^{12}5s^25p^3$	4f-5(5)5.4f+7(7)2.5p-1(1)3.5p+2(4)5	35.832089
181	$4f^{12}5s^25p^3$	4f-4(8)8.5p-1(1)9.5p+2(0)9	35.889007
182	$4f^{12}5s^25p^3$	4f-5(5)5.4f+7(7)8.5p-1(1)7.5p+2(0)7	35.953208
183	$4f^{12}5s^25p^3$	4f-4(4)4.5p-1(1)3.5p+2(4)1	36.137604
184	$4f^{12}5s^25p^3$	4f-5(5)5.4f+7(7)2.5p-1(1)3.5p+2(4)3	36.266912
185	$4f^{12}5s^25p^3$	4f-5(5)5.4f+7(7)6.5p-1(1)5.5p+2(0)5	36.417751
186	$4f^{12}5s^25p^3$	4f-5(5)5.4f+7(7)12.5p-1(1)11.5p+2(4)7	36.686838
187	$4f^{12}5s^25p^3$	4f-5(5)5.4f+7(7)12.5p-1(1)11.5p+2(4)9	36.981241
188	$4f^{12}5s^25p^3$	4f-5(5)5.4f+7(7)2.5p-1(1)1.5p+2(4)3	36.996846
189	$4f^{12}5s^25p^3$	4f+6(4)4.5p-1(1)5.5p+2(0)5	37.131836
190	$4f^{12}5s^25p^3$	4f-5(5)5.4f+7(7)4.5p-1(1)3.5p+2(4)1	37.136391
191	$4f^{12}5s^25p^3$	4f-5(5)5.4f+7(7)12.5p-1(1)11.5p+2(4)7	37.253204
192	$4f^{12}5s^25p^3$	4f-4(4)4.5p-1(1)3.5p+2(4)5	37.454373
193	$4f^{12}5s^25p^3$	4f-5(5)5.4f+7(7)2.5p-1(1)3.5p+2(4)7	37.610500
194	$4f^{12}5s^25p^3$	4f-4(4)4.5p-1(1)3.5p+2(4)3	37.748395

Table 1. *Cont.*

Level	Configuration	2*J*	Energy (eV)
195	$4f^{12}5s^{2}5p^{3}$	4f-4(4)4.5p-1(1)5.5p+2(4)9	37.811969
196	$4f^{12}5s^{2}5p^{3}$	4f-4(8)8.5p-1(1)7.5p+2(0)7	38.345107
197	$4f^{12}5s^{2}5p^{3}$	4f-5(5)5.4f+7(7)4.5p-1(1)3.5p+2(0)3	38.556955
198	$4f^{12}5s^{2}5p^{3}$	4f-5(5)5.4f+7(7)2.5p-1(1)3.5p+2(4)5	38.846072
199	$4f^{12}5s^{2}5p^{3}$	4f-5(5)5.4f+7(7)12.5p-1(1)13.5p+2(0)13	39.722163
200	$4f^{13}5s^{1}5p^{3}$	4f+7(7)7.5s+1(1)8.5p+1(3)11	39.977587
201	$4f^{12}5s^{2}5p^{3}$	4f-5(5)5.4f+7(7)2.5p-1(1)1.5p+2(0)1	40.009869
202	$4f^{13}5s^{1}5p^{3}$	4f+6(0)0.5p-1(1)1.5p+2(0)1	40.143273
203	$4f^{12}5s^{2}5p^{3}$	4f-4(4)4.5p-1(1)3.5p+2(0)3	40.319889
204	$4f^{12}5s^{2}5p^{3}$	4f-5(5)5.4f+7(7)12.5p-1(1)11.5p+2(0)11	40.349004
205	$4f^{14}5s^{1}5p^{2}$	5s+1(1)1.5p-1(1)0.5p+1(3)3	40.558843
206	$4f^{12}5s^{2}5p^{3}$	4f-5(5)5.4f+7(7)4.5p-1(1)5.5p+2(0)5	40.642163
207	$4f^{13}5s^{1}5p^{3}$	4f+7(7)7.5s+1(1)6.5p+1(3)5	40.988890
208	$4f^{13}5s^{1}5p^{3}$	4f+7(7)7.5s+1(1)8.5p+1(3)9	41.140485
209	$4f^{13}5s^{1}5p^{3}$	4f+7(7)7.5s+1(1)6.5p+1(3)7	41.198875
210	$4f^{12}5s^{2}5p^{3}$	4f-5(5)5.4f+7(7)2.5p-1(1)3.5p+2(0)3	41.215262
211	$4f^{13}5s^{1}5p^{3}$	4f+7(7)7.5s+1(1)6.5p+1(3)3	41.408168
212	$4f^{13}5s^{1}5p^{3}$	4f-5(5)5.5s+1(1)4.5p+1(3)1	42.003775
213	$4f^{12}5s^{2}5p^{3}$	4f+6(12)12.5p+3(3)13	43.025335
214	$4f^{12}5s^{2}5p^{3}$	4f+6(12)12.5p+3(3)11	43.297322
215	$4f^{12}5s^{2}5p^{3}$	4f-4(0)0.5p-1(1)1.5p+2(4)3	43.350760
216	$4f^{13}5s^{1}5p^{3}$	4f-5(5)5.5s+1(1)4.5p+1(3)3	43.392389
217	$4f^{12}5s^{2}5p^{3}$	4f+6(12)12.5p+3(3)15	43.406285
218	$4f^{14}5s^{1}5p^{2}$	5s+1(1)1.5p-1(1)2.5p+1(3)5	43.608173
219	$4f^{13}5s^{1}5p^{3}$	4f-5(5)5.5s+1(1)6.5p+1(3)9	43.884680
220	$4f^{12}5s^{2}5p^{3}$	4f+6(8)8.5p+3(3)9	44.013274
221	$4f^{13}5s^{1}5p^{3}$	4f-5(5)5.5s+1(1)4.5p+1(3)5	44.086014
222	$4f^{12}5s^{2}5p^{3}$	4f+6(8)8.5p+3(3)11	44.238316
223	$4f^{13}5s^{1}5p^{3}$	4f-5(5)5.5s+1(1)6.5p+1(3)7	44.238615
224	$4f^{12}5s^{2}5p^{3}$	4f-4(0)0.5p-1(1)1.5p+2(4)5	44.585410
225	$4f^{12}5s^{2}5p^{3}$	4f+6(8)8.5p+3(3)5	45.006992
226	$4f^{12}5s^{2}5p^{3}$	4f-5(5)5.4f+7(7)10.5p+3(3)11	45.017933
227	$4f^{12}5s^{2}5p^{3}$	4f-5(5)5.4f+7(7)10.5p+3(3)9	45.045473
228	$4f^{12}5s^{2}5p^{3}$	4f+6(8)8.5p+3(3)7	45.090392
229	$4f^{12}5s^{2}5p^{3}$	4f-5(5)5.4f+7(7)8.5p+3(3)9	45.574024
230	$4f^{12}5s^{2}5p^{3}$	4f-5(5)5.4f+7(7)10.5p+3(3)13	45.776380
231	$4f^{12}5s^{2}5p^{3}$	4f-5(5)5.4f+7(7)8.5p+3(3)7	45.858203
232	$4f^{12}5s^{2}5p^{3}$	4f-5(5)5.4f+7(7)10.5p+3(3)7	46.339124
233	$4f^{12}5s^{2}5p^{3}$	4f+6(4)4.5p+3(3)1	46.446157
234	$4f^{12}5s^{2}5p^{3}$	4f+6(12)12.5p+3(3)9	46.472647
235	$4f^{12}5s^{2}5p^{3}$	4f-5(5)5.4f+7(7)6.5p+3(3)3	46.568953
236	$4f^{13}5s^{1}5p^{3}$	4f+7(7)7.5s+1(1)8.5p+1(3)5	46.616534
237	$4f^{12}5s^{2}5p^{3}$	4f-5(5)5.4f+7(7)8.5p+3(3)5	46.666498
238	$4f^{13}5s^{1}5p^{3}$	4f+7(7)7.5s+1(1)6.5p+1(3)9	46.718090
239	$4f^{12}5s^{2}5p^{3}$	4f-5(5)5.4f+7(7)6.5p+3(3)5	46.804436
240	$4f^{12}5s^{2}5p^{3}$	4f-5(5)5.4f+7(7)8.5p+3(3)11	46.818182
241	$4f^{12}5s^{2}5p^{3}$	4f+6(4)4.5p+3(3)3	46.867630
242	$4f^{12}5s^{2}5p^{3}$	4f-5(5)5.4f+7(7)6.5p+3(3)9	46.897059
243	$4f^{12}5s^{2}5p^{3}$	4f+6(4)4.5p+3(3)7	47.131872
244	$4f^{12}5s^{2}5p^{3}$	4f-4(8)8.5p+3(3)7	47.498949
245	$4f^{12}5s^{2}5p^{3}$	4f-4(0)0.5p-1(1)1.5p+2(0)1	47.601261
246	$4f^{14}5s^{1}5p^{2}$	5s+1(1)1.5p-1(1)2.5p+1(3)3	47.867842
247	$4f^{13}5s^{1}5p^{3}$	4f+7(7)7.5s+1(1)8.5p+1(3)7	47.963146
248	$4f^{12}5s^{2}5p^{3}$	4f-5(5)5.4f+7(7)6.5p+3(3)7	48.284880
249	$4f^{12}5s^{2}5p^{3}$	4f-4(8)8.5p+3(3)9	48.314230

Table 1. *Cont.*

Level	Configuration	2*J*	Energy (eV)
250	$4f^{12}5s^{2}5p^{3}$	4f-4(8)8.5p+3(3)11	48.357492
251	$4f^{12}5s^{2}5p^{3}$	4f+6(4)4.5p+3(3)5	48.358299
252	$4f^{12}5s^{2}5p^{3}$	4f-4(8)8.5p+3(3)5	48.625980
253	$4f^{12}5s^{2}5p^{3}$	4f-5(5)5.4f+7(7)4.5p+3(3)1	48.890449
254	$4f^{13}5s^{1}5p^{3}$	4f-5(5)5.5s+1(1)6.5p+1(3)3	48.914054
255	$4f^{12}5s^{2}5p^{3}$	4f-5(5)5.4f+7(7)12.5p+3(3)13	49.313778
256	$4f^{13}5s^{1}5p^{3}$	4f-5(5)5.5s+1(1)6.5p+1(3)7	49.571514
257	$4f^{12}5s^{2}5p^{3}$	4f+6(4)4.5p+3(3)3	49.586195
258	$4f^{12}5s^{2}5p^{3}$	4f-5(5)5.4f+7(7)4.5p+3(3)7	49.919408
259	$4f^{12}5s^{2}5p^{3}$	4f-5(5)5.4f+7(7)12.5p+3(3)11	50.371537
260	$4f^{14}5s^{1}5p^{2}$	5s+1(1)1.5p-1(1)2.5p+1(3)1	50.452949
261	$4f^{13}5s^{1}5p^{3}$	4f-5(5)5.5s+1(1)6.5p+1(3)5	50.744707
262	$4f^{12}5s^{2}5p^{3}$	4f-4(4)4.5p+3(3)1	50.746650
263	$4f^{12}5s^{2}5p^{3}$	4f-4(4)4.5p+3(3)3	50.893695
264	$4f^{12}5s^{2}5p^{3}$	4f+6(4)4.5p+3(3)5	50.970529
265	$4f^{13}5s^{1}5p^{3}$	4f+7(7)7.5s+1(1)8.5p-1(1)7.5p+2(4)11	51.131667
266	$4f^{12}5s^{2}5p^{3}$	4f-5(5)5.4f+7(7)12.5p+3(3)15	51.788425
267	$4f^{12}5s^{2}5p^{3}$	4f-4(4)4.5p+3(3)7	51.985278
268	$4f^{12}5s^{2}5p^{3}$	4f-5(5)5.4f+7(7)2.5p+3(3)5	52.093916
269	$4f^{13}5s^{1}5p^{3}$	4f+7(7)7.5s+1(1)8.5p-1(1)7.5p+2(4)9	52.398490
270	$4f^{12}5s^{2}5p^{3}$	4f+6(0)0.5p+3(3)3	52.440969
271	$4f^{13}5s^{1}5p^{3}$	4f+7(7)7.5s+1(1)6.5p-1(1)7.5p+2(4)3	52.516271
272	$4f^{13}5s^{1}5p^{3}$	4f+7(7)7.5s+1(1)6.5p-1(1)7.5p+2(4)7	52.871630
273	$4f^{13}5s^{1}5p^{3}$	4f+7(7)7.5s+1(1)6.5p-1(1)7.5p+2(4)5	52.967365
274	$4f^{13}5s^{1}5p^{3}$	4f-5(5)5.5s+1(1)4.5p-1(1)5.5p+2(4)1	53.136186
275	$4f^{12}5s^{2}5p^{3}$	4f-5(5)5.4f+7(7)12.5p+3(3)9	53.148205
276	$4f^{12}5s^{2}5p^{3}$	4f-5(5)5.4f+7(7)4.5p+3(3)3	53.432744
277	$4f^{12}5s^{2}5p^{3}$	4f-4(4)4.5p+3(3)5	53.482487
278	$4f^{13}5s^{1}5p^{3}$	4f-5(5)5.5s+1(1)4.5p-1(1)5.5p+2(4)3	53.556245
279	$4f^{13}5s^{1}5p^{3}$	4f-5(5)5.5s+1(1)4.5p-1(1)5.5p+2(4)5	54.072377
280	$4f^{12}5s^{2}5p^{3}$	4f-5(5)5.4f+7(7)2.5p+3(3)1	54.212902
281	$4f^{14}5s^{1}5p^{2}$	5s+1(1)1.5p+2(4)5	54.710411
282	$4f^{13}5s^{1}5p^{3}$	4f-5(5)5.5s+1(1)6.5p-1(1)5.5p+2(4)9	54.778699
283	$4f^{13}5s^{1}5p^{3}$	4f+7(7)7.5s+1(1)8.5p-1(1)9.5p+2(4)13	55.063904
284	$4f^{13}5s^{1}5p^{3}$	4f+7(7)7.5s+1(1)8.5p-1(1)9.5p+2(4)11	55.118007
285	$4f^{13}5s^{1}5p^{3}$	4f-5(5)5.5s+1(1)4.5p-1(1)5.5p+2(4)7	55.233560
286	$4f^{13}5s^{1}5p^{3}$	4f+7(7)7.5s+1(1)6.5p-1(1)7.5p+2(4)9	55.423570
287	$4f^{13}5s^{1}5p^{3}$	4f+7(7)7.5s+1(1)6.5p-1(1)7.5p+2(4)7	55.687604
288	$4f^{13}5s^{1}5p^{3}$	4f+7(7)7.5s+1(1)6.5p-1(1)5.5p+2(4)1	56.090306
289	$4f^{13}5s^{1}5p^{3}$	4f+7(7)7.5s+1(1)6.5p-1(1)5.5p+2(4)3	56.104775
290	$4f^{14}5s^{1}5p^{2}$	5s+1(1)1.5p+2(4)5	57.091806
291	$4f^{13}5s^{1}5p^{3}$	4f-5(5)5.5s+1(1)6.5p-1(1)7.5p+2(4)11	57.767247
292	$4f^{13}5s^{1}5p^{3}$	4f-5(5)5.5s+1(1)6.5p-1(1)5.5p+2(4)7	58.051208
293	$4f^{13}5s^{1}5p^{3}$	4f-5(5)5.5s+1(1)4.5p-1(1)3.5p+2(4)3	58.085215
294	$4f^{13}5s^{1}5p^{3}$	4f-5(5)5.5s+1(1)4.5p-1(1)5.5p+2(4)9	58.102775
295	$4f^{13}5s^{1}5p^{3}$	4f-5(5)5.5s+1(1)4.5p-1(1)3.5p+2(4)5	58.108579
296	$4f^{13}5s^{1}5p^{3}$	4f-5(5)5.5s+1(1)4.5p-1(1)3.5p+2(4)1	58.157443
297	$4f^{13}5s^{1}5p^{3}$	4f+7(7)7.5s+1(1)8.5p-1(1)7.5p+2(0)7	58.332193
298	$4f^{13}5s^{2}5p^{1}5d^{1}$	4f+7(7)7.5p-1(1)6.5d-1(3)3	58.415197
299	$4f^{13}5s^{2}5p^{1}5d^{1}$	4f+7(7)7.5p-1(1)8.5d-1(3)9	58.772385
300	$4f^{13}5s^{2}5p^{1}5d^{1}$	4f+7(7)7.5p-1(1)6.5d-1(3)5	58.867240
301	$4f^{13}5s^{2}5p^{1}5d^{1}$	4f+7(7)7.5p-1(1)8.5d-1(3)11	59.062629
302	$4f^{13}5s^{2}5p^{1}5d^{1}$	4f+7(7)7.5p-1(1)6.5d-1(3)7	59.176646
303	$4f^{13}5s^{1}5p^{3}$	4f+7(7)7.5s+1(1)6.5p-1(1)7.5p+2(0)7	59.486179
304	$4f^{12}5s^{2}5p^{3}$	4f-4(0)0.5p+3(3)3	59.792970

A widely used method of accuracy assessment is to match the calculated results with the critically evaluated data compiled by National institute of Standard and Technology (NIST). For Eu-like W, there is only one energy value present in the Atomic Spectra Database (ASD) [9] for the level $4f^{14}5s^{2}5p$ $^{2}P_{1/2,}$ which is 0.10 Rydberg (Ryd) with the uncertainty of 0.18 Ryd., while our calculated result for the same level is 0.105 Ryd. The NIST value was obtained in a very primitive Cowan-code (HFR) calculation made with only a few configurations included. Furthermore, Li et al. [36] reported the calculated value for the energies of the lowest 18 levels for W^{11+}. They have included $4f^{13}5s^{2}5p^{2}$, $4f^{14}5s^{2}5p$, $4f^{12}5s^{2}5p^{3}$, $4f^{13}5s^{2}5p5l$, $4f^{13}5s^{2}5p6l$, $4f^{12}5p^{2}5s^{2}5l$, $4f^{12}5p^{2}5s^{2}6l$, $4f^{14}5s^{2}5l$, and $4f^{14}5s^{2}6l$ configurations, which generate 16,752 levels. The $4f^{14}5s^{2}5p$ $^{2}P_{1/2}$ level does not appear among their list of the lowest 18 levels, while, in our calculation, this is the second level, which is also suggested by Kramida and Shirai [25]. We have performed a calculation by taking the same configurations as Li et al. [37] and found that $4f^{14}5s^{2}5p$ $^{2}P_{1/2}$ is the second level, but they have not reported that. Our level designations for the first three levels are unambiguous, as the dominant eigenvector components constitute 96.3%, 97%, and 95.7%, respectively. For some levels, designations can be ambiguous due to mixing. The basis state given as the label of our calculated level 211 (59%) is mixed with that of level 217 (23%). Level designations of Li et al. [37] differ from our present calculation for some levels. This is because they have not included many important configurations within n = 5. Furthermore, for the $4f^{13}5s^{2}5p^{2}$ $^{2}F^{\circ}_{7/2}$–$^{2}F^{\circ}_{5/2}$ transition, Li et al. [37] reported the transition wavelength calculated using FAC. They have also measured the transition wavelength for the same transition using SH-HtscEBIT, which is 527.60 ± 0.06 nm, while their calculated wavelength is 516.37 nm for the same transition. Our wavelength for this transition calculated using FAC is 472.06 nm.

In Table 2, we present a comparison of wavelengths calculated with FAC with other experimental and theoretical wavelengths [30] for the $(4f^{13}5s^{2}5p^{2})_{5/2}$–$(4f^{13}5s5p^{3})_{3/2,5/2,7/2}$ transitions in Eu-like W, which is also shown in Figure 1. For all transitions, our calculated transition wavelengths agree with the experimental results of Li et al. [30] within 4.7%, while the theoretical results of Li et al. [30] deviate from their experimental results by up to 3.1%. Li et al. [30] also used FAC as in the present calculations, but with a different number of configurations. They have included the $4f^{14}5s^{2}5p$, $4f^{14}5s5p^{2}$, $4f^{14}5s5p5d$, $4f^{13}5s^{2}5p^{2}$, $4f^{13}5s^{2}5p5d$, $4f^{13}5s5p^{3}$, $4f^{13}5s5p^{2}5d$, $4f^{12}5s^{2}5p^{3}$, and $4f^{12}5s^{2}5p^{2}5d$ configurations, which generate 2538 fine structure levels.

Table 2. Comparison of calculated wavelengths (in nm) using FAC with other wavelengths for various transitions in Eu-like W. i and j represent the sequential numbers assigned in Table 1 to the lower and upper levels, respectively.

Transition	i	j	Our Work	Experimental [1]	Other Theory [1]
$\{[(4f^{13})_{5/2}5s]_3(5p^2{}_{1/2}5p_{3/2})_{3/2}\}_{3/2}\rightarrow\{[(4f^{13})_{5/2}5s^2]_{5/2}(5p^2{}_{1/2})_0\}_{5/2}$	2	278	24.349	24.623 ± 0.012	25.084
$\{[(4f^{13})_{5/2}5s]_2(5p^2{}_{1/2}5p_{3/2})_{3/2}\}_{7/2}\rightarrow\{[(4f^{13})_{5/2}5s^2]_{5/2}(5p^2{}_{1/2})_0\}_{5/2}$	2	256	26.416	25.225 ± 0.018	25.746
$\{[(4f^{13})_{5/2}5s]_3(5p^2{}_{1/2}5p_{3/2})_{3/2}\}_{5/2}\rightarrow\{[(4f^{13})_{5/2}5s^2]_{5/2}(5p^2{}_{1/2})_0\}_{5/2}$	2	261	25.772	25.409 ± 0.017	26.198

[1] Reference [30].

Table 3 presents transition data for some strong electric dipole (E1) transitions (transition probability $A > 10^{8}$ s^{-1}), respectively, from the ground state to various levels among the lowest 304 levels. We present a transition wavelength λ (in nm), a weighted oscillator strength gf (dimensionless) (both the length and velocity forms), and a transition rate A_{ji} (s^{-1}) calculated using FAC for Eu-like W. In Figure 2, a comparison of the 'length' and 'velocity' forms of gf (actually, results in the Babushkin and Coulomb gauges) is made for a few of the strongest transitions given in Table 3. One can see that the plot has the usual regular behaviour of increasing scatter with a decreasing line strength. However, for the strongest transitions, although the scatter is small, there is a systematic offset. The velocity form is smaller than the length form by 30%. Thus, all E1 transitions in Table 3 are estimated to have a common uncertainty of 30%.

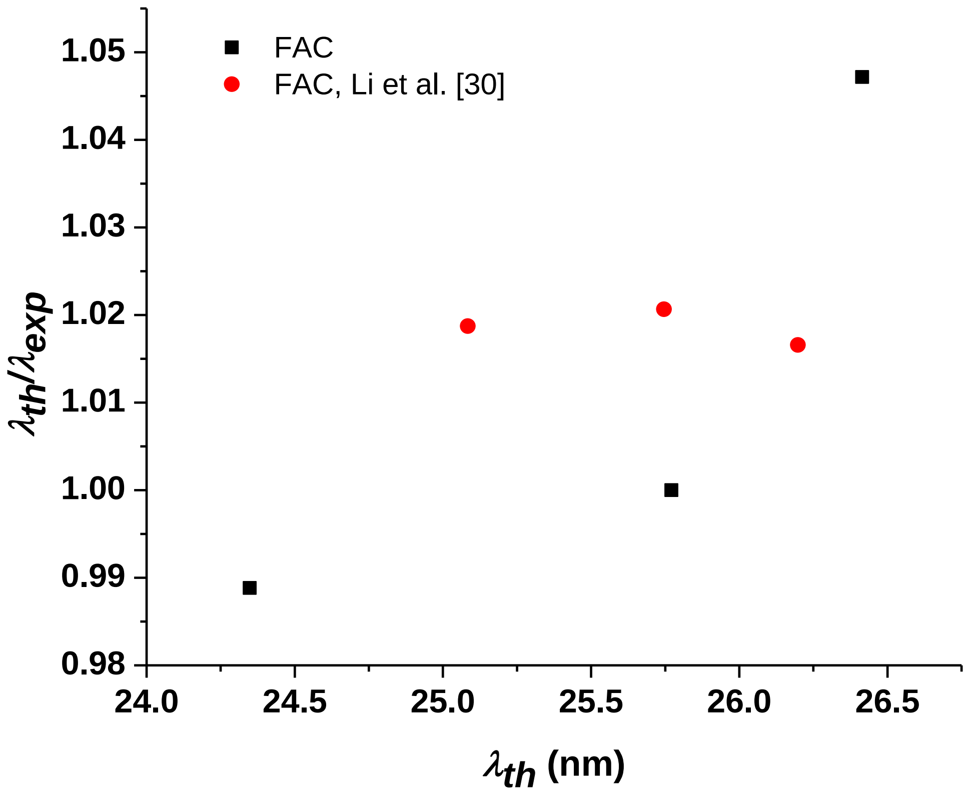

Figure 1. Comparison of theoretical wavelengths with the experimental wavelengths of Reference [30].

Table 3. Oscillator strengths (length and velocity form) gf_L and gf_v, vacuum wavelengths λ (in nm), and transition probabilities A_{ji} (in s^{-1}) for some strong electric dipole (E1) transitions from the ground state to various levels of Eu-like W.

I	j	λ (nm)	gf_L	gf_v	A_{ji}
0	207	30.2482	1.532E-02	1.181E-02	1.861E+08
0	209	30.0941	1.647E-02	1.400E-02	1.516E+08
0	219	28.2523	6.616E-02	6.040E-02	5.529E+08
0	223	28.0262	1.887E-02	1.607E-02	2.003E+08
0	236	26.5966	8.246E-01	6.311E-01	1.296E+10
0	238	26.5388	1.685E+00	1.322E+00	1.596E+10
0	247	25.8499	1.118E+00	8.577E-01	1.395E+10
0	256	25.0112	3.056E-01	2.369E-01	4.073E+09
0	282	22.6337	1.033E-02	1.017E-02	1.345E+08
0	297	21.2548	3.173E-02	4.308E-02	5.857E+08

Tables 4 and 5 present transition data for magnetic dipole (M1) and magnetic quadrupole (M2) transitions from the ground state to some of the lowest 304 levels. We have presented transition wavelength λ (in nm), weighted oscillator strength gf (dimensionless), and transition rate A_{ji} (s^{-1}) calculated using FAC for Eu-like W. We predict new oscillator strength and transition probability data, where no other theoretical or experimental results are available, which will form the basis for future experimental work.

Table 4. Oscillator strengths gf_{ij}, vacuum wavelengths λ (in nm), and transition probabilities A_{ji} (in s^{-1}) for magnetic dipole (M1) transitions from the ground state calculated for Eu-like W.

i	J	λ (nm)	gf_{ij}	$A_{ji}(s^{-1})$
0	2	470.3942	3.751E-06	1.885E+02
0	3	119.1397	1.653E-05	7.768E+03
0	4	109.3488	9.150E-06	8.507E+03
0	6	103.4700	1.244E-05	9.688E+03
0	9	98.4066	2.064E-07	2.369E+02
0	10	96.1341	2.104E-06	1.519E+03
0	11	95.4681	1.038E-06	9.496E+02
0	13	89.1730	2.619E-08	2.746E+01
0	14	87.7895	5.872E-07	8.470E+02
0	16	84.7958	2.574E-09	2.388E+00
0	19	84.0012	4.295E-08	4.060E+01
0	20	82.2056	1.588E-07	1.959E+02
0	21	80.5164	1.239E-07	1.275E+02
0	23	79.9458	3.759E-10	6.538E-01
0	25	78.1530	9.817E-09	1.340E+01
0	28	76.7914	1.085E-08	2.045E+01
0	29	75.5970	1.530E-07	2.232E+02
0	30	73.6928	1.854E-08	3.795E+01
0	31	73.5500	5.146E-08	6.345E+01
0	34	70.8100	8.218E-10	1.367E+00
0	36	69.7334	6.906E-09	9.473E+00
0	37	69.5175	1.369E-08	3.149E+01
0	39	68.6769	3.374E-10	7.953E-01
0	40	68.1151	2.651E-11	4.764E-02
0	41	67.5410	1.421E-09	2.078E+00
0	42	66.6703	2.688E-08	5.042E+01
0	44	63.8355	6.616E-09	1.805E+01
0	45	63.1427	1.790E-08	3.743E+01
0	47	62.0424	2.034E-09	3.525E+00
0	48	61.2594	4.736E-10	1.403E+00
0	50	59.5464	1.348E-09	3.170E+00
0	53	58.1357	1.264E-08	2.495E+01
0	55	55.9250	1.177E-09	4.184E+00
0	59	53.6671	5.867E-10	2.265E+00
0	61	52.8860	1.829E-11	5.452E-02
0	66	48.6902	2.296E-09	6.460E+00
0	75	45.2437	7.166E-10	2.919E+00
0	80	44.2595	2.668E-10	1.514E+00
0	81	44.2545	3.462E-10	1.474E+00
0	83	44.1648	7.762E-09	2.654E+01
0	87	43.8159	6.396E-09	2.778E+01
0	89	43.2959	2.130E-09	9.474E+00
0	90	42.9156	8.688E-10	5.244E+00
0	91	42.7064	6.188E-09	2.263E+01
0	94	42.5506	5.833E-09	2.686E+01
0	95	42.3921	1.434E-11	8.871E-02
0	96	42.0806	5.565E-09	2.096E+01
0	98	41.9130	1.867E-09	8.861E+00
0	102	41.6016	2.435E-09	1.173E+01
0	104	41.4176	8.900E-09	3.461E+01
0	105	41.3380	1.757E-09	6.858E+00
0	106	41.1418	2.075E-09	1.363E+01
0	107	41.0424	4.872E-09	2.412E+01
0	110	40.8286	1.550E-11	1.034E-01
0	112	40.6298	1.542E-09	1.038E+01
0	114	40.4507	2.878E-10	1.173E+00

Table 4. *Cont.*

i	J	λ (nm)	gf_{ij}	$A_{ji}(s^{-1})$
0	116	40.0584	1.399E-10	7.269E-01
0	118	39.8211	3.407E-09	2.389E+01
0	120	39.6115	1.780E-08	7.567E+01
0	124	39.1970	3.920E-09	1.702E+01
0	125	39.1610	7.961E-09	5.771E+01
0	126	39.1237	1.382E-10	7.528E-01
0	128	39.0151	2.709E-09	1.484E+01
0	133	38.6006	6.222E-09	4.642E+01
0	135	38.5379	6.191E-11	3.476E-01
0	139	38.3723	2.555E-09	1.157E+01
0	140	38.2304	6.538E-10	4.973E+00
0	141	38.0327	1.381E-09	7.960E+00
0	142	37.9035	3.474E-09	2.688E+01
0	143	37.8891	2.346E-09	1.090E+01
0	146	37.7958	2.487E-10	1.452E+00
0	147	37.3556	6.913E-09	5.508E+01
0	148	37.2195	5.742E-10	2.765E+00
0	153	36.9644	3.356E-10	2.731E+00
0	155	36.8574	5.074E-10	3.114E+00
0	157	36.7846	1.956E-09	9.642E+00
0	158	36.6062	8.529E-10	4.246E+00
0	164	35.9836	4.992E-11	3.215E-01
0	165	35.9342	1.351E-10	1.163E+00
0	167	35.8530	1.308E-10	8.484E-01
0	168	35.6425	2.604E-10	1.367E+00
0	169	35.5131	1.517E-10	8.025E-01
0	170	35.4919	2.602E-09	2.296E+01
0	173	35.0880	2.364E-09	1.601E+01
0	180	34.6014	1.203E-09	1.117E+01
0	181	34.5466	2.024E-09	1.131E+01
0	182	34.4849	2.403E-09	1.685E+01
0	185	34.0450	1.289E-09	1.236E+01
0	186	33.7953	3.482E-09	2.542E+01
0	187	33.5262	5.150E-09	3.056E+01
0	189	33.3903	2.300E-10	2.293E+00
0	191	33.2815	1.441E-08	1.085E+02
0	192	33.1027	1.192E-10	1.209E+00
0	193	32.9653	2.964E-11	2.274E-01
0	195	32.7897	7.813E-10	4.847E+00
0	196	32.3338	4.930E-10	3.932E+00
0	198	31.9168	1.226E-10	1.338E+00
0	206	30.5063	1.277E-10	1.525E+00
0	225	27.5478	7.954E-11	1.165E+00
0	231	27.0364	5.195E-11	5.926E-01
0	232	26.7558	1.034E-10	1.204E+00
0	234	26.6790	5.105E-11	4.784E-01
0	237	26.5681	9.262E-12	1.459E-01
0	239	26.4898	3.333E-11	5.280E-01
0	242	26.4375	3.896E-11	3.718E-01
0	243	26.3058	7.933E-11	9.558E-01
0	248	25.6776	8.008E-11	1.013E+00
0	249	25.6620	2.285E-11	2.314E-01
0	251	25.6387	1.583E-11	2.677E-01
0	258	24.8369	2.726E-11	3.685E-01
0	267	23.8499	9.560E-11	1.401E+00
0	268	23.8001	2.857E-11	5.607E-01
0	275	23.3280	1.146E-10	1.405E+00

Table 5. Oscillator strengths gf_{ij}, vacuum wavelengths λ (in nm), and transition probabilities A_{ji} (in s^{-1}) for magnetic quadrupole (M2) transitions from the ground state in Eu-like W.

i	j	λ (nm)	gf_{ij}	A_{ji} (s^{-1})
0	200	31.0134	4.147E-09	2.397E+01
0	205	30.5690	3.013E-10	5.377E+00
0	207	30.2482	1.820E-09	2.211E+01
0	208	30.1368	3.279E-09	2.408E+01
0	209	30.0941	2.665E-09	2.454E+01
0	211	29.9420	8.454E-10	1.572E+01
0	216	28.5728	5.206E-10	1.063E+01
0	218	28.4314	6.824E-11	9.385E-01
0	219	28.2523	3.457E-10	2.889E+00
0	221	28.1233	4.822E-10	6.778E+00
0	223	28.0262	3.373E-10	3.580E+00
0	236	26.5966	5.529E-12	8.689E-02
0	238	26.5388	2.201E-13	2.084E-03
0	246	25.9014	6.804E-11	1.691E+00
0	247	25.8499	1.913E-11	2.387E-01
0	254	25.3474	7.382E-12	1.916E-01
0	256	25.0112	8.935E-12	1.191E-01
0	261	24.4329	6.642E-13	1.237E-02
0	265	24.2480	1.490E-09	1.409E+01
0	269	23.6618	1.444E-09	1.720E+01
0	271	23.6087	5.501E-10	1.646E+01
0	272	23.4500	9.282E-10	1.407E+01
0	273	23.4077	7.612E-10	1.544E+01
0	278	23.1503	9.312E-12	2.897E-01
0	279	22.9293	4.199E-11	8.879E-01
0	281	22.6619	5.448E-11	1.179E+00
0	284	22.4943	1.238E-11	1.360E-01
0	285	22.4473	1.773E-10	2.934E+00
0	286	22.3703	1.152E-11	1.536E-01
0	287	22.2642	4.283E-11	7.204E-01
0	289	22.0987	5.163E-13	1.763E-02
0	290	21.7166	5.489E-12	1.294E-01
0	291	21.4627	6.646E-12	8.020E-02
0	292	21.3577	4.977E-12	9.097E-02
0	294	21.3388	1.916E-12	2.807E-02
0	295	21.3366	2.720E-12	6.642E-02
0	297	21.2549	7.816E-11	1.443E+00
0	298	21.2246	3.513E-11	1.300E+00
0	299	21.0957	3.285E-11	4.924E-01
0	300	21.0617	4.574E-12	1.146E-01
0	301	20.9920	2.376E-11	2.997E-01
0	302	20.9515	1.754E-11	3.332E-01
0	303	20.8425	3.451E-12	6.624E-02

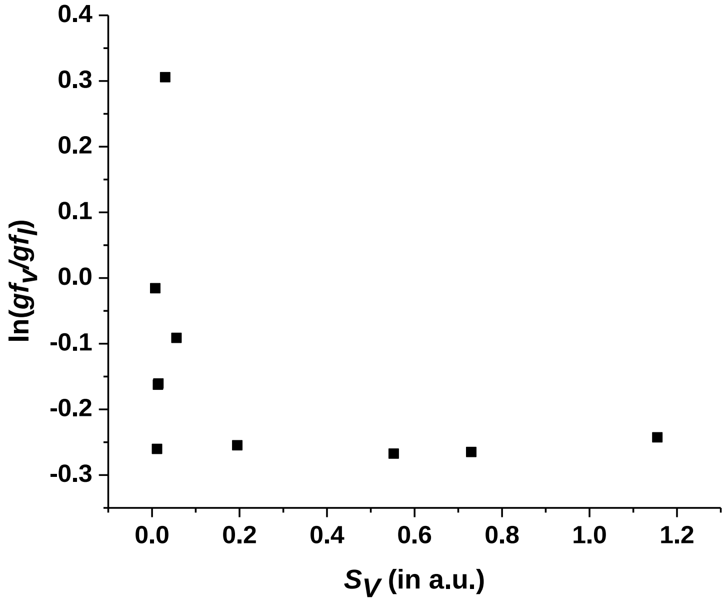

Figure 2. A comparison of the length and velocity forms of oscillator strengths for a few of the strongest transitions of W^{11+}.

In Table 6, we provide collisional excitation cross-sections of Eu-like W from the ground state for the incident electron energy range of 65 to 125 eV. To the best of our knowledge, there are no other data points for collisional cross sections of Eu-like W in the literature within the given energy range.

4.2. Pm-Like W

Realizing the importance of Pm-like W and considering the paucity of atomic data for this ion, in the present work, we have calculated energy levels and radiative transition rates using FAC. To check the convergence of results, we have calculated results with different sets of configurations. Table 7 shows the configurations used in various calculations and the number of levels generated using these configurations. In the present work, we have increased the number of configurations in the sets in a systematic way to study the CI effect. In INP1, we have included $4f^{14}5s$, $4f^{13}5s^2$, $4f^{13}5s5p$, $4f^{14}5p$, and $4f^{13}5p^2$ configurations, which generate 59 fine structure levels. In INP2, we have added the $4f^{12}5s^25p$, $4f^{12}5s5p^2$, and $4f^{12}5p^3$ configurations. These three configurations generate 621 levels. Furthermore, in order to check the effect on energies, INP3 forms a complex system by adding $4f^{11}5s^25p^2$, $4f^{11}5s5p^3$, $4f^{10}5s^25p^3$, and $4f^{10}5s5p^4$ to INP2, which generates a total of 7790 fine structure levels. We observe that the energies of these additional configurations are distributed inside the interval between the $4f^{14}5s$ and $4f^{145}p$ energies, which shows the importance of adding these configurations. Finally, in the INPF column of Table 7, we have considered a larger CI for Pm-like W, which includes $4f^{14}5s$, $4f^{13}5s^2$, $4f^{13}5s5p$, $4f^{14}5p$, $4f^{13}5p^2$, $4f^{12}5s^25p$, $4f^{12}5s5p^2$, $4f^{12}5p^3$, $4f^{11}5s^25p^2$, $4f^{11}5s5p^3$, $4f^{10}5s^25p^3$, $4f^{10}5s5p^4$, $4f^{12}5s^25d$, $4f^{12}5s5d^2$, $4f^{13}5d^2$, $4f^{13}5p5d$, $4f^{13}5d^2$, $4f^{13}5p5d$, $4f^{12}5p5d^2$, $4f^{12}5p^25d$, and $4f^{13}5s5d$ configurations. This set generates 13,160 levels. Table 8 shows the list of configurations included and the number of fine structure levels arising from each configuration of Pm-like W. The ground state configuration in each case is the same. Table 9 lists the energy values from each input for the $4f^{13}5s5p$ configuration. To check convergence, the difference between various output levels (Out1, Out2, Out3) and OutF is plotted in Figure 3. The different colors correspond to the different levels of Table 9. For levels 19 to 24, the difference is very large. Although the differences do not tend to zero with an increasing size of the calculation, the level splitting is almost the same in each output using different configuration sets for the first 18 levels, as shown in Figure 4. The root-mean-square (rms) difference from OUTF for the intervals ΔE_j is 0.16 eV for OUT1, 0.10 eV for OUT2, and 0.08 eV for OUT3.

Table 6. Collisional excitation cross-sections (100 Mb) of Eu-like W from the ground state to various levels.

Energy (eV) /Transition	0–3	0–4	0–5	Energy (eV) /Transition	0–1	Energy (eV) /Transition	0–2	Energy (eV) /Transition	0–29
4.47E-01	2.63E+02	1.07E+02	1.79E+02	1.61E-01	3.14E+02	1.11E-01	2.73E+03	6.30E-01	8.61E+00
1.42E+01	1.03E+02	4.29E+01	8.40E+01	6.82E+00	8.81E+01	5.37E+00	9.22E+02	1.74E+01	4.29E+00
4.80E+01	3.40E+01	1.34E+01	3.68E+01	2.65E+01	2.55E+01	2.24E+01	2.79E+02	5.51E+01	1.98E+00
1.31E+02	9.42E+00	3.14E+00	1.61E+01	8.48E+01	6.25E+00	7.77E+01	7.50E+01	1.40E+02	8.90E-01
3.30E+02	2.60E+00	5.62E-01	7.06E+00	2.55E+02	1.08E+00	2.54E+02	1.49E+01	3.28E+02	4.06E-01
7.95E+02	8.12E-01	7.11E-02	3.01E+00	7.34E+02	2.30E-01	7.95E+02	1.60E+00	7.34E+02	1.83E-01

Energy (eV) /Transition	0–6	0–7	0–8	0–9	0–10	0–11	0–13	0–14	0–16
8.77E-01	1.65E+02	4.82E+01	7.03E+02	2.79E+02	1.39E+02	3.13E+02	8.94E+00	9.00E+00	2.89E+01
2.22E+01	5.29E+01	1.85E+01	2.70E+02	1.08E+02	4.93E+01	1.23E+02	3.93E+00	3.03E+00	1.21E+01
6.79E+01	1.78E+01	8.14E+00	1.18E+02	4.74E+01	1.80E+01	5.50E+01	2.12E+00	9.23E-01	5.35E+00
1.66E+02	6.34E+00	3.86E+00	5.57E+01	2.23E+01	6.60E+00	2.67E+01	1.30E+00	2.44E-01	2.47E+00
3.72E+02	2.59E+00	1.87E+00	2.69E+01	1.08E+01	2.63E+00	1.34E+01	7.94E-01	5.98E-02	1.18E+00
7.95E+02	1.22E+00	8.94E-01	1.28E+01	5.10E+00	1.12E+00	6.67E+00	4.56E-01	1.47E-02	5.62E-01

Energy (eV) /Transition	0–18	0–22	0–24	Energy (eV) /Transition	0–12	0–15	0–17	0–19	0–20
8.77E-01	1.27E+00	6.97E+01	8.56E+00	6.08E-01	7.78E+01	3.22E+02	5.48E+01	5.88E+01	3.03E+01
2.22E+01	4.80E-01	3.06E+01	3.56E+00	2.14E+01	2.64E+01	1.35E+02	2.01E+01	2.25E+01	1.29E+01
6.79E+01	1.73E-01	1.40E+01	1.48E+00	7.59E+01	6.78E+00	5.42E+01	5.67E+00	6.98E+00	5.09E+00
1.66E+02	5.76E-02	6.64E+00	6.19E-01	2.17E+02	1.06E+00	2.19E+01	1.15E+00	1.78E+00	2.07E+00
3.72E+02	1.95E-02	3.21E+00	2.71E-01	5.74E+02	1.37E-01	8.93E+00	2.86E-01	5.32E-01	9.19E-01
7.95E+02	7.33E-03	1.54E+00	1.21E-01	1.43E+03	2.02E-02	3.60E+00	1.06E-01	1.93E-01	3.78E-01

Energy (eV) /Transition	0–21	0–23	0–25	0–26	0–27	Energy (eV) /Transition	0–28	0–30	0–31
6.08E-01	5.35E+02	9.02E+01	5.04E+02	2.71E+01	7.70E+01	1.22E+00	7.15E+01	6.76E+01	2.60E+02
2.14E+01	2.39E+02	3.80E+01	2.41E+02	1.08E+01	3.43E+01	3.42E+01	2.51E+01	2.38E+01	9.53E+01
7.59E+01	1.02E+02	1.44E+01	1.19E+02	3.54E+00	1.41E+01	1.09E+02	1.04E+01	9.56E+00	4.08E+01
2.17E+02	4.34E+01	5.40E+00	6.74E+01	1.11E+00	5.69E+00	2.78E+02	4.95E+00	4.14E+00	1.88E+01
5.74E+02	1.81E+01	2.15E+00	3.88E+01	4.41E-01	2.32E+00	6.50E+02	2.52E+00	1.86E+00	8.68E+00
1.43E+03	7.33E+00	8.78E-01	1.71E+01	1.99E-01	9.37E-01	1.43E+03	1.22E+00	8.44E-01	4.00E+00

Table 6. *Cont.*

Energy (eV) /Transition	0–28	0–30	0–31	0–32	0–33	0–34	0–35	0–36	0–37
1.22E+00	7.15E+01	6.76E+01	2.60E+02	6.66E+01	7.88E+01	8.88E+01	2.09E+01	4.37E+01	1.34E+02
3.42E+01	2.51E+01	2.38E+01	9.53E+01	2.34E+01	2.94E+01	3.23E+01	6.37E+00	1.53E+01	5.09E+01
1.09E+02	1.04E+01	9.56E+00	4.08E+01	9.30E+00	1.26E+01	1.34E+01	1.94E+00	5.94E+00	2.21E+01
2.78E+02	4.95E+00	4.14E+00	1.88E+01	4.05E+00	5.73E+00	6.11E+00	6.65E-01	2.52E+00	1.02E+01
6.50E+02	2.52E+00	1.86E+00	8.68E+00	1.84E+00	2.62E+00	2.88E+00	2.94E-01	1.14E+00	4.74E+00
1.43E+03	1.22E+00	8.44E-01	4.00E+00	8.46E-01	1.20E+00	1.35E+00	1.46E-01	5.23E-01	2.18E+00

Energy (eV) /Transition	0–38	0–39	0–40	0–41	0–42	0–43	0–44	0–45	0–46
1.22E+00	4.06E+00	3.24E+01	4.00E+01	2.40E+01	4.00E+01	2.37E+01	7.58E+00	2.61E+00	2.05E+00
3.42E+01	1.17E+00	1.17E+01	1.59E+01	8.06E+00	1.58E+01	9.02E+00	2.33E+00	9.78E-01	7.32E-01
1.09E+02	2.81E-01	4.61E+00	7.79E+00	2.85E+00	7.52E+00	3.76E+00	5.88E-01	4.14E-01	2.70E-01
2.78E+02	4.71E-02	1.98E+00	4.75E+00	1.12E+00	4.40E+00	1.68E+00	1.05E-01	2.24E-01	1.08E-01
6.50E+02	8.72E-03	8.87E-01	2.98E+00	5.00E-01	2.70E+00	7.70E-01	2.10E-02	1.42E-01	4.79E-02
1.43E+03	2.32E-03	4.05E-01	1.61E+00	2.36E-01	1.44E+00	3.54E-01	5.58E-03	7.83E-02	2.21E-02

Energy (eV) /Transition	0–47	0–48	0–49	0–50
1.22E+00	1.27E+01	9.06E+00	2.66E+01	1.08E+01
3.42E+01	4.46E+00	3.00E+00	8.92E+00	3.48E+00
1.09E+02	1.51E+00	9.06E-01	2.87E+00	9.59E-01
2.78E+02	5.11E-01	2.70E-01	1.02E+00	2.37E-01
6.50E+02	2.04E-01	1.03E-01	4.61E-01	7.70E-02
1.43E+03	8.86E-02	4.63E-02	2.30E-01	3.09E-02

Table 7. Configurations included in the different inputs with the number of fine structure levels for Pm-like W.

	INP1	INP2	INP3	INPF
Configuration	$4f^{14}5s$, $4f^{13}5s^2$, $4f^{13}5s5p$, $4f^{14}5p$, $4f^{13}5p^2$	$4f^{14}5s$, $4f^{13}5s^2$, $4f^{13}5s5p$, $4f^{14}5p$, $4f^{13}5p^2$, $4f^{12}5s^25p$, $4f^{12}5s5p^2$, $4f^{12}5p^3$	$4f^{14}5s$, $4f^{13}5s^2$, $4f^{13}5s5p$, $4f^{14}5p$, $4f^{13}5p^2$, $4f^{12}5s^25p$, $4f^{12}5s5p^2$, $4f^{12}5p^3$, $4f^{11}5s^25p^2$, $4f^{11}5s5p^3$, $4f^{10}5s^25p^3$, $4f^{10}5s5p^4$	$4f^{14}5s$, $4f^{13}5s^2$, $4f^{13}5s5p$, $4f^{14}5p$, $4f^{13}5p^2$, $4f^{12}5s^25p$, $4f^{12}5s5p^2$, $4f^{12}5p^3$, $4f^{11}5s^25p^2$, $4f^{11}5s5p^3$, $4f^{10}5s^25p^3$, $4f^{10}5s5p^4$, $4f^{12}5s^25d$, $4f^{12}5s5d^2$, $4f^{13}5d^2$, $4f^{13}5p5d$, $4f^{13}5d^2$, $4f^{13}5p5d$, $4f^{12}5p5d^2$, $4f^{12}5p^25d$, $4f^{13}5s5d$
Levels	59	680	7790	13,160
Ground state	$4f^{13}5s^2\ {}^2F_{7/2}$	$4f^{13}5s^2\ {}^2F_{7/2}$	$4f^{13}5s^2\ {}^2F_{7/2}$	$4f^{13}5s^2\ {}^2F_{7/2}$

Table 8. List of configurations included and the number of fine-structure levels arising from each configuration of Pm-like W.

Configuration	Total
$4f^{14}5s^1$	1
$4f^{13}5s^2$	2
$4f^{13}5s^1\ 5p^1$	24
$4f^{14}5p^1$	2
$4f^{13}5p^2$	36
$4f^{12}5s^25p^1$	69
$4f^{12}5s^15p^2$	335
$4f^{12}5p^3$	231
$4f^{11}5s^25p^2$	594
$4f^{11}5s^15p^3$	1542
$4f^{10}5s^25p^3$	1971
$4f^{10}5s^15p^4$	2947
$4f^{12}5s^25d^1$	139
$4f^{12}5s^15d^2$	910
$4f^{13}5d^2$	82
$4f^{13}5p^15d^1$	121
$4f^{12}5p^15d^2$	2617
$4f^{12}5p^25d^1$	1499
$4f^{13}5s^15d^1$	38

Table 9. Energy values (in eV) from each input for the $4f^{13}5s5p$ configuration of Pm-like W.

S. No.	Level Index	2*J*	out1	out2	out3	outF
1	69	4f+7(7)7.5s+1(1)8.5p-1(1)7	28.34084	28.23032	28.33804	28.05699
2	85	4f+7(7)7.5s+1(1)6.5p-1(1)7	30.49845	30.39207	30.49463	30.07793
3	89	4f-5(5)5.5s+1(1)4.5p-1(1)5	30.51904	30.42783	30.53146	30.24463
4	91	4f+7(7)7.5s+1(1)8.5p-1(1)9	30.93588	30.81385	30.91735	30.53786
5	94	4f+7(7)7.5s+1(1)6.5p-1(1)5	31.59384	31.48818	31.59510	31.22191
6	108	4f-5(5)5.5s+1(1)6.5p-1(1)5	33.51591	33.39925	33.48623	33.07156
7	110	4f-5(5)5.5s+1(1)6.5p-1(1)7	33.59234	33.50230	33.60730	33.22125
8	114	4f-5(5)5.5s+1(1)4.5p-1(1)3	33.94001	33.79424	33.89133	33.52918
9	222	4f+7(7)7.5s+1(1)8.5p+1(3)11	42.28670	42.17790	42.21274	41.88907
10	250	4f+7(7)7.5s+1(1)6.5p+1(3)3	43.33967	43.16711	43.21708	42.84671

Table 9. *Cont.*

S. No.	Level Index	2*J*	out1	out2	out3	outF
11	263	4f+7(7)7.5s+1(1)6.5p+1(3)5	43.69655	43.48007	43.54132	43.20679
12	266	4f-5(5)5.5s+1(1)4.5p+1(3)1	43.73023	43.55966	43.63034	43.25833
13	277	4f+7(7)7.5s+1(1)6.5p+1(3)7	44.14760	43.88220	43.94818	43.64971
14	279	4f+7(7)7.5s+1(1)8.5p+1(3)9	44.15898	43.88693	43.95022	43.67102
15	317	4f-5(5)5.5s+1(1)4.5p+1(3)3	45.52535	45.30258	45.36262	45.02438
16	326	4f-5(5)5.5s+1(1)6.5p+1(3)9	45.65222	45.44028	45.52273	45.17111
17	351	4f-5(5)5.5s+1(1)4.5p+1(3)5	46.47208	46.22915	46.29386	45.99735
18	357	4f-5(5)5.5s+1(1)6.5p+1(3)7	46.61544	46.37682	46.44845	46.14563
19	433	4f+7(7)7.5s+1(1)8.5p+1(3)5	51.21205	50.85405	50.89800	49.88168
20	434	4f+7(7)7.5s+1(1)6.5p+1(3)9	51.31237	50.99615	51.05140	49.98717
21	451	4f+7(7)7.5s+1(1)8.5p+1(3)7	52.80963	52.14431	52.20551	51.07045
22	460	4f-5(5)5.5s+1(1)6.5p+1(3)3	53.12149	52.74996	52.80752	51.79452
23	475	4f-5(5)5.5s+1(1)4.5p+1(3)7	53.89587	53.42507	53.48859	52.41451
24	493	4f-5(5)5.5s+1(1)6.5p+1(3)5	55.31426	54.63896	54.70557	53.48189

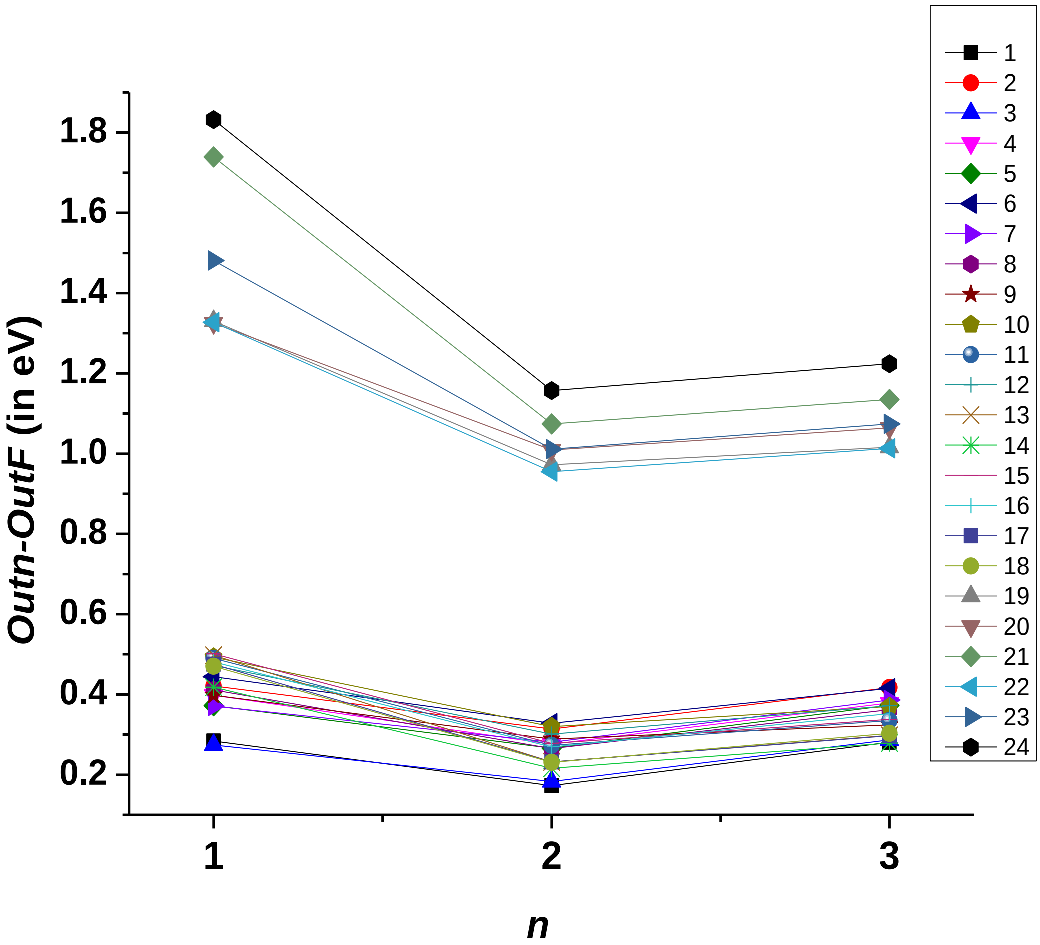

Figure 3. Difference of energy values of each output OUT*n* (*n* = 1, 2, 3) from the final calculation for the $4f^{13}5s5p$ configuration.

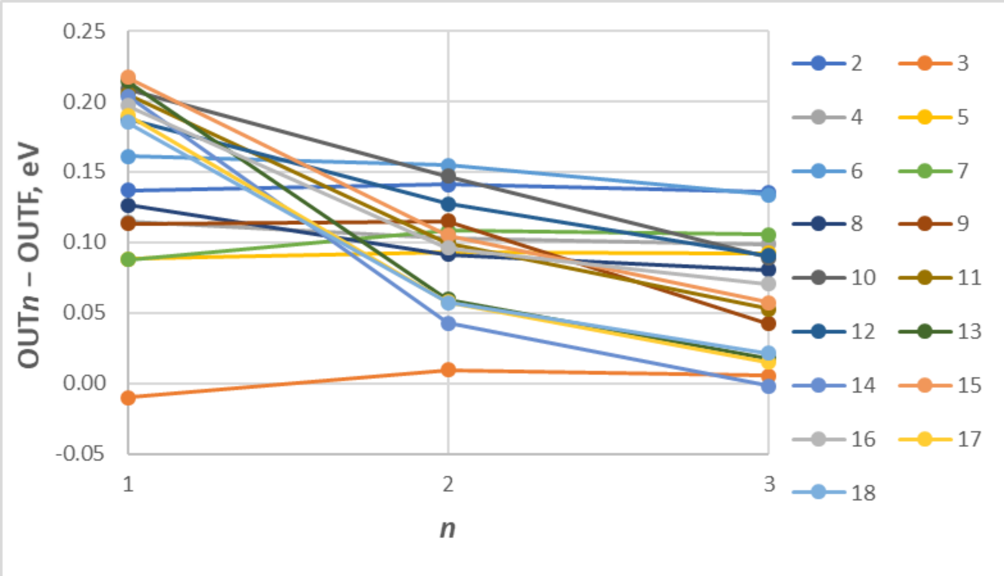

Figure 4. Differences of energy intervals relative to the lowest level (with index 1) for each output OUTn (n = 1, 2, 3) from the final calculation for the 4f135s5p configuration.

Table 10 presents the energy levels (in Rydberg) for the lowest 500 levels calculated with FAC for Pm-like W. As can be seen from this table, we report results for many new levels that are not listed in the NIST tables [9]. The format of Table 10 is the same as in Table 1. Since 85 levels out of 500 of Table 8 have the same '2*J*' label as some other levels, we report the eigenvector compositions and mixing coefficients of W^{13+} in Table S2 of the supplementary material. In this table, we report the composition of the levels given in Table 10. In the column, the 'Comp. No.' of Table S2 contains sequential numbers of the basis states in decreasing order of contribution. We have included only a few basis states with the largest contributions. For each basis state, Table S2 gives an electronic configuration in the *JJ* coupling scheme. In these designations, '4f13' represents that there are 13 electrons in the 4f subshell. In '4f+7(7)7,' the '+' sign denotes the larger of the two possible values of the angular momentum for the f electron, i.e., '4f+' corresponds to 4f7/2. '7' after the '+' sign shows the number of electrons in the relativistic subshell 4f7/2, '(7),' which means that the total 2*J* value of the 4f7/2 subshell is 7, and '7' at the end denotes the final 2*J* value of the configuration.

Table 10. Energy levels (in eV) for the lowest 500 levels calculated with FAC using INPF configurations for Pm-like W.

Level No.	Configuration	2*J*	FAC
0	$4f^{13}5s^2$	4f+7(7)7	0.000000
1	$4f^{13}5s^2$	4f-5(5)5	2.255395
2	$4f^{12}5s^25p^1$	4f+6(12)12.5p-1(1)11	7.276828
3	$4f^{12}5s^25p^1$	4f+6(12)12.5p-1(1)13	8.000018
4	$4f^{12}5s^25p^1$	4f+6(8)8.5p-1(1)7	8.504221
5	$4f^{12}5s^25p^1$	4f+6(8)8.5p-1(1)9	8.898153
6	$4f^{12}5s^25p^1$	4f-5(5)5.4f+7(7)10.5p-1(1)11	9.837877
7	$4f^{12}5s^25p^1$	4f-5(5)5.4f+7(7)10.5p-1(1)9	9.857320
8	$4f^{12}5s^25p^1$	4f-5(5)5.4f+7(7)8.5p-1(1)7	10.537519
9	$4f^{12}5s^25p^1$	4f-5(5)5.4f+7(7)6.5p-1(1)5	10.821138
10	$4f^{12}5s^25p^1$	4f+6(4)4.5p-1(1)3	10.938403
11	$4f^{12}5s^25p^1$	4f-5(5)5.4f+7(7)8.5p-1(1)9	11.036302
12	$4f^{12}5s^25p^1$	4f-5(5)5.4f+7(7)6.5p-1(1)5	11.306358

Table 10. *Cont.*

Level No.	Configuration	2J	FAC
13	$4f^{12}5s^25p^1$	4f-5(5)5.4f+7(7)6.5p-1(1)7	11.775166
14	$4f^{12}5s^25p^1$	4f-4(8)8.5p-1(1)9	12.546322
15	$4f^{12}5s^25p^1$	4f-5(5)5.4f+7(7)4.5p-1(1)3	13.724712
16	$4f^{12}5s^25p^1$	4f-4(8)8.5p-1(1)7	13.755493
17	$4f^{12}5s^25p^1$	4f-4(4)4.5p-1(1)5	13.957189
18	$4f^{12}5s^25p^1$	4f-5(5)5.4f+7(7)12.5p-1(1)13	14.902679
19	$4f^{12}5s^25p^1$	4f-5(5)5.4f+7(7)2.5p-1(1)1	15.077341
20	$4f^{12}5s^25p^1$	4f+6(0)0.5p-1(1)1	15.148716
21	$4f^{12}5s^25p^1$	4f-5(5)5.4f+7(7)12.5p-1(1)11	15.246453
22	$4f^{12}5s^25p^1$	4f-5(5)5.4f+7(7)2.5p-1(1)3	16.064828
23	$4f^{12}5s^25p^1$	4f-4(4)4.5p-1(1)5	16.335222
24	$4f^{12}5s^25p^1$	4f-4(4)4.5p-1(1)3	16.845319
25	$4f^{11}5s^25p^2$	4f+5(15)15	20.958997
26	$4f^{12}5s^25p^1$	4f+6(12)12.5p+1(3)15	21.711928
27	$4f^{12}5s^25p^1$	4f+6(12)12.5p+1(3)11	22.687480
28	$4f^{12}5s^25p^1$	4f+6(12)12.5p+1(3)9	22.793061
29	$4f^{11}5s^25p^2$	4f-5(5)5.4f+6(12)13	23.259954
30	$4f^{12}5s^25p^1$	4f-4(0)0.5p-1(1)1	23.263519
31	$4f^{12}5s^25p^1$	4f+6(12)12.5p+1(3)13	23.414228
32	$4f^{12}5s^25p^1$	4f+6(8)8.5p+1(3)9	23.475916
33	$4f^{12}5s^25p^1$	4f-5(5)5.4f+7(7)10.5p+1(3)7	23.595130
34	$4f^{11}5s^25p^2$	4f+5(9)9	23.615822
35	$4f^{11}5s^25p^2$	4f+5(11)11	23.666002
36	$4f^{12}5s^25p^1$	4f+6(8)8.5p+1(3)5	23.951175
37	$4f^{12}5s^25p^1$	4f+6(8)8.5p+1(3)11	24.192841
38	$4f^{12}5s^25p^1$	4f-5(5)5.4f+7(7)10.5p+1(3)13	24.205246
39	$4f^{12}5s^25p^1$	4f+6(8)8.5p+1(3)7	24.241919
40	$4f^{11}5s^25p^2$	4f+5(3)3	24.903151
41	$4f^{12}5s^25p^1$	4f-5(5)5.4f+7(7)10.5p+1(3)9	25.000189
42	$4f^{12}5s^25p^1$	4f+6(8)8.5p+1(3)5	25.137622
43	$4f^{14}5s^1$	5s+1(1)1	25.146356
44	$4f^{11}5s^25p^2$	4f-5(5)5.4f+6(8)9	25.192432
45	$4f^{12}5s^25p^1$	4f-5(5)5.4f+7(7)8.5p+1(3)11	25.518823
46	$4f^{12}5s^25p^1$	4f-5(5)5.4f+7(7)6.5p+1(3)5	25.571768
47	$4f^{12}5s^25p^1$	4f-5(5)5.4f+7(7)10.5p+1(3)11	25.685382
48	$4f^{11}5s^25p^2$	4f-4(8)8.4f+7(7)11	25.733561
49	$4f^{12}5s^25p^1$	4f+6(4)4.5p+1(3)3	25.861534
50	$4f^{12}5s^25p^1$	4f-5(5)5.4f+7(7)8.5p+1(3)7	25.914135
51	$4f^{12}5s^25p^1$	4f-5(5)5.4f+7(7)6.5p+1(3)7	26.087574
52	$4f^{12}5s^25p^1$	4f-5(5)5.4f+7(7)8.5p+1(3)9	26.100478
53	$4f^{11}5s^25p^2$	4f-5(5)5.4f+6(8)7	26.203062
54	$4f^{11}5s^25p^2$	4f+5(5)5	26.274573
55	$4f^{12}5s^25p^1$	4f+6(4)4.5p+1(3)5	26.376467
56	$4f^{11}5s^25p^2$	4f-5(5)5.4f+6(8)3	26.602434
57	$4f^{12}5s^25p^1$	4f-5(5)5.4f+7(7)4.5p+1(3)1	26.748723
58	$4f^{12}5s^25p^1$	4f-5(5)5.4f+7(7)6.5p+1(3)9	26.773530
59	$4f^{12}5s^25p^1$	4f+6(4)4.5p+1(3)7	26.925455
60	$4f^{12}5s^25p^1$	4f-5(5)5.4f+7(7)6.5p+1(3)3	27.023513
61	$4f^{11}5s^25p^2$	4f-5(5)5.4f+6(12)15	27.192388
62	$4f^{11}5s^25p^2$	4f-5(5)5.4f+6(12)9	27.238668
63	$4f^{12}5s^25p^1$	4f-5(5)5.4f+7(7)8.5p+1(3)5	27.250690
64	$4f^{11}5s^25p^2$	4f+5(7)7	27.363071
65	$4f^{12}5s^25p^1$	4f-4(8)8.5p+1(3)11	27.516542
66	$4f^{12}5s^25p^1$	4f-4(8)8.5p+1(3)7	27.543276

Table 10. *Cont.*

Level No.	Configuration	*2J*	FAC
67	$4f^{11}5s^25p^2$	4f-5(5)5.4f+6(12)11	27.655306
68	$4f^{12}5s^25p^1$	4f-4(8)8.5p+1(3)9	27.786327
69	$4f^{13}5s^15p^1$	4f+7(7)7.5s+1(1)8.5p-1(1)7	28.056993
70	$4f^{11}5s^25p^2$	4f-4(8)8.4f+7(7)9	28.081706
71	$4f^{12}5s^25p^1$	4f-5(5)5.4f+7(7)4.5p+1(3)5	28.492190
72	$4f^{11}5s^25p^2$	4f-5(5)5.4f+6(8)13	28.766415
73	$4f^{11}5s^25p^2$	4f-5(5)5.4f+6(4)1	28.772590
74	$4f^{12}5s^25p^1$	4f-5(5)5.4f+7(7)12.5p+1(3)15	28.841463
75	$4f^{11}5s^25p^2$	4f+5(5)5	28.862296
76	$4f^{11}5s^25p^2$	4f-4(4)4.4f+7(7)3	28.863668
77	$4f^{11}5s^25p^2$	4f-5(5)5.4f+6(4)5	29.139885
78	$4f^{12}5s^25p^1$	4f-4(4)4.5p+1(3)3	29.272728
79	$4f^{12}5s^25p^1$	4f-5(5)5.4f+7(7)12.5p+1(3)9	29.390448
80	$4f^{12}5s^25p^1$	4f+6(4)4.5p+1(3)7	29.431457
81	$4f^{12}5s^25p^1$	4f+6(4)4.5p+1(3)1	29.536806
82	$4f^{11}5s^25p^2$	4f-4(8)8.4f+7(7)7	29.698561
83	$4f^{11}5s^25p^2$	4f-4(8)8.4f+7(7)7	29.938896
84	$4f^{11}5s^25p^2$	4f-5(5)5.4f+6(8)11	29.992013
85	$4f^{13}5s^15p^1$	4f+7(7)7.5s+1(1)6.5p-1(1)7	30.077928
86	$4f^{11}5s^25p^2$	4f-5(5)5.4f+6(12)17	30.107356
87	$4f^{11}5s^25p^2$	4f-4(8)8.4f+7(7)5	30.194314
88	$4f^{12}5s^25p^1$	4f+6(0)0.5p+1(3)3	30.244202
89	$4f^{13}5s^15p^1$	4f-5(5)5.5s+1(1)4.5p-1(1)5	30.244635
90	$4f^{12}5s^25p^1$	4f-4(4)4.5p+1(3)5	30.530323
91	$4f^{13}5s^15p^1$	4f+7(7)7.5s+1(1)8.5p-1(1)9	30.537856
92	$4f^{11}5s^25p^2$	4f-3(9)9	30.925077
93	$4f^{11}5s^25p^2$	4f-5(5)5.4f+6(4)3	31.052591
94	$4f^{13}5s^15p^1$	4f+7(7)7.5s+1(1)6.5p-1(1)5	31.221911
95	$4f^{11}5s^25p^2$	4f-4(8)8.4f+7(7)13	31.222353
96	$4f^{12}5s^25p^1$	4f-5(5)5.4f+7(7)12.5p+1(3)11	31.228435
97	$4f^{12}5s^25p^1$	4f-5(5)5.4f+7(7)2.5p+1(3)1	31.443892
98	$4f^{12}5s^25p^1$	4f-5(5)5.4f+7(7)2.5p+1(3)5	31.618803
99	$4f^{12}5s^25p^1$	4f-5(5)5.4f+7(7)12.5p+1(3)13	31.626541
100	$4f^{12}5s^25p^1$	4f+6(0)0.5p+1(3)3	31.690676
101	$4f^{12}5s^25p^1$	4f-4(4)4.5p+1(3)7	31.855806
102	$4f^{11}5s^25p^2$	4f-4(4)4.4f+7(7)3	31.860288
103	$4f^{11}5s^25p^2$	4f-5(5)5.4f+6(4)9	31.868845
104	$4f^{11}5s^25p^2$	4f-4(8)8.4f+7(7)15	32.320684
105	$4f^{12}5s^25p^1$	4f-5(5)5.4f+7(7)2.5p+1(3)3	32.411987
106	$4f^{11}5s^25p^2$	4f-4(8)8.4f+7(7)1	32.619662
107	$4f^{11}5s^25p^2$	4f-4(4)4.4f+7(7)5	32.672403
108	$4f^{13}5s^15p^1$	4f-5(5)5.5s+1(1)6.5p-1(1)5	33.071560
109	$4f^{11}5s^25p^2$	4f-4(4)4.4f+7(7)11	33.185265
110	$4f^{13}5s^15p^1$	4f-5(5)5.5s+1(1)6.5p-1(1)7	33.221250
111	$4f^{12}5s^25p^1$	4f-4(4)4.5p+1(3)1	33.350995
112	$4f^{11}5s^25p^2$	4f-4(4)4.4f+7(7)7	33.371350
113	$4f^{11}5s^25p^2$	4f+5(15)15.5p-1(1)14.5p+1(3)17	33.384989
114	$4f^{13}5s^15p^1$	4f-5(5)5.5s+1(1)4.5p-1(1)3	33.529177
115	$4f^{11}5s^25p^2$	4f+5(15)15.5p-1(1)14.5p+1(3)15	34.395525
116	$4f^{11}5s^25p^2$	4f+5(15)15.5p-1(1)14.5p+1(3)13	34.979542
117	$4f^{11}5s^25p^2$	4f-3(3)3	34.983491
118	$4f^{11}5s^25p^2$	4f-5(5)5.4f+6(4)7	35.157994
119	$4f^{11}5s^25p^2$	4f+5(15)15.5p-1(1)16.5p+1(3)19	35.632188
120	$4f^{11}5s^25p^2$	4f-5(5)5.4f+6(12)13.5p-1(1)14.5p+1(3)11	35.873969
121	$4f^{11}5s^25p^2$	4f-5(5)5.4f+6(12)13.5p-1(1)12.5p+1(3)15	36.103905

Table 10. *Cont.*

Level No.	Configuration	*2J*	FAC
122	$4f^{11}5s^25p^2$	4f-3(5)5	36.132441
123	$4f^{11}5s^25p^2$	4f+5(15)15.5p-1(1)16.5p+1(3)17	36.289379
124	$4f^{11}5s^25p^2$	4f+5(11)11.5p-1(1)10.5p+1(3)13	36.421597
125	$4f^{11}5s^25p^2$	4f+5(9)9.5p-1(1)8.5p+1(3)11	36.524088
126	$4f^{11}5s^25p^2$	4f+5(9)9.5p-1(1)8.5p+1(3)9	36.532534
127	$4f^{11}5s^25p^2$	4f+5(15)15.5p-1(1)16.5p+1(3)15	36.572398
128	$4f^{11}5s^25p^2$	4f+5(9)9.5p-1(1)8.5p+1(3)9	36.677277
129	$4f^{11}5s^25p^2$	4f+5(15)15.5p-1(1)16.5p+1(3)13	36.697402
130	$4f^{11}5s^25p^2$	4f-4(4)4.4f+7(7)9	36.795762
131	$4f^{11}5s^25p^2$	4f+5(9)9.5p-1(1)10.5p+1(3)7	36.952634
132	$4f^{11}5s^25p^2$	4f+5(15)15.5p-1(1)14.5p+1(3)11	37.082975
133	$4f^{11}5s^25p^2$	4f-5(5)5.4f+6(12)13.5p-1(1)14.5p+1(3)13	37.411724
134	$4f^{11}5s^25p^2$	4f+5(9)9.5p-1(1)10.5p+1(3)11	37.597102
135	$4f^{11}5s^25p^2$	4f+5(9)9.5p-1(1)8.5p+1(3)7	37.813602
136	$4f^{11}5s^25p^2$	4f-5(5)5.4f+6(12)13.5p-1(1)14.5p+1(3)17	37.826275
137	$4f^{11}5s^25p^2$	4f+5(3)3.5p-1(1)2.5p+1(3)5	37.898919
138	$4f^{12}5s^15p^2$	4f+6(12)12.5s+1(1)13	38.071969
139	$4f^{11}5s^25p^2$	4f-5(5)5.4f+6(12)13.5p-1(1)12.5p+1(3)11	38.248034
140	$4f^{11}5s^25p^2$	4f+5(3)3.5p-1(1)4.5p+1(3)3	38.277848
141	$4f^{11}5s^25p^2$	4f-5(5)5.4f+6(12)9.5p-1(1)8.5p+1(3)9	38.297614
142	$4f^{11}5s^25p^2$	4f-5(5)5.4f+6(8)9.5p-1(1)8.5p+1(3)11	38.321917
143	$4f^{11}5s^25p^2$	4f-5(5)5.4f+6(12)13.5p-1(1)14.5p+1(3)13	38.367848
144	$4f^{11}5s^25p^2$	4f-5(5)5.4f+6(8)5.5p-1(1)4.5p+1(3)5	38.377390
145	$4f^{11}5s^25p^2$	4f-5(5)5.4f+6(12)13.5p-1(1)14.5p+1(3)15	38.419868
146	$4f^{11}5s^25p^2$	4f+5(11)11.5p-1(1)10.5p+1(3)9	38.462512
147	$4f^{11}5s^25p^2$	4f+5(9)9.5p-1(1)10.5p+1(3)13	38.561854
148	$4f^{11}5s^25p^2$	4f+5(3)3.5p-1(1)4.5p+1(3)1	38.700658
149	$4f^{11}5s^25p^2$	4f+5(9)9.5p-1(1)10.5p+1(3)7	38.714756
150	$4f^{11}5s^25p^2$	4f+5(11)11.5p-1(1)10.5p+1(3)9	38.717201
151	$4f^{11}5s^25p^2$	4f+5(9)9.5p-1(1)8.5p+1(3)7	38.777407
152	$4f^{11}5s^25p^2$	4f+5(9)9.5p-1(1)8.5p+1(3)5	38.786312
153	$4f^{11}5s^25p^2$	4f+5(11)11.5p-1(1)12.5p+1(3)15	38.840427
154	$4f^{12}5s^25p^1$	4f-4(0)0.5p+1(3)3	38.850279
155	$4f^{11}5s^25p^2$	4f+5(9)9.5p-1(1)10.5p+1(3)11	38.857099
156	$4f^{11}5s^25p^2$	4f+5(11)11.5p-1(1)10.5p+1(3)13	38.931170
157	$4f^{11}5s^25p^2$	4f-4(8)8.4f+7(7)11.5p-1(1)12.5p+1(3)11	39.036573
158	$4f^{12}5s^15p^2$	4f+6(12)12.5s+1(1)11	39.094106
159	$4f^{11}5s^25p^2$	4f+5(11)11.5p-1(1)12.5p+1(3)9	39.211350
160	$4f^{12}5s^15p^2$	4f+6(8)8.5s+1(1)9	39.332591
161	$4f^{11}5s^25p^2$	4f+5(11)11.5p-1(1)12.5p+1(3)13	39.344217
162	$4f^{11}5s^25p^2$	4f+5(9)9.5p-1(1)10.5p+1(3)9	39.354890
163	$4f^{11}5s^25p^2$	4f-5(5)5.4f+6(8)3.5p-1(1)4.5p+1(3)3	39.466359
164	$4f^{11}5s^25p^2$	4f+5(5)5.5p-1(1)4.5p+1(3)7	39.469231
165	$4f^{11}5s^25p^2$	4f-5(5)5.4f+6(12)13.5p-1(1)12.5p+1(3)9	39.696083
166	$4f^{11}5s^25p^2$	4f+5(3)3.5p-1(1)4.5p+1(3)5	39.739705
167	$4f^{11}5s^25p^2$	4f+5(3)3.5p-1(1)4.5p+1(3)7	39.748882
168	$4f^{11}5s^25p^2$	4f-5(5)5.4f+6(12)9.5p-1(1)8.5p+1(3)11	39.768124
169	$4f^{11}5s^25p^2$	4f-5(5)5.4f+6(12)15.5p-1(1)14.5p+1(3)17	39.864491
170	$4f^{11}5s^25p^2$	4f-5(5)5.4f+6(12)13.5p-1(1)12.5p+1(3)11	39.955178
171	$4f^{11}5s^25p^2$	4f-5(5)5.4f+6(4)3.5p-1(1)4.5p+1(3)1	40.023281
172	$4f^{11}5s^25p^2$	4f-5(5)5.4f+6(12)15.5p-1(1)16.5p+1(3)13	40.030831
173	$4f^{11}5s^25p^2$	4f+5(3)3.5p-1(1)4.5p+1(3)5	40.042976
174	$4f^{12}5s^15p^2$	4f+6(8)8.5s+1(1)7	40.076237
175	$4f^{11}5s^25p^2$	4f-5(5)5.4f+6(8)3.5p-1(1)4.5p+1(3)7	40.103966

Table 10. *Cont.*

Level No.	Configuration	2J	FAC
176	$4f^{11}5s^25p^2$	4f-5(5)5.4f+6(8)9.5p-1(1)10.5p+1(3)13	40.159488
177	$4f^{11}5s^25p^2$	4f+5(3)3.5p-1(1)4.5p+1(3)5	40.186407
178	$4f^{11}5s^25p^2$	4f+5(3)3.5p-1(1)2.5p+1(3)3	40.201850
179	$4f^{11}5s^25p^2$	4f-5(5)5.4f+6(12)13.5p-1(1)12.5p+1(3)9	40.205703
180	$4f^{11}5s^25p^2$	4f+5(5)5.5p-1(1)6.5p+1(3)3	40.289325
181	$4f^{11}5s^25p^2$	4f-5(5)5.4f+6(8)9.5p-1(1)8.5p+1(3)11	40.382701
182	$4f^{11}5s^25p^2$	4f-5(5)5.4f+6(0)5	40.407623
183	$4f^{11}5s^25p^2$	4f-4(8)8.4f+7(7)11.5p-1(1)12.5p+1(3)15	40.546845
184	$4f^{11}5s^25p^2$	4f-5(5)5.4f+6(12)9.5p-1(1)8.5p+1(3)7	40.567874
185	$4f^{11}5s^25p^2$	4f-4(8)8.4f+7(7)11.5p-1(1)12.5p+1(3)9	40.574136
186	$4f^{11}5s^25p^2$	4f-5(5)5.4f+6(8)13.5p-1(1)14.5p+1(3)11	40.623030
187	$4f^{11}5s^25p^2$	4f-5(5)5.4f+6(8)9.5p-1(1)8.5p+1(3)7	40.652418
188	$4f^{11}5s^25p^2$	4f-5(5)5.4f+6(8)3.5p-1(1)2.5p+1(3)3	40.706965
189	$4f^{11}5s^25p^2$	4f-5(5)5.4f+6(8)9.5p-1(1)8.5p+1(3)9	40.755795
190	$4f^{11}5s^25p^2$	4f-5(5)5.4f+6(4)1.5p-1(1)2.5p+1(3)1	40.779964
191	$4f^{11}5s^25p^2$	4f+5(11)11.5p-1(1)10.5p+1(3)7	40.854550
192	$4f^{12}5s^15p^2$	4f-5(5)5.4f+7(7)10.5s+1(1)9	40.863392
193	$4f^{11}5s^25p^2$	4f-5(5)5.4f+6(12)15.5p-1(1)16.5p+1(3)13	40.890074
194	$4f^{11}5s^25p^2$	4f-5(5)5.4f+6(8)7.5p-1(1)8.5p+1(3)11	40.891647
195	$4f^{11}5s^25p^2$	4f+5(9)9.5p-1(1)8.5p+1(3)5	40.977267
196	$4f^{11}5s^25p^2$	4f-5(5)5.4f+6(8)7.5p-1(1)8.5p+1(3)9	41.011051
197	$4f^{11}5s^25p^2$	4f-5(5)5.4f+6(12)11.5p-1(1)12.5p+1(3)13	41.066343
198	$4f^{11}5s^25p^2$	4f-5(5)5.4f+6(12)15.5p-1(1)16.5p+1(3)15	41.092734
199	$4f^{11}5s^25p^2$	4f-5(5)5.4f+6(4)1.5p-1(1)2.5p+1(3)3	41.127133
200	$4f^{11}5s^25p^2$	4f-5(5)5.4f+6(12)9.5p-1(1)10.5p+1(3)7	41.160989
201	$4f^{11}5s^25p^2$	4f-5(5)5.4f+6(4)1.5p-1(1)2.5p+1(3)1	41.192857
202	$4f^{11}5s^25p^2$	4f-5(5)5.4f+6(8)7.5p-1(1)6.5p+1(3)9	41.210887
203	$4f^{11}5s^25p^2$	4f-5(5)5.4f+6(8)7.5p-1(1)8.5p+1(3)5	41.254861
204	$4f^{11}5s^25p^2$	4f-5(5)5.4f+6(8)5.5p-1(1)4.5p+1(3)5	41.317661
205	$4f^{11}5s^25p^2$	4f-5(5)5.4f+6(12)15.5p-1(1)16.5p+1(3)19	41.471568
206	$4f^{11}5s^25p^2$	4f-5(5)5.4f+6(12)9.5p-1(1)8.5p+1(3)11	41.504783
207	$4f^{11}5s^25p^2$	4f-5(5)5.4f+6(12)11.5p-1(1)12.5p+1(3)11	41.534879
208	$4f^{12}5s^15p^2$	4f+6(4)4.5s+1(1)3	41.558156
209	$4f^{11}5s^25p^2$	4f+5(5)5.5p-1(1)6.5p+1(3)9	41.567579
210	$4f^{12}5s^15p^2$	4f-5(5)5.4f+7(7)6.5s+1(1)5	41.581960
211	$4f^{11}5s^25p^2$	4f+5(11)11.5p-1(1)10.5p+1(3)7	41.590698
212	$4f^{11}5s^25p^2$	4f-5(5)5.4f+6(8)3.5p-1(1)4.5p+1(3)5	41.615627
213	$4f^{11}5s^25p^2$	4f-4(8)8.4f+7(7)3.5p-1(1)4.5p+1(3)5	41.684795
214	$4f^{11}5s^25p^2$	4f-5(5)5.4f+6(8)3.5p-1(1)2.5p+1(3)1	41.689852
215	$4f^{11}5s^25p^2$	4f-5(5)5.4f+6(12)9.5p-1(1)10.5p+1(3)9	41.695204
216	$4f^{11}5s^25p^2$	4f-5(5)5.4f+6(12)9.5p-1(1)8.5p+1(3)7	41.718644
217	$4f^{12}5s^15p^2$	4f-5(5)5.4f+7(7)8.5s+1(1)7	41.720355
218	$4f^{11}5s^25p^2$	4f-4(8)8.4f+7(7)9.5p-1(1)10.5p+1(3)11	41.740916
219	$4f^{11}5s^25p^2$	4f-5(5)5.4f+6(8)3.5p-1(1)4.5p+1(3)3	41.772383
220	$4f^{11}5s^25p^2$	4f+5(5)5.5p-1(1)4.5p+1(3)1	41.821878
221	$4f^{11}5s^25p^2$	4f-5(5)5.4f+6(8)13.5p-1(1)12.5p+1(3)15	41.824746
222	$4f^{13}5s^15p^1$	4f+7(7)7.5s+1(1)8.5p+1(3)11	41.889066
223	$4f^{11}5s^25p^2$	4f-5(5)5.4f+6(8)9.5p-1(1)10.5p+1(3)9	41.903860
224	$4f^{11}5s^25p^2$	4f-5(5)5.4f+6(8)7.5p-1(1)8.5p+1(3)7	41.906544
225	$4f^{12}5s^15p^2$	4f-5(5)5.4f+7(7)10.5s+1(1)11	41.954094
226	$4f^{11}5s^25p^2$	4f+5(7)7.5p-1(1)8.5p+1(3)7	42.030961
227	$4f^{11}5s^25p^2$	4f+5(5)5.5p-1(1)4.5p+1(3)3	42.044655
228	$4f^{11}5s^25p^2$	4f+5(5)5.5p-1(1)6.5p+1(3)5	42.063989
229	$4f^{11}5s^25p^2$	4f-5(5)5.4f+6(12)15.5p-1(1)14.5p+1(3)11	42.163110

Table 10. *Cont.*

Level No.	Configuration	2J	FAC
230	$4f^{11}5s^{2}5p^{2}$	4f-4(0)0.4f+7(7)7	42.205120
231	$4f^{11}5s^{2}5p^{2}$	4f-5(5)5.4f+6(12)15.5p-1(1)14.5p+1(3)13	42.221158
232	$4f^{11}5s^{2}5p^{2}$	4f-5(5)5.4f+6(12)11.5p-1(1)12.5p+1(3)15	42.276307
233	$4f^{11}5s^{2}5p^{2}$	4f-5(5)5.4f+6(8)3.5p-1(1)4.5p+1(3)7	42.291003
234	$4f^{11}5s^{2}5p^{2}$	4f-5(5)5.4f+6(8)5.5p-1(1)6.5p+1(3)9	42.294626
235	$4f^{11}5s^{2}5p^{2}$	4f-5(5)5.4f+6(8)7.5p-1(1)6.5p+1(3)5	42.367551
236	$4f^{11}5s^{2}5p^{2}$	4f-5(5)5.4f+6(8)7.5p-1(1)6.5p+1(3)3	42.411801
237	$4f^{11}5s^{2}5p^{2}$	4f-5(5)5.4f+6(12)9.5p-1(1)10.5p+1(3)13	42.426365
238	$4f^{11}5s^{2}5p^{2}$	4f-4(0)0.4f+7(7)7	42.471082
239	$4f^{11}5s^{2}5p^{2}$	4f-5(5)5.4f+6(12)17.5p-1(1)16.5p+1(3)19	42.488306
240	$4f^{11}5s^{2}5p^{2}$	4f-5(5)5.4f+6(12)17.5p-1(1)18.5p+1(3)15	42.490099
241	$4f^{11}5s^{2}5p^{2}$	4f-4(8)8.4f+7(7)9.5p-1(1)10.5p+1(3)13	42.510407
242	$4f^{11}5s^{2}5p^{2}$	4f-5(5)5.4f+6(8)3.5p-1(1)4.5p+1(3)3	42.601749
243	$4f^{11}5s^{2}5p^{2}$	4f+5(7)7.5p-1(1)8.5p+1(3)11	42.668342
244	$4f^{12}5s^{1}5p^{2}$	4f-5(5)5.4f+7(7)8.5s+1(1)9	42.675456
245	$4f^{11}5s^{2}5p^{2}$	4f-5(5)5.4f+6(12)11.5p-1(1)12.5p+1(3)9	42.676572
246	$4f^{11}5s^{2}5p^{2}$	4f-5(5)5.4f+6(12)15.5p-1(1)16.5p+1(3)17	42.747113
247	$4f^{11}5s^{2}5p^{2}$	4f-4(4)4.4f+7(7)3.5p-1(1)2.5p+1(3)5	42.761996
248	$4f^{11}5s^{2}5p^{2}$	4f-5(5)5.4f+6(12)9.5p-1(1)10.5p+1(3)7	42.778821
249	$4f^{11}5s^{2}5p^{2}$	4f-5(5)5.4f+6(12)11.5p-1(1)12.5p+1(3)11	42.844266
250	$4f^{13}5s^{1}5p^{1}$	4f+7(7)7.5s+1(1)6.5p+1(3)3	42.846710
251	$4f^{11}5s^{2}5p^{2}$	4f-5(5)5.4f+6(12)9.5p-1(1)8.5p+1(3)9	42.850480
252	$4f^{11}5s^{2}5p^{2}$	4f-5(5)5.4f+6(12)15.5p-1(1)16.5p+1(3)13	42.883478
253	$4f^{11}5s^{2}5p^{2}$	4f-4(4)4.4f+7(7)3.5p-1(1)4.5p+1(3)1	42.940906
254	$4f^{11}5s^{2}5p^{2}$	4f-5(5)5.4f+6(4)5.5p-1(1)6.5p+1(3)5	42.960119
255	$4f^{11}5s^{2}5p^{2}$	4f+5(7)7.5p-1(1)8.5p+1(3)11	42.979710
256	$4f^{11}5s^{2}5p^{2}$	4f-5(5)5.4f+6(8)13.5p-1(1)14.5p+1(3)17	43.036815
257	$4f^{11}5s^{2}5p^{2}$	4f-3(9)9.5p-1(1)10.5p+1(3)9	43.045039
258	$4f^{12}5s^{1}5p^{2}$	4f-5(5)5.4f+7(7)6.5s+1(1)7	43.067672
259	$4f^{11}5s^{2}5p^{2}$	4f-5(5)5.4f+6(4)5.5p-1(1)6.5p+1(3)7	43.115484
260	$4f^{11}5s^{2}5p^{2}$	4f-5(5)5.4f+6(12)9.5p-1(1)8.5p+1(3)5	43.123252
261	$4f^{11}5s^{2}5p^{2}$	4f-4(8)8.4f+7(7)1.5p-1(1)2.5p+1(3)1	43.184025
262	$4f^{11}5s^{2}5p^{2}$	4f-5(5)5.4f+6(12)9.5p-1(1)10.5p+1(3)13	43.193490
263	$4f^{13}5s^{1}5p^{1}$	4f+7(7)7.5s+1(1)6.5p+1(3)5	43.206794
264	$4f^{11}5s^{2}5p^{2}$	4f-5(5)5.4f+6(12)9.5p-1(1)8.5p+1(3)7	43.247479
265	$4f^{11}5s^{2}5p^{2}$	4f-5(5)5.4f+6(4)1.5p-1(1)0.5p+1(3)3	43.253889
266	$4f^{13}5s^{1}5p^{1}$	4f-5(5)5.5s+1(1)4.5p+1(3)1	43.258331
267	$4f^{11}5s^{2}5p^{2}$	4f-5(5)5.4f+6(12)15.5p-1(1)14.5p+1(3)11	43.283855
268	$4f^{12}5s^{1}5p^{2}$	4f+6(4)4.5s+1(1)5	43.285472
269	$4f^{11}5s^{2}5p^{2}$	4f+5(7)7.5p-1(1)6.5p+1(3)3	43.317624
270	$4f^{11}5s^{2}5p^{2}$	4f-5(5)5.4f+6(4)7.5p-1(1)8.5p+1(3)9	43.319875
271	$4f^{11}5s^{2}5p^{2}$	4f-5(5)5.4f+6(12)17.5p-1(1)18.5p+1(3)15	43.352594
272	$4f^{11}5s^{2}5p^{2}$	4f-4(8)8.4f+7(7)9.5p-1(1)8.5p+1(3)5	43.417388
273	$4f^{11}5s^{2}5p^{2}$	4f-5(5)5.4f+6(12)11.5p-1(1)10.5p+1(3)9	43.498409
274	$4f^{11}5s^{2}5p^{2}$	4f-4(8)8.4f+7(7)5.5p-1(1)6.5p+1(3)7	43.511747
275	$4f^{11}5s^{2}5p^{2}$	4f-3(9)9.5p-1(1)8.5p+1(3)7	43.580865
276	$4f^{11}5s^{2}5p^{2}$	4f-4(8)8.4f+7(7)7.5p-1(1)8.5p+1(3)5	43.641796
277	$4f^{13}5s^{1}5p^{1}$	4f+7(7)7.5s+1(1)6.5p+1(3)7	43.649705
278	$4f^{11}5s^{2}5p^{2}$	4f-4(4)4.4f+7(7)5.5p-1(1)6.5p+1(3)3	43.660656
279	$4f^{13}5s^{1}5p^{1}$	4f+7(7)7.5s+1(1)8.5p+1(3)9	43.671016
280	$4f^{11}5s^{2}5p^{2}$	4f-4(8)8.4f+7(7)15.5p-1(1)16.5p+1(3)13	43.717882
281	$4f^{11}5s^{2}5p^{2}$	4f-4(8)8.4f+7(7)9.5p-1(1)10.5p+1(3)9	43.750006
282	$4f^{11}5s^{2}5p^{2}$	4f-5(5)5.4f+6(12)9.5p-1(1)10.5p+1(3)11	43.751161
283	$4f^{11}5s^{2}5p^{2}$	4f-4(8)8.4f+7(7)7.5p-1(1)8.5p+1(3)7	43.810325

Table 10. *Cont.*

Level No.	Configuration	*2J*	FAC
284	$4f^{11}5s^25p^2$	4f-5(5)5.4f+6(8)13.5p-1(1)12.5p+1(3)13	43.816105
285	$4f^{11}5s^25p^2$	4f-5(5)5.4f+6(4)1.5p-1(1)2.5p+1(3)5	43.827070
286	$4f^{11}5s^25p^2$	4f-4(8)8.4f+7(7)7.5p-1(1)6.5p+1(3)9	43.851458
287	$4f^{11}5s^25p^2$	4f-5(5)5.4f+6(12)11.5p-1(1)10.5p+1(3)7	43.912980
288	$4f^{11}5s^25p^2$	4f-4(8)8.4f+7(7)3.5p-1(1)4.5p+1(3)5	43.980542
289	$4f^{11}5s^25p^2$	4f-3(9)9.5p-1(1)10.5p+1(3)11	44.031655
290	$4f^{11}5s^25p^2$	4f-5(5)5.4f+6(8)5.5p-1(1)6.5p+1(3)3	44.052047
291	$4f^{11}5s^25p^2$	4f-5(5)5.4f+6(8)13.5p-1(1)14.5p+1(3)15	44.055037
292	$4f^{11}5s^25p^2$	4f-5(5)5.4f+6(4)5.5p-1(1)6.5p+1(3)9	44.067255
293	$4f^{11}5s^25p^2$	4f-5(5)5.4f+6(12)17.5p-1(1)18.5p+1(3)21	44.093153
294	$4f^{11}5s^25p^2$	4f-4(4)4.4f+7(7)5.5p-1(1)4.5p+1(3)7	44.180961
295	$4f^{11}5s^25p^2$	4f-4(8)8.4f+7(7)13.5p-1(1)12.5p+1(3)15	44.272026
296	$4f^{11}5s^25p^2$	4f-4(4)4.4f+7(7)3.5p-1(1)2.5p+1(3)3	44.273736
297	$4f^{11}5s^25p^2$	4f-4(8)8.4f+7(7)15.5p-1(1)16.5p+1(3)13	44.307366
298	$4f^{11}5s^25p^2$	4f-5(5)5.4f+6(12)17.5p-1(1)18.5p+1(3)17	44.323538
299	$4f^{11}5s^25p^2$	4f-5(5)5.4f+6(4)1.5p-1(1)2.5p+1(3)5	44.328986
300	$4f^{11}5s^25p^2$	4f-5(5)5.4f+6(4)3.5p-1(1)4.5p+1(3)7	44.359708
301	$4f^{11}5s^25p^2$	4f-5(5)5.4f+6(8)13.5p-1(1)12.5p+1(3)11	44.376938
302	$4f^{11}5s^25p^2$	4f-4(8)8.4f+7(7)13.5p-1(1)12.5p+1(3)9	44.401158
303	$4f^{11}5s^25p^2$	4f-4(4)4.4f+7(7)3.5p-1(1)4.5p+1(3)1	44.423800
304	$4f^{11}5s^25p^2$	4f-4(4)4.4f+7(7)5.5p-1(1)6.5p+1(3)5	44.470206
305	$4f^{11}5s^25p^2$	4f+5(5)5.5p-1(1)6.5p+1(3)3	44.493374
306	$4f^{11}5s^25p^2$	4f-5(5)5.4f+6(8)11.5p-1(1)10.5p+1(3)11	44.531032
307	$4f^{11}5s^25p^2$	4f-4(4)4.4f+7(7)3.5p-1(1)2.5p+1(3)1	44.542990
308	$4f^{11}5s^25p^2$	4f+5(5)5.5p-1(1)4.5p+1(3)5	44.577555
309	$4f^{11}5s^25p^2$	4f+5(5)5.5p-1(1)6.5p+1(3)7	44.585082
310	$4f^{11}5s^25p^2$	4f-5(5)5.4f+6(12)17.5p-1(1)16.5p+1(3)13	44.619176
311	$4f^{12}5s^15p^2$	4f-4(8)8.5s+1(1)7	44.655880
312	$4f^{11}5s^25p^2$	4f-5(5)5.4f+6(4)5.5p-1(1)6.5p+1(3)9	44.663143
313	$4f^{11}5s^25p^2$	4f-4(4)4.4f+7(7)3.5p-1(1)2.5p+1(3)5	44.734290
314	$4f^{11}5s^25p^2$	4f-5(5)5.4f+6(4)5.5p-1(1)4.5p+1(3)7	44.812548
315	$4f^{11}5s^25p^2$	4f-4(8)8.4f+7(7)7.5p-1(1)8.5p+1(3)11	44.879029
316	$4f^{11}5s^25p^2$	4f-5(5)5.4f+6(4)5.5p-1(1)4.5p+1(3)3	44.933982
317	$4f^{13}5s^15p^1$	4f-5(5)5.5s+1(1)4.5p+1(3)3	45.024375
318	$4f^{11}5s^25p^2$	4f-5(5)5.4f+6(4)5.5p-1(1)4.5p+1(3)5	45.026303
319	$4f^{12}5s^15p^2$	4f-5(5)5.4f+7(7)4.5s+1(1)5	45.079574
320	$4f^{11}5s^25p^2$	4f+5(5)5.5p-1(1)4.5p+1(3)1	45.082661
321	$4f^{11}5s^25p^2$	4f-5(5)5.4f+6(8)11.5p-1(1)12.5p+1(3)15	45.085685
322	$4f^{12}5s^15p^2$	4f+6(4)4.5s+1(1)3	45.096066
323	$4f^{11}5s^25p^2$	4f-5(5)5.4f+6(8)11.5p-1(1)10.5p+1(3)9	45.139443
324	$4f^{11}5s^25p^2$	4f-5(5)5.4f+6(8)5.5p-1(1)4.5p+1(3)3	45.160972
325	$4f^{11}5s^25p^2$	4f-5(5)5.4f+6(12)7.5p-1(1)6.5p+1(3)7	45.169732
326	$4f^{13}5s^15p^1$	4f-5(5)5.5s+1(1)6.5p+1(3)9	45.171113
327	$4f^{11}5s^25p^2$	4f-4(8)8.4f+7(7)15.5p-1(1)14.5p+1(3)17	45.207091
328	$4f^{12}5s^15p^2$	4f+6(0)0.5s+1(1)1	45.226338
329	$4f^{12}5s^15p^2$	4f-4(8)8.5s+1(1)9	45.263813
330	$4f^{11}5s^25p^2$	4f-5(5)5.4f+6(8)5.5p-1(1)6.5p+1(3)9	45.287098
331	$4f^{11}5s^25p^2$	4f-5(5)5.4f+6(8)11.5p-1(1)10.5p+1(3)7	45.311729
332	$4f^{11}5s^25p^2$	4f-3(9)9.5p-1(1)10.5p+1(3)13	45.364459
333	$4f^{11}5s^25p^2$	4f-4(8)8.4f+7(7)7.5p-1(1)8.5p+1(3)11	45.366640
334	$4f^{11}5s^25p^2$	4f-4(8)8.4f+7(7)5.5p-1(1)4.5p+1(3)7	45.369971
335	$4f^{11}5s^25p^2$	4f-5(5)5.4f+6(4)3.5p-1(1)4.5p+1(3)5	45.394036
336	$4f^{11}5s^25p^2$	4f-4(8)8.4f+7(7)7.5p-1(1)6.5p+1(3)5	45.452376
337	$4f^{11}5s^25p^2$	4f-5(5)5.4f+6(8)11.5p-1(1)12.5p+1(3)13	45.454850
338	$4f^{11}5s^25p^2$	4f-5(5)5.4f+6(12)7.5p-1(1)8.5p+1(3)11	45.503849

Table 10. *Cont.*

Level No.	Configuration	2J	FAC
339	$4f^{11}5s^25p^2$	4f-4(8)8.4f+7(7)5.5p-1(1)6.5p+1(3)9	45.532680
340	$4f^{11}5s^25p^2$	4f-5(5)5.4f+6(12)7.5p-1(1)6.5p+1(3)3	45.547802
341	$4f^{11}5s^25p^2$	4f-3(9)9.5p-1(1)8.5p+1(3)9	45.569721
342	$4f^{11}5s^25p^2$	4f-4(8)8.4f+7(7)5.5p-1(1)4.5p+1(3)3	45.714391
343	$4f^{11}5s^25p^2$	4f-5(5)5.4f+6(8)11.5p-1(1)10.5p+1(3)11	45.747075
344	$4f^{11}5s^25p^2$	4f-5(5)5.4f+6(12)7.5p-1(1)6.5p+1(3)5	45.758919
345	$4f^{11}5s^25p^2$	4f-4(4)4.4f+7(7)3.5p-1(1)4.5p+1(3)1	45.785356
346	$4f^{11}5s^25p^2$	4f-3(9)9.5p-1(1)8.5p+1(3)7	45.798358
347	$4f^{11}5s^25p^2$	4f-3(9)9.5p-1(1)8.5p+1(3)9	45.878309
348	$4f^{11}5s^25p^2$	4f-3(3)3.5p-1(1)4.5p+1(3)1	45.896710
349	$4f^{11}5s^25p^2$	4f-4(8)8.4f+7(7)3.5p-1(1)2.5p+1(3)3	45.906397
350	$4f^{11}5s^25p^2$	4f-4(8)8.4f+7(7)3.5p-1(1)4.5p+1(3)7	45.926221
351	$4f^{13}5s^15p^1$	4f-5(5)5.5s+1(1)4.5p+1(3)5	45.997353
352	$4f^{11}5s^25p^2$	4f-5(5)5.4f+6(12)17.5p-1(1)16.5p+1(3)13	46.001588
353	$4f^{11}5s^25p^2$	4f-5(5)5.4f+6(12)7.5p-1(1)6.5p+1(3)5	46.007526
354	$4f^{11}5s^25p^2$	4f-5(5)5.4f+6(12)17.5p-1(1)16.5p+1(3)17	46.084963
355	$4f^{11}5s^25p^2$	4f-3(9)9.5p-1(1)8.5p+1(3)11	46.106557
356	$4f^{11}5s^25p^2$	4f-4(8)8.4f+7(7)15.5p-1(1)16.5p+1(3)19	46.119690
357	$4f^{13}5s^15p^1$	4f-5(5)5.5s+1(1)6.5p+1(3)7	46.145634
358	$4f^{11}5s^25p^2$	4f-4(8)8.4f+7(7)7.5p-1(1)6.5p+1(3)3	46.160789
359	$4f^{11}5s^25p^2$	4f-5(5)5.4f+6(12)17.5p-1(1)18.5p+1(3)19	46.198266
360	$4f^{11}5s^25p^2$	4f-3(9)9.5p-1(1)8.5p+1(3)7	46.238815
361	$4f^{11}5s^25p^2$	4f-5(5)5.4f+6(4)3.5p-1(1)2.5p+1(3)3	46.264864
362	$4f^{12}5s^15p^2$	4f-5(5)5.4f+7(7)2.5s+1(1)3	46.305166
363	$4f^{12}5s^15p^2$	4f-5(5)5.4f+7(7)12.5s+1(1)13	46.313076
364	$4f^{11}5s^25p^2$	4f-4(4)4.4f+7(7)11.5p-1(1)10.5p+1(3)13	46.330883
365	$4f^{11}5s^25p^2$	4f-4(8)8.4f+7(7)5.5p-1(1)6.5p+1(3)9	46.359567
366	$4f^{12}5s^15p^2$	4f-5(5)5.4f+7(7)12.5s+1(1)11	46.359947
367	$4f^{11}5s^25p^2$	4f-4(8)8.4f+7(7)13.5p-1(1)14.5p+1(3)15	46.375372
368	$4f^{11}5s^25p^2$	4f-5(5)5.4f+6(12)17.5p-1(1)18.5p+1(3)17	46.447493
369	$4f^{11}5s^25p^2$	4f-4(8)8.4f+7(7)5.5p-1(1)4.5p+1(3)1	46.467329
370	$4f^{11}5s^25p^2$	4f-4(8)8.4f+7(7)13.5p-1(1)12.5p+1(3)11	46.470016
371	$4f^{11}5s^25p^2$	4f-4(8)8.4f+7(7)15.5p-1(1)16.5p+1(3)15	46.479449
372	$4f^{11}5s^25p^2$	4f-3(3)3.5p-1(1)4.5p+1(3)5	46.524453
373	$4f^{11}5s^25p^2$	4f-4(8)8.4f+7(7)5.5p-1(1)4.5p+1(3)7	46.566212
374	$4f^{11}5s^25p^2$	4f-4(8)8.4f+7(7)1.5p-1(1)2.5p+1(3)3	46.614030
375	$4f^{11}5s^25p^2$	4f-3(3)3.5p-1(1)4.5p+1(3)5	46.627077
376	$4f^{11}5s^25p^2$	4f-5(5)5.4f+6(4)3.5p-1(1)4.5p+1(3)7	46.762017
377	$4f^{11}5s^25p^2$	4f-5(5)5.4f+6(12)7.5p-1(1)8.5p+1(3)9	46.768387
378	$4f^{11}5s^25p^2$	4f-4(4)4.4f+7(7)11.5p-1(1)12.5p+1(3)9	46.837656
379	$4f^{11}5s^25p^2$	4f-5(5)5.4f+6(12)17.5p-1(1)16.5p+1(3)15	46.923650
380	$4f^{11}5s^25p^2$	4f-4(4)4.4f+7(7)5.5p-1(1)4.5p+1(3)1	46.925950
381	$4f^{11}5s^25p^2$	4f-4(4)4.4f+7(7)3.5p-1(1)2.5p+1(3)3	46.940582
382	$4f^{11}5s^25p^2$	4f-4(8)8.4f+7(7)15.5p-1(1)14.5p+1(3)11	46.990451
383	$4f^{11}5s^25p^2$	4f-4(8)8.4f+7(7)13.5p-1(1)12.5p+1(3)9	47.012767
384	$4f^{11}5s^25p^2$	4f-4(8)8.4f+7(7)3.5p-1(1)2.5p+1(3)5	47.019958
385	$4f^{11}5s^25p^2$	4f-5(5)5.4f+6(4)9.5p-1(1)10.5p+1(3)13	47.046126
386	$4f^{11}5s^25p^2$	4f+5(7)7.5p-1(1)8.5p+1(3)5	47.224165
387	$4f^{11}5s^25p^2$	4f-4(8)8.4f+7(7)13.5p-1(1)12.5p+1(3)13	47.329489
388	$4f^{11}5s^25p^2$	4f-4(8)8.4f+7(7)1.5p-1(1)2.5p+1(3)3	47.357200
389	$4f^{11}5s^25p^2$	4f-4(8)8.4f+7(7)3.5p-1(1)4.5p+1(3)7	47.366743
390	$4f^{11}5s^25p^2$	4f-4(8)8.4f+7(7)15.5p-1(1)14.5p+1(3)11	47.371560
391	$4f^{11}5s^25p^2$	4f-4(8)8.4f+7(7)1.5p-1(1)2.5p+1(3)5	47.400267
392	$4f^{11}5s^25p^2$	4f-5(5)5.4f+6(4)9.5p-1(1)8.5p+1(3)9	47.490240
393	$4f^{12}5s^15p^2$	4f+6(12)12.5s+1(1)13.5p-1(1)12.5p+1(3)15	47.566220

Table 10. *Cont.*

Level No.	Configuration	*2J*	FAC
394	$4f^{11}5s^25p^2$	4f-4(4)4.4f+7(7)3.5p-1(1)2.5p+1(3)1	47.576112
395	$4f^{12}5s^15p^2$	4f-4(4)4.5s+1(1)5	47.608356
396	$4f^{11}5s^25p^2$	4f-5(5)5.4f+6(4)9.5p-1(1)8.5p+1(3)7	47.626404
397	$4f^{11}5s^25p^2$	4f-4(8)8.4f+7(7)3.5p-1(1)4.5p+1(3)3	47.630702
398	$4f^{11}5s^25p^2$	4f-4(4)4.4f+7(7)7.5p-1(1)8.5p+1(3)5	47.856467
399	$4f^{11}5s^25p^2$	4f-5(5)5.4f+6(4)9.5p-1(1)8.5p+1(3)7	47.906232
400	$4f^{11}5s^25p^2$	4f-4(4)4.4f+7(7)5.5p-1(1)6.5p+1(3)9	47.942764
401	$4f^{11}5s^25p^2$	4f-4(4)4.4f+7(7)5.5p-1(1)4.5p+1(3)3	48.044767
402	$4f^{11}5s^25p^2$	4f-4(4)4.4f+7(7)11.5p-1(1)12.5p+1(3)15	48.051851
403	$4f^{11}5s^25p^2$	4f-4(4)4.4f+7(7)11.5p-1(1)12.5p+1(3)11	48.152857
404	$4f^{11}5s^25p^2$	4f-4(4)4.4f+7(7)5.5p-1(1)4.5p+1(3)5	48.241588
405	$4f^{11}5s^25p^2$	4f-4(8)8.4f+7(7)15.5p-1(1)16.5p+1(3)17	48.262896
406	$4f^{11}5s^25p^2$	4f-4(4)4.4f+7(7)5.5p-1(1)6.5p+1(3)7	48.340247
407	$4f^{11}5s^25p^2$	4f-4(8)8.4f+7(7)1.5p-1(1)2.5p+1(3)5	48.405696
408	$4f^{12}5s^15p^2$	4f-5(5)5.4f+7(7)2.5s+1(1)1	48.416353
409	$4f^{11}5s^25p^2$	4f-4(4)4.4f+7(7)11.5p-1(1)12.5p+1(3)13	48.461446
410	$4f^{11}5s^25p^2$	4f-4(4)4.4f+7(7)7.5p-1(1)8.5p+1(3)11	48.477197
411	$4f^{11}5s^25p^2$	4f-3(3)3.5p-1(1)2.5p+1(3)1	48.497669
412	$4f^{11}5s^25p^2$	4f-4(4)4.4f+7(7)11.5p-1(1)10.5p+1(3)7	48.743022
413	$4f^{11}5s^25p^2$	4f-4(8)8.4f+7(7)3.5p-1(1)2.5p+1(3)5	48.754213
414	$4f^{11}5s^25p^2$	4f-4(4)4.4f+7(7)11.5p-1(1)10.5p+1(3)9	48.792651
415	$4f^{11}5s^25p^2$	4f-4(4)4.4f+7(7)11.5p-1(1)10.5p+1(3)11	48.831990
416	$4f^{11}5s^25p^2$	4f-4(8)8.4f+7(7)5.5p-1(1)4.5p+1(3)1	48.876547
417	$4f^{12}5s^15p^2$	4f-5(5)5.4f+7(7)4.5s+1(1)3	48.891319
418	$4f^{11}5s^25p^2$	4f-4(8)8.4f+7(7)15.5p-1(1)14.5p+1(3)13	48.923501
419	$4f^{11}5s^25p^2$	4f-4(4)4.4f+7(7)7.5p-1(1)6.5p+1(3)5	48.991206
420	$4f^{11}5s^25p^2$	4f-4(8)8.4f+7(7)15.5p-1(1)14.5p+1(3)15	49.005761
421	$4f^{11}5s^25p^2$	4f-4(4)4.4f+7(7)7.5p-1(1)8.5p+1(3)9	49.073201
422	$4f^{11}5s^25p^2$	4f-4(8)8.4f+7(7)1.5p-1(1)0.5p+1(3)3	49.092208
423	$4f^{11}5s^25p^2$	4f-5(5)5.4f+6(4)7.5p-1(1)8.5p+1(3)7	49.107584
424	$4f^{12}5s^15p^2$	4f+6(8)8.5s+1(1)9.5p-1(1)8.5p+1(3)11	49.225409
425	$4f^{11}5s^25p^2$	4f-4(4)4.4f+7(7)7.5p-1(1)6.5p+1(3)3	49.318118
426	$4f^{11}5s^25p^2$	4f-4(4)4.4f+7(7)5.5p-1(1)4.5p+1(3)5	49.398585
427	$4f^{11}5s^25p^2$	4f-3(3)3.5p-1(1)4.5p+1(3)7	49.458758
428	$4f^{12}5s^15p^2$	4f+6(12)12.5s+1(1)13.5p-1(1)12.5p+1(3)13	49.511467
429	$4f^{12}5s^15p^2$	4f+6(8)8.5s+1(1)9.5p-1(1)8.5p+1(3)9	49.549600
430	$4f^{11}5s^25p^2$	4f-5(5)5.4f+6(4)7.5p-1(1)6.5p+1(3)9	49.803106
431	$4f^{11}5s^25p^2$	4f-3(3)3.5p-1(1)4.5p+1(3)3	49.819068
432	$4f^{11}5s^25p^2$	4f-4(4)4.4f+7(7)5.5p-1(1)6.5p+1(3)7	49.856027
433	$4f^{13}5s^15p^1$	4f+7(7)7.5s+1(1)8.5p+1(3)5	49.881682
434	$4f^{13}5s^15p^1$	4f+7(7)7.5s+1(1)6.5p+1(3)9	49.987168
435	$4f^{11}5s^25p^2$	4f-3(3)3.5p-1(1)2.5p+1(3)3	50.028605
436	$4f^{11}5s^25p^2$	4f-5(5)5.4f+6(4)7.5p-1(1)8.5p+1(3)5	50.077842
437	$4f^{11}5s^25p^2$	4f-4(4)4.4f+7(7)9.5p-1(1)10.5p+1(3)7	50.111402
438	$4f^{12}5s^15p^2$	4f-5(5)5.4f+7(7)10.5s+1(1)9.5p-1(1)10.5p+1(3)7	50.183762
439	$4f^{12}5s^15p^2$	4f+6(8)8.5s+1(1)9.5p-1(1)8.5p+1(3)9	50.198350
440	$4f^{11}5s^25p^2$	4f+5(15)15.5p+2(4)19	50.226742
441	$4f^{12}5s^15p^2$	4f-5(5)5.4f+7(7)8.5s+1(1)7.5p-1(1)8.5p+1(3)5	50.328400
442	$4f^{12}5s^15p^2$	4f+6(8)8.5s+1(1)7.5p-1(1)8.5p+1(3)7	50.426385
443	$4f^{11}5s^25p^2$	4f-3(3)3.5p-1(1)2.5p+1(3)1	50.466901
444	$4f^{11}5s^25p^2$	4f-4(4)4.4f+7(7)9.5p-1(1)10.5p+1(3)7	50.502712
445	$4f^{12}5s^15p^2$	4f+6(8)8.5s+1(1)9.5p-1(1)8.5p+1(3)11	50.590776
446	$4f^{11}5s^25p^2$	4f-5(5)5.4f+6(4)7.5p-1(1)6.5p+1(3)9	50.597918
447	$4f^{11}5s^25p^2$	4f-5(5)5.4f+6(4)7.5p-1(1)8.5p+1(3)11	50.610624
448	$4f^{11}5s^25p^2$	4f-4(4)4.4f+7(7)9.5p-1(1)8.5p+1(3)5	50.949017

Table 10. *Cont.*

Level No.	Configuration	2J	FAC
449	$4f^{11}5s^25p^2$	4f-3(5)5.5p-1(1)6.5p+1(3)9	51.020195
450	$4f^{11}5s^25p^2$	4f-4(4)4.4f+7(7)9.5p-1(1)8.5p+1(3)11	51.068131
451	$4f^{13}5s^15p^1$	4f+7(7)7.5s+1(1)8.5p+1(3)7	51.070448
452	$4f^{11}5s^25p^2$	4f+5(15)15.5p+2(4)17	51.116024
453	$4f^{12}5s^15p^2$	4f-5(5)5.4f+7(7)10.5s+1(1)11.5p-1(1)10.5p+1(3)13	51.334835
454	$4f^{11}5s^25p^2$	4f-5(5)5.4f+6(4)7.5p-1(1)6.5p+1(3)3	51.363160
455	$4f^{12}5s^15p^2$	4f-5(5)5.4f+7(7)6.5s+1(1)5.5p-1(1)6.5p+1(3)5	51.370276
456	$4f^{11}5s^25p^2$	4f-5(5)5.4f+6(4)7.5p-1(1)6.5p+1(3)7	51.373528
457	$4f^{12}5s^15p^2$	4f+6(12)12.5s+1(1)13.5p-1(1)14.5p+1(3)17	51.564277
458	$4f^{11}5s^25p^2$	4f-5(5)5.4f+6(4)7.5p-1(1)6.5p+1(3)5	51.616242
459	$4f^{11}5s^25p^2$	4f-3(5)5.5p-1(1)6.5p+1(3)9	51.669738
460	$4f^{13}5s^15p^1$	4f-5(5)5.5s+1(1)6.5p+1(3)3	51.794518
461	$4f^{12}5s^15p^2$	4f+6(12)12.5s+1(1)11.5p-1(1)12.5p+1(3)9	51.808742
462	$4f^{11}5s^25p^2$	4f+5(15)15.5p+2(4)15	51.873567
463	$4f^{11}5s^25p^2$	4f-4(4)4.4f+7(7)9.5p-1(1)10.5p+1(3)13	51.894895
464	$4f^{11}5s^25p^2$	4f-3(5)5.5p-1(1)4.5p+1(3)7	51.949134
465	$4f^{11}5s^25p^2$	4f-3(5)5.5p-1(1)4.5p+1(3)1	52.008321
466	$4f^{12}5s^15p^2$	4f-5(5)5.4f+7(7)10.5s+1(1)9.5p-1(1)10.5p+1(3)7	52.026776
467	$4f^{11}5s^25p^2$	4f-5(5)5.4f+6(4)7.5p-1(1)6.5p+1(3)5	52.033636
468	$4f^{12}5s^15p^2$	4f-5(5)5.4f+7(7)8.5s+1(1)9.5p-1(1)8.5p+1(3)11	52.083735
469	$4f^{12}5s^15p^2$	4f+6(4)4.5s+1(1)3.5p-1(1)4.5p+1(3)3	52.119437
470	$4f^{11}5s^25p^2$	4f-3(5)5.5p-1(1)4.5p+1(3)3	52.127458
471	$4f^{11}5s^25p^2$	4f-4(4)4.4f+7(7)9.5p-1(1)10.5p+1(3)11	52.249539
472	$4f^{12}5s^15p^2$	4f-4(8)8.5s+1(1)7.5p-1(1)8.5p+1(3)5	52.272296
473	$4f^{11}5s^25p^2$	4f+5(15)15.5p+2(4)13	52.359709
474	$4f^{12}5s^15p^2$	4f+6(12)12.5s+1(1)13.5p-1(1)14.5p+1(3)15	52.368597
475	$4f^{13}5s^15p^1$	4f-5(5)5.5s+1(1)4.5p+1(3)7	52.414510
476	$4f^{11}5s^25p^2$	4f+5(15)15.5p+2(4)11	52.547263
477	$4f^{12}5s^15p^2$	4f+6(12)12.5s+1(1)11.5p-1(1)12.5p+1(3)13	52.589880
478	$4f^{11}5s^25p^2$	4f-3(5)5.5p-1(1)4.5p+1(3)5	52.607852
479	$4f^{12}5s^15p^2$	4f-5(5)5.4f+7(7)10.5s+1(1)9.5p-1(1)10.5p+1(3)9	52.686118
480	$4f^{11}5s^25p^2$	4f-5(5)5.4f+6(12)13.5p+2(4)17	52.735714
481	$4f^{12}5s^15p^2$	4f+6(4)4.5s+1(1)3.5p-1(1)4.5p+1(3)1	52.825991
482	$4f^{12}5s^15p^2$	4f+6(8)8.5s+1(1)7.5p-1(1)8.5p+1(3)5	52.888739
483	$4f^{11}5s^25p^2$	4f-4(4)4.4f+7(7)9.5p-1(1)10.5p+1(3)9	52.889924
484	$4f^{12}5s^15p^2$	4f+6(12)12.5s+1(1)13.5p-1(1)12.5p+1(3)11	52.905137
485	$4f^{11}5s^25p^2$	4f-5(5)5.4f+6(12)13.5p+2(4)15	53.036541
486	$4f^{12}5s^15p^2$	4f+6(8)8.5s+1(1)9.5p-1(1)10.5p+1(3)13	53.151612
487	$4f^{11}5s^25p^2$	4f-5(5)5.4f+6(12)13.5p+2(4)13	53.161837
488	$4f^{12}5s^15p^2$	4f-5(5)5.4f+7(7)8.5s+1(1)9.5p-1(1)8.5p+1(3)11	53.245023
489	$4f^{12}5s^15p^2$	4f+6(8)8.5s+1(1)9.5p-1(1)10.5p+1(3)11	53.248825
490	$4f^{12}5s^15p^2$	4f+6(12)12.5s+1(1)11.5p-1(1)10.5p+1(3)9	53.381515
491	$4f^{12}5s^15p^2$	4f+6(8)8.5s+1(1)7.5p-1(1)8.5p+1(3)7	53.404688
492	$4f^{11}5s^25p^2$	4f-4(4)4.4f+7(7)9.5p-1(1)8.5p+1(3)7	53.434223
493	$4f^{13}5s^15p^1$	4f-5(5)5.5s+1(1)6.5p+1(3)5	53.481890
494	$4f^{12}5s^15p^2$	4f+6(12)12.5s+1(1)11.5p-1(1)10.5p+1(3)7	53.583051
495	$4f^{11}5s^25p^2$	4f-5(5)5.4f+6(12)13.5p+2(4)11	53.620775
496	$4f^{11}5s^25p^2$	4f-5(5)5.4f+6(0)5.5p-1(1)6.5p+1(3)3	53.620908
497	$4f^{11}5s^25p^2$	4f+5(9)9.5p+2(4)13	53.694318
498	$4f^{11}5s^25p^2$	4f-5(5)5.4f+6(12)13.5p+2(4)9	53.695742
499	$4f^{11}5s^25p^2$	4f+5(11)11.5p+2(4)15	53.722950
500	$4f^{12}5s^15p^2$	4f+6(8)8.5s+1(1)7.5p-1(1)8.5p+1(3)9	53.767747
634	$4f^{14}5p^1$	5p-1(1)1	58.282075
1292	$4f^{14}5p^1$	5p+1(3)3	72.160271

In Table 11, some of the calculated energies are compared with those from critically evaluated data compiled by NIST [9], which are commonly used as a reference set for atomic results. The calculated values of Safronova et al. [28] and Zhou et al. [32] are also presented for comparison in Table 11. For the level $4f^{13}5s^2\,^2F_{5/2}$, our calculated value matches the results of Zhou et al. [32]. For this level, the NIST value is from Vilkas et al. [24] whose results have been proven wrong by many authors in the recent past. They have used the MR-MP method for their calculation. For the $4f^{13}5s5p$ levels, the maximum difference between our calculation using FAC and the calculation of Safronova et al. [28] is 3.1%.

Table 11. Comparison of energy levels (in Rydberg) calculated with FAC for Pm-like W with other available results.

Level No.	Configuration	$2J$	FAC	NIST	Safronova [a]
1	$4f^{13}5s^2$	5	0.1658	0.24(3) + x	0.165 [b]
43	$4f^{14}5s^1$	1	1.8482	1.62(3) + y	1.79
91	$4f^{13}5s5p$	9	2.2445	2.3379(12)	2.294
263	$4f^{13}5s5p$	5	3.1756	3.350(3)	3.212
326	$4f^{13}5s5p$	9	3.3200	3.490(3)	3.361
451	$4f^{13}5s5p$	7	3.7536	3.826(3)	3.878

a—Reference [28]. b—Reference [32].

In Table 12, we present the transition data for the $4f^{13}5s^{2}$–$4f^{13}5s5p$ and $4f^{14}5s$-$4f^{14}5p$ transitions including transition wavelengths (in nm), transition probabilities (A_{ji} in s^{-1}), and oscillator strengths (gf_{ij}, dimensionless). We give the oscillator strengths both in the velocity and length forms to check the accuracy of the calculated results, as it is one of the criteria used to assess the accuracy. The ratio of the velocity and length forms of the oscillator strength should be close to unity in accurate calculations. It is a necessary condition, even though it is not sufficient. As one can see in Table 12, this ratio is close to unity for most of the strong transitions. It is plotted in Figure 5 against line strength. For the Pm-like W, the systematic offset between the length and velocity forms is significantly smaller, at only about 10%. Therefore, the strongest E1 transitions with the line strength $S_V > 0.017$ a.u. can be assigned an uncertainty of 10%. Those with 0.004 a.u. $< S_V <$ 0.017 a.u. can be assigned an uncertainty of 15%, and weaker transitions can be estimated as accurate to 30%. In Table 12, we also present the transition rates from the OUT3 results for comparison since, for magnetic transitions, the velocity form is not available. From Table 12, one can see that transition rates of OUTF have large differences from OUT3 for many levels, which is due to additional configurations in OUTF. In Table S1 of the supplementary material, we report M1 and E2 transition data for the transitions to various levels for $4f^{12}5s^25p$ of Pm-like W, as these transitions could help to analyze experimental EBIT and tokamak spectra.

Table 12. Transition data for the $4f^{13}5s^2\,^2F$-$4f^{13}5s5p$ and $4f^{14}5s$-$4f^{14}5p$ transitions in Pm-like W. Oscillator strength are given in both the length form (gf_L) and velocity form (gf_v).

$4f^{13}5s^2\,^2F$-$4f^{13}5s5p$ Transition									
j	$2J_j$	i	$2J_i$	λ(nm)	gf_L	gf_v	A_{ji}(s^{-1}) OUT3	A_{ji}(s^{-1}) OUTF	Type
69	7	0	7	44.1901	2.41E-02	2.20E-02	8.84E+07	1.03E+08	E1
69	7	1	5	48.0529	6.40E-04	8.21E-04	3.20E+06	2.31E+06	E1
69	7	0	7	44.1901	9.18E-12	9.18E-12	2.95E-02	3.92E-02	M2
69	7	1	5	48.0529	1.16E-12	1.16E-12	3.81E-03	4.18E-03	M2
85	7	0	7	41.2210	2.75E-01	2.40E-01	1.40E+09	1.35E+09	E1
85	7	1	5	44.5625	1.67E-02	1.68E-02	7.72E+07	7.02E+07	E1
85	7	0	7	41.2210	2.05E-12	2.05E-12	1.15E-02	1.01E-02	M2
85	7	1	5	44.5625	6.20E-14	6.20E-14	4.67E-04	2.60E-04	M2
89	5	0	7	40.9938	8.27E-02	7.26E-02	4.68E+08	5.47E+08	E1
89	5	1	5	44.2971	4.68E-03	4.16E-03	2.93E+07	2.65E+07	E1

Table 12. *Cont.*

4f^{13}5s^2 ^{2}F-4f^{13}5s5p Transition									
j	$2J_j$	i	$2J_i$	λ(nm)	gf_L	gf_v	A_{ji}(s^{-1}) OUT3	A_{ji}(s^{-1}) OUTF	Type
89	5	0	7	40.9938	1.81E-12	1.81E-12	9.39E-03	1.19E-02	M2
89	5	1	5	44.2971	4.19E-12	4.19E-12	1.92E-02	2.38E-02	M2
91	9	0	7	40.6002	5.38E-01	5.00E-01	2.18E+09	2.18E+09	E1
91	9	0	7	40.6002	7.31E-12	7.31E-12	2.23E-02	2.96E-02	M2
91	9	1	5	43.8378	2.25E-12	2.25E-12	1.01E-02	7.81E-03	M2
94	5	0	7	39.7106	2.42E-01	2.19E-01	1.78E+09	1.71E+09	E1
94	5	1	5	42.8026	5.97E-02	5.49E-02	3.36E+08	3.62E+08	E1
94	5	0	7	39.7106	1.48E-11	1.48E-11	9.30E-02	1.04E-01	M2
94	5	1	5	42.8026	1.10E-13	1.10E-13	1.35E-03	6.68E-04	M2
108	5	0	7	37.4897	5.80E-02	5.69E-02	4.50E+08	4.59E+08	E1
108	5	1	5	40.2335	1.76E-01	1.50E-01	1.29E+09	1.21E+09	E1
108	5	0	7	37.4897	8.94E-13	8.94E-13	1.10E-02	7.07E-03	M2
108	5	1	5	40.2335	3.24E-12	3.24E-12	1.31E-02	2.22E-02	M2
110	7	0	7	37.3208	2.07E-02	1.76E-02	1.31E+08	1.24E+08	E1
110	7	1	5	40.0390	4.29E-01	3.86E-01	2.17E+09	2.23E+09	E1
110	7	0	7	37.3208	3.07E-12	3.07E-12	1.50E-02	1.84E-02	M2
110	7	1	5	40.0390	8.68E-12	8.68E-12	3.70E-02	4.51E-02	M2
114	3	1	5	39.6448	2.25E-01	1.95E-01	2.38E+09	2.38E+09	E1
114	3	0	7	36.9780	4.52E-12	4.52E-12	6.28E-02	5.51E-02	M2
114	3	1	5	39.6448	7.47E-12	7.47E-12	6.67E-02	7.93E-02	M2
222	11	0	7	29.5982	3.95E-09	3.95E-09	2.50E+01	2.51E+01	M2
250	3	1	5	30.5445	4.58E-03	3.26E-03	8.20E+07	8.18E+07	E1
250	3	0	7	28.9367	1.25E-09	1.25E-09	2.45E+01	2.48E+01	M2
250	3	1	5	30.5445	3.70E-10	3.70E-10	6.94E+00	6.62E+00	M2
263	5	0	7	28.6955	1.85E-02	1.53E-02	2.10E+08	2.50E+08	E1
263	5	1	5	30.2759	1.96E-02	1.80E-02	2.04E+08	2.37E+08	E1
263	5	0	7	28.6955	2.16E-09	2.16E-09	2.98E+01	2.92E+01	M2
263	5	1	5	30.2759	2.74E-10	2.74E-10	3.47E+00	3.32E+00	M2
266	1	1	5	30.2379	7.45E-10	7.45E-10	2.74E+01	2.72E+01	M2
277	7	0	7	28.4044	3.29E-02	3.06E-02	2.69E+08	3.40E+08	E1
277	7	1	5	29.9520	4.30E-03	4.51E-03	3.61E+07	4.00E+07	E1
277	7	0	7	28.4044	3.21E-09	3.21E-09	3.44E+01	3.32E+01	M2
277	7	1	5	29.9520	1.24E-10	1.24E-10	1.26E+00	1.15E+00	M2
279	9	0	7	28.3905	2.12E-02	1.76E-02	1.30E+08	1.75E+08	E1
279	9	0	7	28.3905	4.13E-09	4.13E-09	3.53E+01	3.42E+01	M2
279	9	1	5	29.9366	9.21E-11	9.21E-11	7.97E-01	6.85E-01	M2
317	3	1	5	28.9893	2.36E-02	2.32E-02	3.72E+08	4.68E+08	E1
317	3	0	7	27.5371	5.07E-10	5.07E-10	1.15E+01	1.12E+01	M2
317	3	1	5	28.9893	1.16E-09	1.16E-09	2.36E+01	2.30E+01	M2
326	9	0	7	27.4477	4.27E-02	4.56E-02	3.18E+08	3.78E+08	E1
326	9	0	7	27.4477	1.26E-10	1.26E-10	1.12E+00	1.12E+00	M2
326	9	1	5	28.8902	3.90E-09	3.90E-09	3.02E+01	3.12E+01	M2
351	5	0	7	26.9546	1.60E-02	1.60E-02	1.80E+08	2.45E+08	E1
351	5	1	5	28.3445	2.01E-03	2.06E-03	2.35E+07	2.79E+07	E1
351	5	0	7	26.9546	3.86E-10	3.86E-10	6.32E+00	5.91E+00	M2
351	5	1	5	28.3445	2.22E-09	2.22E-09	3.17E+01	3.07E+01	M2
357	7	0	7	26.8680	1.38E-02	1.33E-02	1.21E+08	1.59E+08	E1
357	7	1	5	28.2487	5.85E-02	5.66E-02	5.11E+08	6.11E+08	E1
357	7	0	7	26.8680	1.59E-10	1.59E-10	2.11E+00	1.84E+00	M2
357	7	1	5	28.2487	3.26E-09	3.26E-09	3.55E+01	3.41E+01	M2
433	5	0	7	24.8557	3.27E+00	3.03E+00	6.52E+10	5.88E+10	E1
433	5	1	5	26.0327	3.84E-02	3.41E-02	7.37E+08	6.29E+08	E1
433	5	0	7	24.8557	3.52E-14	3.52E-14	8.78E-04	6.33E-04	M2
433	5	1	5	26.0327	1.45E-11	1.45E-11	2.74E-01	2.38E-01	M2

Table 12. *Cont.*

$4f^{13}5s^2\,^2F$-$4f^{13}5s5p$ Transition									
j	$2J_j$	i	$2J_i$	λ(nm)	gf_L	gf_v	$A_{ji}(s^{-1})$ OUT3	$A_{ji}(s^{-1})$ OUTF	Type
434	9	0	7	24.8032	5.16E+00	4.84E+00	6.74E+10	5.59E+10	E1
434	9	0	7	24.8032	6.56E-12	6.56E-12	3.56E-03	7.11E-02	M2
434	9	1	5	25.9752	3.47E-11	3.47E-11	3.20E-01	3.43E-01	M2
451	7	0	7	24.2771	3.97E+00	3.75E+00	4.92E+10	5.62E+10	E1
451	7	1	5	25.3988	4.19E-01	4.00E-01	4.99E+09	5.42E+09	E1
451	7	0	7	24.2771	1.29E-11	1.29E-11	1.45E-01	1.83E-01	M2
451	7	1	5	25.3988	1.73E-12	1.73E-12	1.80E-02	2.23E-02	M2
460	3	1	5	25.0275	2.23E+00	2.06E+00	6.66E+10	5.93E+10	E1
460	3	0	7	23.9377	1.38E-12	1.38E-12	7.80E-02	4.03E-02	M2
460	3	1	5	25.0275	6.03E-12	6.03E-12	2.44E-01	1.61E-01	M2
475	7	0	7	23.6546	4.17E-01	3.92E-01	8.91E+09	6.21E+09	E1
475	7	1	5	24.7182	3.77E+00	3.54E+00	5.84E+10	5.14E+10	E1
475	7	0	7	23.6546	9.03E-12	9.03E-12	2.22E-01	1.35E-01	M2
475	7	1	5	24.7182	2.69E-11	2.69E-11	3.70E-01	3.66E-01	M2
493	5	0	7	23.1825	4.11E-02	3.86E-02	8.33E+08	8.51E+08	E1
493	5	1	5	24.2031	3.28E+00	3.09E+00	6.74E+10	6.23E+10	E1
493	5	0	7	23.1825	1.09E-11	1.09E-11	2.19E-01	2.26E-01	M2
493	5	1	5	24.2031	1.82E-12	1.82E-12	1.32E-02	3.45E-02	M2
$4f^{14}5s$-$4f^{14}5p$ transition									
J	$2J_j$	i	$2J_i$	λ(in nm)	gf_L	gf_v	$A_{ji}(s^{-1})$ OUT3	$A_{ji}(s^{-1})$ OUTF	Type
634	1	43	1	37.4171	4.89E-01	4.61E-01	1.29E+10	1.16E+10	E1
1292	3	43	1	26.3718	1.33E+00	1.29E+00	3.50E+10	3.18E+10	E1
1292	3	43	1	26.3718	2.40E-09	2.40E-09	5.53E+01	5.75E+01	M2

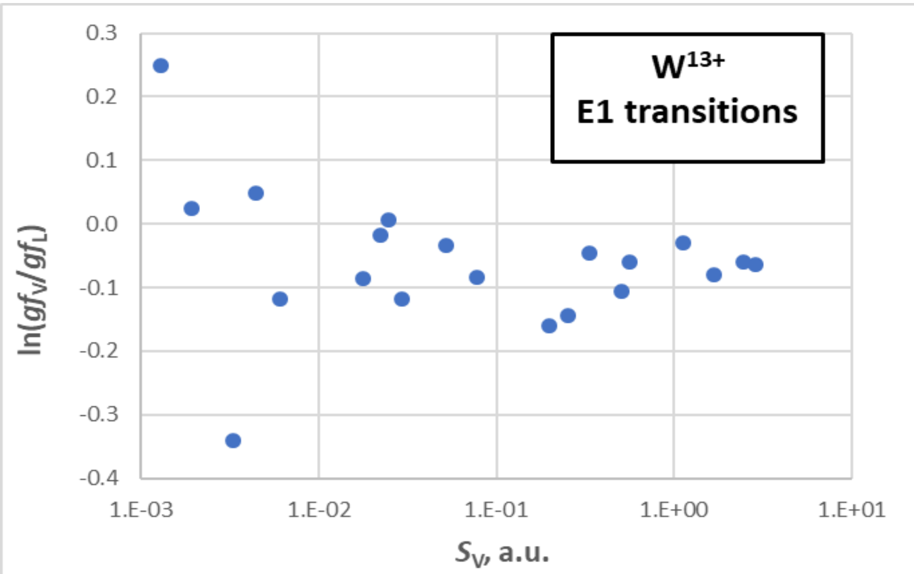

Figure 5. A comparison of the velocity and length forms of oscillator strength for a few of the strongest transitions (E1) of W^{13+}.

In the $4f^{13}5s^2\,^2F_{7/2}$ and $4f^{13}5s^2\,^2F_{5/2}$ levels, the mixing is very low, and their labeling is unambiguous. For both levels, the dominant eigenvector component contributes 98.3% and 98.4%, respectively. We would also like to mention that mixing among some of the levels is strong in our calculations.

We found that level 250 is strongly coupled with level 317 with percentages of the corresponding components of 71% and 23%, respectively. We found that the level 277 is composed of 52% of the basis state used in its label mixed with 39% of the state used to label the level 357. Similarly, mixing among some other levels is very strong. Hence, the labeling of a particular level is not always based on the dominant eigenvector component. The configuration and J values given in Table 8 are definite, but the labels are not unique and can be interchanged.

Table S1 provides the means to estimate the uncertainties of the M1 and E2 transitions in Pm-like W. For example, Figure 6 plots the natural logarithm of the ratio $A_{\rm outF}/A_{\rm out3}$ of the E2 transition rates calculated in the two largest calculations. From this figure, one can see that, except for a few strongly discrepant transitions, the two data sets agree with each other fairly well. This figure is consistent with a typical behavior of calculated transition rates. For the strongest transitions (in this case, $S_{\rm outF} > 0.94$ a.u.), the mean (i.e., root-mean-square, rms) of the logarithmic ratio is 0.014, corresponding to an agreement within 1.4% on average. For weaker transitions, the scatter of the data points increases, but, even for the weakest transitions with $S < 0.00212$ a.u., the mean disagreement is only 52%.

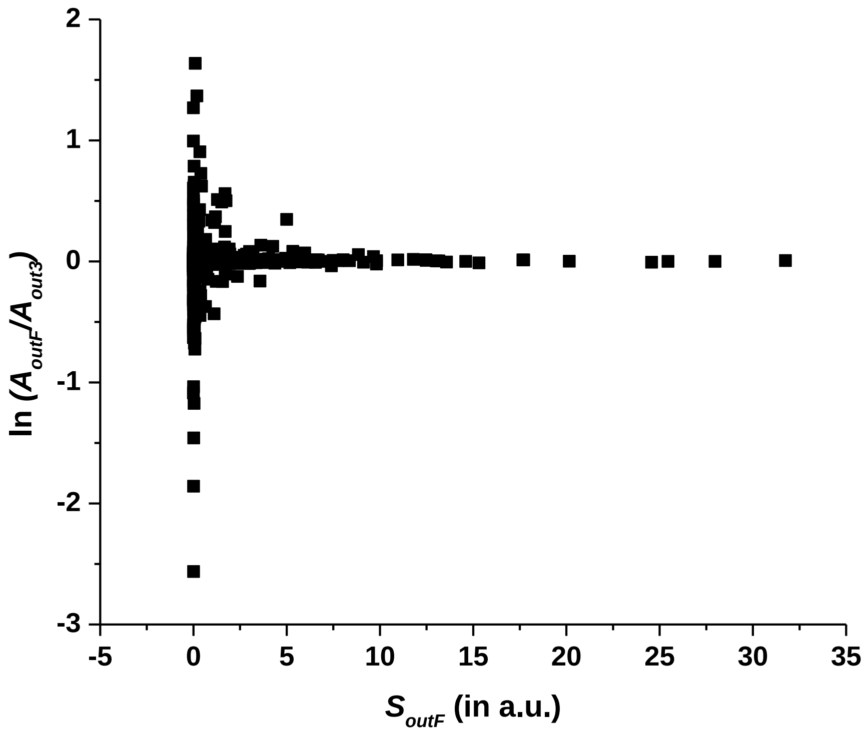

Figure 6. Natural logarithm of the ratio $A_{\rm outF}/A_{\rm out3}$ of the E2 transition rates calculated in the two largest calculations for W^{13+}. The horizontal axis contains the line strengths $S_{\rm outF}$ of the largest calculation in atomic units.

For M1 transitions, if three strongly discrepant transitions are excluded, the comparison of out3 and outF looks qualitatively similar, as shown in Figure 7. Here again, the strongest transitions ($S_{\rm outF} > 2.8$ a.u. in this case) exhibit a mean discrepancy of 3.2%, while, for weaker transitions, it increases, but, even for the weakest transitions with $S < 0.1$ a.u., the mean discrepancy is only 15%. The three transitions excluded from this plot are 47 → 38, 65 → 38, and 74 → 38. For them, the discrepancies amount to a factor between 10 and 100.

In Table 13, we compare transition wavelengths (in nm) calculated using FAC with the data compiled by NIST [9] and with experimental and theoretical results of Kobayashi et al. [31] along with theoretical results of Safronova et al. [28] and Ding et al. [33]. For the transitions 0–91, 0–263, and 0–326, our calculated transition wavelengths are comparable (maximum difference of 5%) with the data compiled by NIST. For the transitions 0–433, 0–434, and 0–451, our calculated transition wavelength agrees well with the experimental results of Kobayashi et al. [31] (error within 0.4%) and are more accurate than the theoretical results of Safronova et al. [28] and Kobayashi et al. [31]. Furthermore, our calculated transition wavelengths for all transitions are in excellent agreement with the recent results of Ding et al. [33]. This is a clear indication of accuracy of our results.

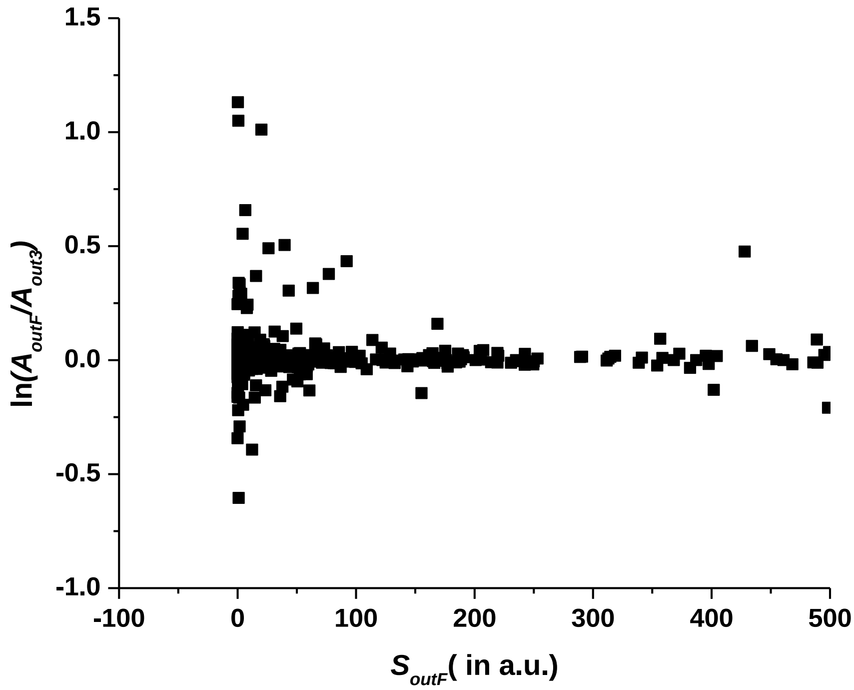

Figure 7. Natural logarithm of the ratio $A_{\mathrm{outF}}/A_{\mathrm{out3}}$ of the M1 transition rates calculated in the two largest calculations for W^{13+}. The horizontal axis contains the line strengths S_{outF} of the largest calculation in atomic units.

Table 13. Comparison of a transition wavelength (in nm) calculated using FAC with NIST [9] and other results for Pm-like W. The indexes of the lower and upper levels, *i* and *j*, respectively, correspond to those given in Table 10.

i	*J*	*λ* (This Work)	*λ* (NIST)	*λ* (Others)
0	91	40.600	38.978(20)	———
0	263	28.696	27.205(20)	———
0	326	27.448	26.110(20)	———
0	433	24.856	———	24.91 [c] 24.70 [a] 24.71 [b] 24.76 [d]
0	434	24.803	———	24.83 [c] 24.64 [a] 24.53 [b] 24.69 [d]
0	451	24.277	———	24.32 [c] 24.06 [a] 23.95 [b] 24.17 [d]
1	451	25.399	25.384(20)	

a—Reference [28] results using COWAN code. b—Reference [31] results using the HULLAC code. c—Experimental results of Reference [31]. d—Reference [33] using FAC.

In Table 14, we have compared transition wavelength (in nm) calculated with FAC for the transition $4f^{13}5s^2\ ^2F_{5/2}$–$^2F_{7/2}$ with other results for Pm-like W. The theoretical wavelengths are calculated in vacuum, while the experimental wavelengths are measured in standard air. Li et al. [30] and Zhao et al. [32] in Shanghai and Kobayashi et al. [31] in Tokyo observed similar spectra, but the charge state assignments differ by one. Recently, the Shanghai group confirmed [36] that their assignment made in References [30,32] was wrong and confirmed the assignment in Reference [31]. In addition, recent theoretical calculations by Ding et al. [33] also support the assignment in Reference [31]. Our theoretical result agrees within 2% with the experimental wavelengths of Kobayashi et al. [31]. This is better than the result of Safronova et al. [28], who used the COWAN code, and Vilkas et al. [24]. The differences of those two results from the measurement of Kobayashi et al. are larger (4% and 30%, respectively). The maximum discrepancy of 29% is between the experimental wavelength and the results of Vilkas et al. [24], which are responsible for discrepancies between our calculated results and the NIST data [9] quoted from Vilkas et al. [24]. Furthermore, our transition wavelength is in good agreement with the recent results of Ding et al. [33] as well as with other theoretical results listed in Table 14. In Table 15, we give the collisional excitation cross-sections of Pm-like W from the ground state for incident electron energy ranging from 45 to 75 eV. The collision cross section is given in units of 100 Mb.

Table 14. Comparison of transition wavelength (nm) calculated with FAC for the transition $4f^{13}5s^2\ ^2F_{5/2}$-$^2F_{7/2}$ with other results for Pm-like W. Experimental wavelengths are given in standard air, while theoretically calculated wavelengths are in vacuum.

Method	Wavelength (nm)
FAC (this work)	549.72
Experiment [f]	560.25
Experiment [a]	549.95 ± 0.06
RMBPT [a]	567.64
FAC [a]	552.08
Safronova et al. (COWAN) [b]	537.63
Vilkas et al. (MR-MP) [c]	388.71
Nandy (CCSD-T) [d]	556.60
FAC [e]	550.80

a—Reference [32]. b—Reference [28]. c—Reference [24]. d—Reference [38]. e—Reference [33]. f—Reference [31].

Table 15. Collisional excitation cross-sections (100 Mb) of Pm-like W from the ground state to various levels.

Energy (eV) /Transition	0–2	0–3	0–4	Energy (eV) /Transition	0–5	0–6	0–7	Energy (eV) /Transition	0–43
0.00E+00	2.54E+04	2.54E+04	2.54E+04	0.00E+00	2.54E+04	2.54E+04	2.54E+04	0.00E+00	3.00E+04
3.72E-01	1.72E+02	1.12E+02	8.80E+01	3.72E-01	8.14E+01	5.64E+01	1.13E+02	1.20E+00	3.06E+01
1.32E+01	5.98E+01	4.14E+01	3.36E+01	1.32E+01	3.19E+01	2.35E+01	4.93E+01	2.43E+01	1.52E+01
4.70E+01	1.89E+01	1.37E+01	1.11E+01	4.70E+01	1.07E+01	8.24E+00	1.91E+01	6.85E+01	7.18E+00
1.36E+02	4.65E+00	3.87E+00	2.93E+00	1.36E+02	2.94E+00	2.36E+00	6.91E+00	1.52E+02	3.21E+00
3.64E+02	8.57E-01	1.10E+00	6.36E-01	3.64E+02	7.57E-01	6.19E-01	2.54E+00	3.11E+02	1.47E+00
9.32E+02	1.97E-01	4.12E-01	1.85E-01	9.32E+02	2.63E-01	1.96E-01	9.75E-01	6.04E+02	7.42E-01

Energy (eV) /Transition	0–8	0–9	0–10	0–11	Energy (eV) /Transition	0–12	0–13	0–14	0–15
0.00E+00	2.54E+04	2.54E+04	2.54E+04	2.54E+04	0.00E+00	2.54E+04	2.54E+04	2.54E+04	2.54E+04
7.44E-01	4.67E+01	2.78E+01	2.96E+01	1.50E+02	7.44E-01	7.69E+01	1.78E+02	1.77E+01	1.62E+01
2.11E+01	1.64E+01	9.12E+00	9.88E+00	5.42E+01	2.11E+01	2.77E+01	6.76E+01	6.84E+00	6.19E+00
6.78E+01	6.91E+00	3.02E+00	3.32E+00	2.17E+01	6.78E+01	1.08E+01	2.78E+01	2.76E+00	2.22E+00
1.74E+02	3.25E+00	9.09E-01	1.01E+00	9.12E+00	1.74E+02	4.27E+00	1.20E+01	1.14E+00	7.23E-01
4.13E+02	1.71E+00	2.85E-01	3.13E-01	3.99E+00	4.13E+02	1.79E+00	5.32E+00	4.88E-01	2.44E-01
9.32E+02	7.91E-01	1.11E-01	1.21E-01	1.78E+00	9.32E+02	7.87E-01	2.39E+00	2.16E-01	9.65E-02

Energy (eV) /Transition	0–16	0–17	0–18	0–19	0–20	0–21	0–22	0–23	0–24
0.00E+00	2.54E+04	2.54E+04	2.54E+04	2.54E+04	2.54E+04	2.54E+04	2.54E+04	2.54E+04	2.54E+04
7.44E-01	1.11E+01	4.92E+01	3.25E+01	5.56E+00	6.88E+00	2.18E+02	3.76E+01	3.07E+01	2.40E+01
2.11E+01	4.71E+00	2.02E+01	1.24E+01	2.16E+00	2.69E+00	9.61E+01	1.69E+01	1.39E+01	1.11E+01
6.78E+01	2.09E+00	8.33E+00	4.08E+00	7.25E-01	9.17E-01	4.22E+01	7.40E+00	6.13E+00	4.98E+00
1.74E+02	9.88E-01	3.47E+00	1.03E+00	1.94E-01	2.52E-01	1.87E+01	3.23E+00	2.68E+00	2.23E+00
4.13E+02	4.94E-01	1.50E+00	2.12E-01	4.75E-02	6.39E-02	8.42E+00	1.44E+00	1.20E+00	1.01E+00
9.32E+02	2.44E-01	6.68E-01	5.14E-02	1.49E-02	2.12E-02	3.81E+00	6.48E-01	5.38E-01	4.57E-01

Energy (eV) /Transition	0–26	0–27	0–28	0–30	0–31	0–32	0–33	0–36	0–37
0.00E+00	2.54E+04	2.54E+04	2.54E+04	2.54E+04	2.54E+04	2.54E+04	2.54E+04	2.54E+04	2.54E+04
1.48E+00	3.44E+01	6.29E+01	1.73E+02	1.83E+00	2.50E+01	1.63E+01	5.08E+01	4.80E+01	2.57E+01
3.30E+01	1.15E+01	2.58E+01	7.67E+01	7.06E-01	9.14E+00	5.97E+00	2.20E+01	2.14E+01	1.03E+01
9.59E+01	3.46E+00	1.12E+01	3.69E+01	2.67E-01	3.15E+00	2.03E+00	1.00E+01	1.01E+01	4.20E+00

Table 15. *Cont.*

Energy (eV) /Transition	0–26	0–27	0–28	0–30	0–31	0–32	0–33	0–36	0–37
2.21E+02	8.42E-01	5.07E+00	1.86E+01	9.95E-02	1.05E+00	6.36E-01	4.81E+00	4.99E+00	1.79E+00
4.66E+02	1.97E-01	2.47E+00	9.59E+00	4.19E-02	4.11E-01	2.25E-01	2.41E+00	2.54E+00	8.53E-01
9.32E+02	4.72E-02	1.24E+00	4.96E+00	2.09E-02	1.96E-01	9.44E-02	1.23E+00	1.31E+00	4.40E-01
Energy (eV) /Transition	0–38	0–39	0–41	0–42	0–45	0–46	0–47	0–49	0–50
0.00E+00	2.54E+04	2.54E+04	2.54E+04	2.54E+04	2.54E+04	2.54E+04	2.54E+04	2.54E+04	2.54E+04
1.48E+00	1.38E+01	5.47E+01	7.00E+01	1.12E+01	3.03E+01	2.14E+01	1.31E+01	2.71E+01	3.43E+01
3.30E+01	5.39E+00	2.42E+01	3.25E+01	4.53E+00	1.38E+01	9.78E+00	5.37E+00	1.25E+01	1.63E+01
9.59E+01	2.10E+00	1.12E+01	1.60E+01	1.77E+00	6.51E+00	4.63E+00	2.18E+00	6.04E+00	8.19E+00
2.21E+02	8.62E-01	5.46E+00	8.18E+00	6.91E-01	3.20E+00	2.28E+00	9.22E-01	3.02E+00	4.41E+00
4.66E+02	4.12E-01	2.75E+00	4.26E+00	3.02E-01	1.63E+00	1.16E+00	4.41E-01	1.55E+00	2.57E+00
9.32E+02	2.19E-01	1.41E+00	2.22E+00	1.46E-01	8.42E-01	5.99E-01	2.30E-01	7.99E-01	1.54E+00
Energy (eV) /Transition	0–25	0–29	0–34	0–35	0–40	0–44	0–48	Energy (eV) /Transition	0–1
0.00E+00	2.54E+04	2.54E+04	2.54E+04	2.54E+04	2.54E+04	2.54E+04	2.54E+04	0.00E+00	3.00E+04
1.40E+00	1.37E-01	1.56E-01	9.11E+00	7.74E-01	1.50E-01	2.15E-01	1.30E+00	1.13E-01	2.79E+03
4.18E+01	3.78E-02	5.01E-02	2.89E+00	2.69E-01	6.03E-02	8.22E-02	5.14E-01	2.21E+00	1.47E+03
1.37E+02	8.92E-03	1.55E-02	8.48E-01	9.60E-02	2.57E-02	3.25E-02	2.12E-01	6.17E+00	7.72E+02
3.58E+02	1.66E-03	4.96E-03	2.65E-01	3.77E-02	1.13E-02	1.35E-02	9.14E-02	1.36E+01	4.02E+02
8.57E+02	2.51E-04	1.89E-03	1.01E-01	1.63E-02	5.00E-03	5.83E-03	4.03E-02	2.77E+01	2.06E+02
1.91E+03	3.28E-05	8.74E-04	4.29E-02	7.56E-03	2.28E-03	2.66E-03	1.84E-02	5.41E+01	1.03E+02

5. Conclusions

Motivated by the need of atomic data for fusion plasma research, in the present paper, we have reported energy levels and radiative data, such as transition wavelengths and oscillator strengths, as well as collisional excitation cross sections for W^{11+} and W^{13+}. For the calculations, the fully relativistic FAC has been adopted with the inclusion of CI. The effect of CI has been examined and investigated systematically by including different configurations. The present calculations provide new energy level data and are useful for accuracy assessments. Based on several comparisons with NIST and other available results, our listed energies are accurate (error <1%) for most levels of both ions. Energies have been listed for the lowest 304 and 500 levels of W^{11+} and W^{13+}, respectively, but the remaining data for higher levels can be obtained from the authors on request. We have also presented radiative transition rates for both ions that are expected to be highly useful in analysis and modeling of plasmas. We have presented oscillator strengths in both velocity and length forms for both ions. We have compared our calculated data with the other available theoretical and experimental data and no (major) discrepancies have been found, except for some levels of Pm-like W calculated by Vilkas et al. [24]. Furthermore, we observed discrepancies in the ground state of Eu-like W, which depends on the configurations included. There is scope for further work in these complex systems.

Supplementary Materials: The following are available online at http://www.mdpi.com/2218-2004/8/4/92/s1. Table S1: Magnetic dipole (M1) and electric quadrupole (E2) transition data for transitions within the 4f13.5s2 and 4f12.5s2.5p configurations of Pm-like W. Table S2: Eigenvector compositions and mixing coefficients for Pm-like W.

Author Contributions: All authors have contributed equally in preparation of the manuscript. All authors have read and agreed to the published version of the manuscript.

Funding: This research was funded by IAEA grant number 23244.

Acknowledgments: We are thankful to IAEA for providing financial support through a research coordination project entitled "Atomic data for vapour shielding in fusion devices" contract no. 23244. "Drafts of Figures 2–7, as well as Tables S1 and S2 of the Supplementary Materials, were made for us by an anonymous Reviewer, whose help in preparation of this article for publication is gratefully acknowledged".

Conflicts of Interest: The authors declare no conflict of interest.

References

1. Matthews, G.; Coad, P.; Greuner, H.; Hill, M.; Hirai, T.; Likonen, J.; Maier, H.; Mayer, M.; Neu, R.; Philipps, V.; et al. Development of divertor tungsten coatings for the JET ITER-like wall. *J. Nucl. Mater.* **2009**, *390*, 934–937. [CrossRef]
2. Hirai, T.; Escourbiac, F.; Carpentier-Chouchana, S.; Fedosov, A.; Ferrand, L.; Jokinen, T.; Komarov, V.; Kukushkin, A.; Merola, M.; Mitteau, R.; et al. ITER tungsten divertor design development and qualification program. *Fusion Eng. Des.* **2013**, *88*, 1798–1801. [CrossRef]
3. Clementson, J.; Lennartsson, T.; Beiersdorfer, P. Extreme Ultraviolet Spectra of Few-Times Ionized Tungsten for Divertor Plasma Diagnostics. *Atoms* **2015**, *3*, 407–421. [CrossRef]
4. Radtke, R.; Biedermann, C.; Schwob, J.L.; Mandelbaum, P.; Doron, R. Line and band emission from tungsten ions with charge 21+ to 45+ in the 45–70–Å range. *Phys. Rev. A* **2001**, *64*, 012720. [CrossRef]
5. Harte, C.S.; Suzuki, C.; Kato, T.; Sakaue, H.; Kato, D.; Sato, K.; Tamura, N.; Sudo, S.; D'Arcy, R.; Sokell, E.; et al. Tungsten spectra recorded at the LHD and comparison with calculations. *J. Phys. B At. Mol. Opt. Phys.* **2010**, *43*, 205004. [CrossRef]
6. Suzuki, C.; Koike, F.; Murakami, I.; Tamura, N.; Sudo, S.; Sakaue, H.A.; Nakamura, N.; Morita, S.; Goto, M.; Kato, D.; et al. EUV spectroscopy of highly charged high Z ions in the Large Helical Device plasmas. *Phys. Scripta* **2014**, *89*, 114009. [CrossRef]
7. Jonauskas, V.; Kučas, S.; Karazija, R. On the interpretation of the intense emission of tungsten ions at about 5 nm. *J. Phys. B At. Mol. Opt. Phys.* **2007**, *40*, 2179–2188. [CrossRef]
8. Jonauskas, V.; Kisielius, R.; Kynienė, A.; Kučas, S.; Norrington, P.H. Magnetic dipole transitions in 4 d N configurations of tungsten ions. *Phys. Rev. A* **2010**, *81*, 012506. [CrossRef]

9. Kramida, A.; Ralchenko, Y. Reader and NIST ASD Team 2019. Version 5.7.1. Available online: https://physics.nist.gov/asd (accessed on 8 October 2019).
10. Singh, A.K.; Aggarwal, S.; Mohan, M. Level energies, lifetimes and radiative rates in the 4p44d configurations of bromine-like ions. *Phys. Scr.* **2013**, *88*, 35301. [CrossRef]
11. Goyal, A.; Khatri, I.; Aggarwal, S.; Singh, A.; Mohan, M. Atomic structure calculations for Br-like ions. *Can. J. Phys.* **2015**, *93*, 487–495. [CrossRef]
12. Goyal, A.; Khatri, I.; Aggarwal, S.; Singh, A.; Mohan, M. Atomic structure calculations and identification of EUV and SXR spectral lines in Sr XXX. *J. Quant. Spectrosc. Radiat. Transf.* **2015**, *161*, 157–170. [CrossRef]
13. Goyal, A.; Khatri, I.; Aggarwal, S.; Singh, A.K.; Sharma, R.; Mohan, M. Collisional excitation of Florine like Tungsten using relativistic Dirac atomic R-matrix method. *JAMNCP* **2015**, *2*, 1.
14. Goyal, A.; Khatri, I.; Aggarwal, S.; Singh, A.K.; Mohan, M. Calculation of energy levels, lifetimes and radiative data for La XXIX to Sm XXXIV. *At. Data Nucl. Data Tables* **2016**, *107*, 406. [CrossRef]
15. Aggarwal, S.; Singh, J.; Mohan, M. Atomic structure calculations for Br-like ions. *At. Data Nucl. Data Tables* **2013**, *99*, 394. [CrossRef]
16. Brage, T.; Froese Fischer, C.; Brage, T. Systematic calculations of correlation in complex ions. *PhysicaScripta* **1993**, *T47*, 18. [CrossRef]
17. Fischer, C.F. Correlation effects on transition probabilities in Mo vi. *J. Phys. B At. Mol. Opt. Phys.* **2011**, *44*, 125001. [CrossRef]
18. Berengut, J.C.; Dzuba, V.A.; Flambaum, V.V.; Ong, A. Highly charged ions with E1, M1, and E2 transitions within laser range. *Phys. Rev. A* **2012**, *86*, 22517. [CrossRef]
19. Berengut, J.C.; Dzuba, V.A.; Flambaum, V.V. Enhanced Laboratory Sensitivity to Variation of the Fine-Structure Constant using Highly Charged Ions. *Phys. Rev. Lett.* **2010**, *105*, 120801. [CrossRef]
20. Berengut, J.C.; Dzuba, V.A.; Flambaum, V.V.; Ong, A. Electron-hole transitions in multiply charged ions for precision laser spectroscopy and searching for variations in α. *Phys. Rev. Lett.* **2011**, *106*, 210802. [CrossRef]
21. Curtis, L.J.; Ellis, D.G. Alkalilike spectra in the promethium isoelectronic sequence. *Phys. Rev. Lett.* **1980**, *45*, 2099. [CrossRef]
22. Theodosiou, C.E.; Raftopoulos, V. Further studies of the promethium isoelectronic sequence. *Phys. Rev. A* **1983**, *28*, 1186–1188. [CrossRef]
23. Hutton, R.; Zou, Y.; Almandos, J.R.; Biedermann, R.; Radtke, R.; Greier, A.; Neu, R. EBIT Spectroscopy of Pm-like Tungsten. *Nucl. Instrum. Methods Phys. Res B* **2003**, *205*, 114. [CrossRef]
24. Vilkas, M.J.; Ishikawa, Y.; Träbert, E. Electric-dipole 5 s—5 p transitions in promethiumlike ions. *Phys. Rev. A* **2008**, *77*, 42510. [CrossRef]
25. Kramida, A.; Shirai, T. Energy levels and spectral lines of tungsten, W III through W LXXIV. *At. Data Nucl. Data Tables* **2009**, *95*, 305–474. [CrossRef]
26. Wu, S.; Hutton, R. Applications of EBITs to spectra of multi-electron ions: Some solved and some unsolved problems. *Can. J. Phys.* **2008**, *86*, 125. [CrossRef]
27. Kramida, A. Recent progress in spectroscopy of tungsten1This review is part of a Special Issue on the 10th International Colloquium on Atomic Spectra and Oscillator Strengths for Astrophysical and Laboratory Plasmas. *Can. J. Phys.* **2011**, *89*, 551–570. [CrossRef]
28. Safronova, U.I.; Safronova, A.S.; Beiersdorfer, P. Contribution of the 4f -core-excited states in determination of atomic properties in the promethium isoelectronic sequence. *Phys. Rev. A* **2013**, *88*, 32512. [CrossRef]
29. Qiu, M.L.; Li, W.; Zhao, Z.Z.; Yang, Y.; Xiao, J.; Brage, T.; Hutton, R.; Zou, Y. Review of highly charged tungsten spectroscopy research using low energy EBITs at the Shanghai EBIT laboratory. *J. Phys. B At. Mol. Opt. Phys.* **2015**, *48*, 144029. [CrossRef]
30. Li, W.; Shi, Z.; Yang, Y.; Xiao, J.; Brage, T.; Hutton, R.; Zou, Y. Tungsten spectroscopy in the EUV range observed at a high-temperature superconducting electron-beam ion trap. *Phys. Rev. A* **2015**, *91*, 62501. [CrossRef]
31. Kobayashi, Y.; Kubota, K.; Omote, K.; Komatsu, A.; Sakoda, J.; Minoshima, M.; Kato, D.; Li, J.; Sakaue, H.A.; Murakami, I.; et al. Extreme ultraviolet and visible spectroscopy of promethiumlike heavy ions. *Phys. Rev. A* **2015**, *92*, 022510. [CrossRef]
32. Zhao, Z.; Qiu, M.L.; Zhao, R.F.; Li, W.X.; Guo, X.L.; Xiao, J.; Chen, C.Y.; Zou, Y.; Hutton, R. Experimental and theoretical study of visible transitions in promethium-like tungsten. *J. Phys. B At. Mol. Opt. Phys.* **2015**, *48*, 115004. [CrossRef]

33. Ding, X.; Zhang, F.; Yang, Y.; Zhang, L.; Koike, F.; Murakami, I.; Kato, D.; Sakaue, H.A.; Nakamura, N.; Dong, C. Collisional-radiative modeling of the 5 p—5 s spectrum of W xiv–W xvi ions. *Phys. Rev. A* **2020**, *101*, 42509. [CrossRef]
34. Mita, M.; Sakaue, H.A.; Kato, D.; Murakami, I.; Nakamura, N. Extreme ultraviolet spectra of multiply charged tungsten ions. *J. Phys. Conf. Ser.* **2017**, *875*, 12019. [CrossRef]
35. Gu, M.F. The flexible atomic code. *Can. J. Phys.* **2008**, *86*, 675–689. [CrossRef]
36. Liang, S.; Lu, Q.; Wang, X.; Yang, Y.; Yao, K.; Shen, Y.; Wei, B.; Xiao, J.; Chen, S.; Zhou, P.; et al. A low-energy compact Shanghai-Wuhan electron beam ion trap for extraction of highly charged ions. *Rev. Sci. Instrum.* **2019**, *90*, 93301. [CrossRef]
37. Li, M.; Qiu, M.; Xiao, J.; Yao, K.; Brage, T.; Hutton, R.; Zou, Y. A strong visible line in the spectrum of W11+. *Phys. Scr.* **2016**, *91*, 105401. [CrossRef]
38. Nandy, D.K.; Sahoo, B.K. Highly charged W13+, Ir16+, and Pt17+ ions as promising optical clock candidates for probing variations of the fine-structure constant. *Phys. Rev. A* **2016**, *94*, 032504. [CrossRef]